# A possible role of Werner helicase interacting protein 1 (WRNIP1) in the Fanconi anemia DNA repair pathway




**Alicja Bulsiewicz**

Jesus College

University of Oxford

**A thesis submitted for the degree of Doctor of Philosophy**

**Michaelmas Term 2016**

# Abstract


**A possible role of Werner helicase interacting protein 1 (WRNIP1) in the Fanconi anemia DNA repair pathway**

***Alicja Bulsiewicz, Jesus College, submitted for the degree of Doctor of Philosophy, Michaelmas Term 2016***

The Fanconi anemia (FA) pathway plays a crucial role in resolving DNA interstrand crosslinks (ICLs), which can form as a result of DNA damage by genotoxic agents (Lopez-Martinez *et al.,* 2016). The exact mechanism of FA pathway action is unknown, although 21 proteins have been identified as its components, which, in turn, form at least three known groups, i.e. core, FANCD2/FANCI and downstream effector proteins (Mamrak *et al.,* 2016; Ceccaldi *et al.,* 2016). The FANCD2/FANCI complex is multi-phosphorylated and monoubiquitinated on both FANCD2 and FANCI after ICL-inducing damage. However, how FANCD2/FANCI complex is recruited to damaged chromatin remains elusive (Cohn and D'Andrea, 2008).

This project investigates whether WRNIP1 can function as a protein operating in the Fanconi anemia pathway and examines its interaction with FANCD2 and FANCI.

It was demonstrated here that WRNIP1 behaved similarly to the Fanconi anemia proteins because its depletion resulted in higher sensitivity of cells to the ICL-inducing agents, i.e. mitomycin C (MMC), TMP combined with UVA irradiation as well as cisplatin. Moreover, it was demonstrated that WRNIP1 partially rescued the sensitivity of WRNIP1-depleted cells after their complementation.

It has been demonstrated that following treatment with genotoxic agents of cells and their subsequent fractionation, WRNIP1 did not show any significant increase in its

nuclear fraction levels. Furthermore, WRNIP1-deficient cells treated with ICL-inducing agents and subsequently fractionated did not affect the ubiquitination patterns of FANCD2 nor did WRNIP1 depletion affect the formation of FANCD2 repair foci. These data might indicate that WRNIP1 was already present in the nucleus at the levels necessary to repair DNA. However, the lack of alteration in the FANCD2 ubiquitination and absence of effect of FANCD2 foci formation might suggest that WRNIP1 acted downstream of FANCD2 in the Fanconi anemia pathway or that there was no interaction between these two proteins. Therefore, this part of the project did not establish a functional link between FANCD2 and WRNIP1.

It was demonstrated for the first time by *in vitro* binding analysis that WRNIP1 could bind to the two established components of the Fanconi anemia pathway, i.e. FANCD2 and FANCI. This result was corroborated by a subsequent study which revealed that FANCD2, FANCI and WRNIP1 could also form a complex together. It was shown that WRNIP1 bound to FANCD2 independently of FANCI. The *in vitro* binding analysis also attempted to map a WRNIP1's domain which would be responsible for interaction with FANCD2. However, the three investigated WRNIP1 deletion mutants were shown to bind FANCD2. This outcome indicated the possibility that either WRNIP1 amino acid sequences located in between the three previously-generated regions were responsible for FANCD2-WRNIP1 interaction or, alternatively, WRNIP1 might bind to FANCD2 via two or more domains.

It was also shown here that WRNIP1 was purified in two forms, one of which was demonstrated to be ubiquitinated. However, the type of ubiquitination has not been determined yet. It was demonstrated that deletion of WRNIP1's UBZ domain abrogates its ubiquitination but the consequences of this phenomenon must still be established.

# Acknowledgements

*"Learning to think rigorously,*

*so as to act rightly and to serve humanity better."*

− Pope John Paul II (Karol Wojtyła)

First and foremost, I would like to express my thanks and deepest appreciation to my supervisor Dr Martin Cohn for supporting me with his expertise and plenty of patience throughout the entire course of my doctoral studies. Without his knowledge and constant encouragement, the completion of this project could not be possible.

I am equally indebted and grateful to my second supervisor Prof. David Sherratt and members of my thesis committee: Prof. Lynne Cox and Prof. Catherine Pears as well as my College advisors: Prof. Ilan Davis and Dr Erika Manzini for guiding me throughout my studies and providing me with excellent advice.

I would like to thank BBSRC research council for providing me with the financial assistance for my research projects.

It is a pleasure to thank members of the Micron group, especially, Dr Eva Wegel and Dr Ian Dobbie for their instructions and assistance in introducing me and explaining to me the intricacies of microscopy.

I would like to thank Dr Fumiko Esashi and Dr Conrad Nieduszynski for providing me with advice on my research during our monthly joint meetings.

I am very grateful to all the members, past and present, of Cohn's laboratory for giving me guidance, support and critical evaluation of both my experimental and written work. In particular, I am grateful to Anna Socha, Chih-Chao Liang, Jamie Zhan, Anna

Motnenko, David Lopez-Martinez and Dr Yasunaga Yoshikawa. Moreover, I would like to thank members of Pears, Lakin and Howarth laboratories for their assistance with the experimental work.

Most importantly, I would like to thank my amazing parents, grandmother, younger sister Monika, my beloved boyfriend – Michael, and my dearest friends for their incessant love and support during my doctoral studies. No words can describe how much I am indebted to them and how I admire their strength of personalities which gave me motivation and inspiration when I was at my weakest. I have learnt invaluable life lessons from each one of you.

## Dedication

*In loving memory of*

*Marianna Czechowska, Andrzej Więcek and Dariusz Napoleon Stefański*

## Declaration

I confirm that this DPhil thesis represents my own work. External contributions to the research are acknowledged.

## Abbreviations

- ATM – Ataxia telangiectasia mutated
- ATR – Ataxia telangiectasia and Rad3-related protein
- BER – Base Excision Repair
- bp – base pair
- β-ME – β-mercaptoethanol
- BPB – bromophenol blue
- BSA – bovine serum albumin
- CPD – cyclobutane pyrimidine dimer
- DAPI – 4, 6-Diamidino-2-phenylindole dihydrochloride
- DDR – DNA Damage Response
- DMEM – Dulbecco's Modified Eagle's Medium
- DMSO – dimethyl sulfoxide
- DSB – Double-Strand Breaks
- EtOH – ethanol
- FA – Fanconi anemia
- FBS – Foetal Bovine Serum
- FT – flow-through fraction
- HA tag – Human Influenza Hemagglutinin tag
- HR – Homologous Recombination
- ICL(s) – interstrand crosslink(s)
- IF – immunofluorescence
- IPTG – isopropyl β-D-1-thiogalactopyranoside
- KD – knockdown
- kDa – kilo Dalton
- KO – knockout
- LB – Luria Bertani
- MBP – Maltose-Binding Protein
- MeOH – methanol
- Mgs1 – maintenance of genome stability 1

- MMC – mitomycin C
- MMR – Mismatch Repair
- MQ – Milli-Q
- MRN – Mre11-Rad50-Nbs1 complex
- NER – Nucleotide Excision Repair
- NHEJ – Non-homologous end joining
- NLS – nuclear localisation sequence
- OD – optical density
- PBS – Phosphate Buffered Saline
- PCNA – Proliferating Cell Nuclear Antigen
- PCR – Polymerase Chain Reaction
- PMSF – phenylmethanesulfonyl fluoride
- Pol η – polymerase eta
- rpm – rounds per minute
- RNAi – RNA interference
- RT – room temperature
- SDS-PAGE – sodium dodecyl sulfate - polyacrylamide gel electrophoresis
- Sgs1 – slow growth suppressor 1
- shRNA – small-hairpin RNA
- Tris – Tris(hydroxymethyl)aminomethane
- TLS – Translesion Synthesis
- ub – ubiquitin
- UBZ – ubiquitin-binding zinc-finger domain
- TMP – 4,5',8-trimethylpsolaren
- UV – ultraviolet radiation
- v/v – volume per volume
- WB – Western blot
- WRN – Werner helicase
- WS – Werner syndrome
- WT – Wild type
- w/v – weight per volume

# Table of Contents


Abstract ..... 2
Acknowledgements ..... 4
Dedication ..... 6
Declaration ..... 7
Abbreviations ..... 8
Table of Contents ..... 10
1 Introduction ..... 17
1.1 DNA Damage Response……..……...17
1.1.1 DNA damage and associated diseases ..... 18
1.1.2 Homologous recombination repair pathway ..... 20
1.1.3 Non-homologous end joining ..... 24
1.1.4 Base excision repair ..... 25
1.1.5 Nucleotide excision repair ..... 26
1.1.6 Translesion synthesis ..... 27
1.1.7 Fanconi anemia pathway ..... 28
1.2 Fanconi anemia DNA repair pathway……..……..29
1.2.1 Fanconi anemia background ..... 29
1.2.2 Molecular mechanism of the Fanconi anemia pathway ..... 30
1.2.3 Ubiquitination and ubiquitin-binding domains in the Fanconi anemia pathway ..... 38
1.3 Werner helicase interacting protein 1 (WRNIP1)……..42
1.3.1 Werner helicase interacting protein 1 ..... 42
1.3.2 Post-translational modifications of WRNIP1 ..... 44
1.3.3 WRNIP1 and its interacting partners ..... 46
1.3.4 WRNIP1's role in DNA repair ..... 46
1.5 Aims of the thesis……..…….51
2 Materials and Methods ..... 55
2.1 Materials…….55
2.1.1 Reagents and solvents ..... 55
2.1.2 Cell lines and antibodies ..... 57
2.1.3 Primers ..... 60
2.2 Methods……..……61

2.2.1 Cell survival (clonogenic) assay ..... 61
2.2.2 Immunofluorescence microscopy (IF) ..... 62
2.2.3 Cell transformation ..... 64
2.2.4 Restriction enzyme digestion ..... 65
2.2.5 Plasmid fragment dephosphorylation ..... 66
2.2.6 Ligation ..... 66
2.2.7 *In vitro* binding assay ..... 66
2.2.8 Fractionation of HeLa cells (Intact nuclei method) ..... 67
2.2.9 Fractionation of HeLa cells ..... 69
2.2.10 Reverse transcription reaction ..... 71
2.2.11 Polymerase chain reaction (PCR) ..... 71
2.2.12 Lysis of the Sf9 insect cells ..... 72
2.2.13 Western blot (WB) sample preparation ..... 74
2.2.14 Transformation of cells ..... 75
2.2.15 Transfection ..... 75
2.2.16 $Ni^{2+}$-NTA Purification ..... 76
2.2.17 StrepTactin Purification ..... 78
2.2.18 Preparation of the desthiobiotin stock ..... 80
2.2.19 Preparation of 4% (w/v) paraformaldehyde ..... 80
2.2.20 Cell competency ..... 81
2.2.21 Collection of baculovirus particles and harvesting of Sf9 insect cells for WB ..... 82
2.2.22 FANCD2/FANCI heterodimeric complex purification ..... 82
2.2.23 Gene knockdown ..... 83
2.2.24 Heat inactivation of FBS ..... 84
2.2.25 *In vivo* α-Flag binding assay ..... 84
2.2.26 Preparation of X-gal Luria Agar (LB) plates for baculovirus selection ..... 86
2.2.27 α-Flag M2 agarose purification of Flag-tagged proteins ..... 86
2.2.28 SDS-PAGE gel stack preparation ..... 88
2.2.29 Plasmid purification ..... 89
2.2.30 Mycoplasma detection protocol ..... 91
2.2.31 PCR-based colony screening ..... 92
2.2.32 Transfection of Sf9 insect cells ..... 93
2.2.33 Infection of Sf9 insect cells with a baculovirus ..... 94
2.2.34 TMP-UVA cell treatment for Western blot ..... 95

2.2.35 Western blot preparation ..... 95
2.2.36 Sequencing ..... 97
2.2.37 Statistical analysis ..... 97
2.2.38 Plating efficiency calculation ..... 98
3 Analysis of WRNIP1's impact on cell survival upon exposure to genotoxic agents ..... 99
3.1 Introduction……99
3.2 WRNIP1 knockdown cells exhibit lower survival than control cells…….99
3.3 WRNIP1 knockout cells show lower survival than control cells after treatment with genotoxic agents…….104
3.4 WRNIP1 partially rescues the ICL-induced DNA damage……..114
3.5 Discussion…….117
4 An *in vivo* study of WRNIP1's response to various DNA damaging agents ..... 118
4.1 Introduction……..118
4.2 WRNIP1 is not significantly enriched in nuclear fractions after genotoxic agent treatment…….119
4.3 FANCD2 deficiency does not influence WRNIP1's levels in the nucleus……..121
4.4 WRNIP1 deficiency does not influence FANCD2 foci formation……...127
4.5 Discussion…….129
5 *In vitro* interactions between WRNIP1 and components of FANCD2/FANCI heterogeneous complex ..... 131
5.1 Introduction……..131
5.2 Cloning, expression, purification and characterization of WRNIP1……133
5.3 *In vitro* binding between WRNIP1 and FANCD2……...136
5.4 *In vitro* binding between FANCD2 and WRNIP1 deletion mutants……137
5.5 *In vitro* binding between WRNIP1 and FANCI……...142
5.6 *In vitro* binding between FANCD2/FANCI heterodimeric complex and WRNIP1……146
5.7 *In vitro* interaction between FANCD2, WRNIP1 and FANCI……148
5.8 Discussion…….152
6 A study of ubiquitination of WRNIP1 ..... 158
6.1 Introduction……..158
6.2 WRNIP1 has an ubiquitinated upper form……...159
6.3 UBZ domain directs WRNIP1's ubiquitination……...162
6.4 WRNIP1's ubiquitinated upper form is not directed for proteasome degradation…….165
6.5 Discussion…….167

7 Discussion and Conclusions ..... 169
8 Future Directions ..... 176
9 Bibliography ..... 180

## List of Figures

Figure 1. Simplified diagrammatic representation of the Fanconi anemia ICL-repair pathway. 30
Figure 2. Diagrammatic representation of the Fanconi anemia pathway-dependent mechanism of DNA ICL resolution during DNA replication and the proteins involved in this process (Part 1) ..... 36
Figure 3. Diagrammatic representation of the Fanconi anemia pathway-dependent mechanism of ICL resolution during DNA replication and the proteins involved in this process (Part 2) ..... 37
Figure 4. Diagrammatic representation of the Werner helicase interacting protein 1 (WRNIP1). ..... 43
Figure 5. Interactions between WRNIP1's UBZ domain and ubiquitin. ..... 45
Figure 6. Quantification of WRNIP1 knockdown in HeLa cells ..... 101
Figure 7. WRNIP1 knockdown cells are sensitive to the treatment with MMC ..... 102
Figure 8. WRNIP1 knockdown cells are not sensitive to the treatment with cisplatin ..... 103
Figure 9. Western blot of HeLa WRNIP1 knockout (HeLa WRNIP1$^{-/-}$) cells. ..... 105
Figure 10. WRNIP1 knockout cells are sensitive to the treatment with MMC ..... 106
Figure 11. WRNIP1 knockout cells are sensitive to the treatment with TMP-UVA ..... 108
Figure 12. WRNIP1 knockout cells are not sensitive to the treatment with TMP only ..... 109
Figure 13. WRNIP1 knockout and FANCD2 knockout cells are sensitive to the treatment with TMP-UVA ..... 111
Figure 14. WRNIP1 knockout cells are sensitive to the treatment with cisplatin. ..... 113
Figure 15. WRNIP1 partially complements the cellular sensitivity to the treatment with MMC ..... 115
Figure 16. WRNIP1 partially complements the cellular sensitivity to the treatment with TMP-UVA. ..... 116
Figure 17. Western blot analysis of MMC-treated and fractionated HeLa cells ..... 120
Figure 18. Western blot analysis of UVC-treated and fractionated HeLa cells ..... 121
Figure 19. Western blot analysis of MMC-treated nuclear fractions of HeLa cells ..... 123
Figure 20. Westrn blot analysis of TMP-UVA-treated nuclear fractions of HeLa cells. ..... 124
Figure 21. Western blot analysis of MMC-treated nuclear and cytoplasmic fractions of HeLa cells ..... 125
Figure 22. Western blot analysis of TMP-UVA-treated nuclear and cytoplasmic fractions of HeLa cells ..... 126
Figure 23. WRNIP1 does not influence FANCD2 foci formation ..... 128
Figure 24. Generation of recombinant baculovirus and the expression of WRNIP1 with the use of Bac-to-Bac® Baculovirus Expression System ..... 134

Figure 25. Coomassie blue stain and Western blot analysis of Sf9 insect cell purified His- and Strep(II)-tagged WRNIP1 ..... 135
Figure 26. WRNIP1 interacts with FANCD2 in vitro. ..... 137
Figure 27. Diagrammatic representation of WRNIP1 and three WRNIP1 deletion mutants. ..... 138
Figure 28. Diagrammatic representation and Western blot analysis of two Sf9-purified WRNIP1 deletion mutants. ..... 139
Figure 29. Purification of WRNIP1 deletion mutants ..... 141
Figure 30. FANCD2 interacts with WRNIP1 and WRNIP1 deletion mutants in vitro ..... 142
Figure 31. WRNIP1 interacts with FANCI in vitro ..... 144
Figure 32. WRNIP1 interacts with FANCI at various concentrations in vitro ..... 145
Figure 33. WRNIP1 interacts with FANCD2/FANCI complex in vitro ..... 147
Figure 34. WRNIP1 interacts with monomeric FANCD2 and monomeric FANCI in vitro ..... 150
Figure 35. WRNIP1 does not compete with FANCI for binding with FANCD2 ..... 151
Figure 36. FANCD2, FANCI and WRNIP1 interaction models. ..... 154
Figure 37. Models of WRNIP1 interaction with FANCD2/FANCI complex ..... 156
Figure 38. Recombinant WRNIP1 purified from Sf9 cells has two forms ..... 160
Figure 39. Analysis of ubiquitination of WRNIP1's upper form ..... 161
Figure 40. Western blot analysis of the ubiquitination of WRNIP1 deletion mutants ..... 163
Figure 41 Interactions between UBZ domain of WRNIP1 and ubiquitin ..... 164
Figure 42. WRNIP1's ubiquitination is not affected by proteasome inhibition ..... 166
Figure 43. Simplified diagrammatic representation of the Fanconi anemia ICL-repair pathway including WRNIP1 ..... 175

# List of Tables

Table 1. Human genetic diseases associated with defects in DNA repair pathways..... 19
Table 2. A list of genes mutated in Fanconi anemia patients. This table has been partially adapted from Wang, A. T. and Smogorzewska, A. (2015), Ceccaldi et al. (2016) and Mamrak et al. (2016). ..... 40
Table 3. A list of Fanconi anemia-associated genes. This table has been partially adapted from Wang, A. T. and Smogorzewska, A. (2015) and Ceccaldi et al. (2016)) ..... 41
Table 4. List of buffers and solutions used in this project. ..... 55
Table 5. Primers used in this project ..... 60
Table 6. The example of conditions applied during Polymerase Chain Reaction (PCR). ..... 72
Table 7. The reagents and their volumes used for polymerase chain reaction (PCR) in order to detect mycoplasma. ..... 91
Table 8. The polymerase chain reaction (PCR) conditions used for mycoplasma detection. ..... 92
Table 9. Components and their volumes used in the PCR-based colony screening. ..... 92
Table 10. Conditions used for polymerase chain reaction (PCR)-based colony screening. ..... 93

# 1 Introduction

The research presented in this thesis provides the preliminary evidence that Werner helicase interacting protein 1 (WRNIP1) could be a component of the Fanconi anemia DNA repair pathway. Through the experimental work performed during the course of this doctoral study, it was possible to demonstrate that WRNIP1, indeed, could play a role in this pathway. This chapter introduces the fundamentals of DNA repair processes predominantly present in mammalian cells and places the Fanconi anemia pathway in their context. Moreover, a scientific background gathered to date and encompassing the information on WRNIP1's functions and structure is presented here.

## 1.1 DNA Damage Response

Genomes are constantly challenged by both endogenous and exogenous agents, which can cause DNA lesions capable of inhibiting replication or transcription and lead to a development of serious conditions such as cancer (Branzei and Foiani, 2008). For this reason, DNA lesions must be repaired effectively during all phases of cell cycle (Harper and Elledge, 2007). Therefore, organisms developed a set of sophisticated signal transduction and DNA repair mechanisms which are collectively known as a DNA damage response (DDR) (Jackson and Bartek, 2009). The DDR encompasses a variety of pathways which can repair DNA, e.g. homologous recombination, non-homologous end joining or Fanconi anemia pathway (Cohn and D'Andrea, 2008). The type of activated pathway depends on the type of lesion as well as the phase of the cell cycle. Interstrand crosslinks (ICLs) are one of the most deleterious lesions which could affect chromatin (Dronkert and Kanaar, 2001; Loper-Martinez *et al.*, 2016). Consequences of

ICL formation involve stalling of replication forks or inhibition of transcription (Wang, 2007). Therefore, a formation of such lesions requires efficiently acting repair pathways which could restore DNA to its original conformation and hence inhibit mutagenesis (Ceccaldi *et al.,* 2016).

### 1.1.1 DNA damage and associated diseases

The mutations in various genes associated with DNA repair can cause a plethora of genetic diseases (Ciccia and Elledge, 2010). Table 1 provides an overview of genes which protein products participate in various DNA repair pathways. The mutations in these genes give rise to genetic disorders which are listed below.

**Table 1. Human genetic diseases associated with defects in DNA repair pathways.**

(partially adapted from Kottemann and Smogorzewska (2013) and Ciccia and Elledge (2010)).

| Disorder | Mutated gene | Affected DNA repair pathway |
|---|---|---|
| Xeroderma pigmentosum | *XPA-G, POLH* | NER |
| Werner syndrome | *WRN* | HR, BER |
| Bloom syndrome | *BLM* | HR |
| Fanconi anemia | *FANCA-C. FANCD1, D2, FANCE-G, FANCI, J, L-N, RAD51C* | ICL repair, HR |
| Familial breast cancer | *ATM, BRCA1, BRCA2, BRIP1, CHK2, NBS1, PALB2, RAD50, RAD51C* | HR, damage signalling |
| Rothmund Thomson syndrome | *RECQL4* | BER, HR |
| Li-Fraumeni syndrome | *TP53* | DNA damage signalling, DSB repair |
| Nijmegen breakage syndrome | *NBS1* | Damage signalling, DSB repair, replication fork repair |
| Ataxia telangiectasia | *ATM* | Damage signalling, DSB repair, oxidative stress |
| Ligase IV syndrome | *LIG4* | NHEJ |
| Cockayne syndrome | *CSA, CSB, XPB, XPD, XPG* | TC-NER |

### 1.1.2 Homologous recombination repair pathway

Double-stand breaks are one of the most deleterious DNA lesions because they disrupt the continuity of the DNA helices and hence the integrity of chromosomes (van Gent *et al.,* 2001; Shiloh and Lehmann, 2004). Double-stand breaks can be created as a consequence of plethora of factors such as ionizing radiation, injury to DNA replication forks or endogenous reactive metabolites (Malkova and Haber, 2012). Therefore, the cells have developed mechanisms which serve to repair these types of breaks effectively. Double-stand breaks can be repaired through the action of two pathways, i.e. homologous recombination or non-homologous end joining (NHEJ) (Chapman *et al.,* 2012). The decision on which repair pathway should be employed depends on the phase of the cell cycle but not only (Aparicio *et al.,* 2014; Liu and Huang, 2016; Kakarougkas and Jeggo, 2014). 53BP1 and BRCA1 have been shown to play opposing roles in double-stand break repair, where BRCA1 promotes choice of homologous recombination, whereas 53BP1 facilitates non-homologous end joining (Daley *et al.,* 2015). Indeed, it was demonstrated that when BRCA1 is depleted from cells in S phase, 53BP1 is recruited. On the other hand, depletion of 53BP1 in G1 phase resulted in BRCA1 recruitment (Escribano-Diaz *et al*., 2013).

Homologous recombination pathway is known to function in the repair of double-strand breaks during S and G2 phases of the cell cycle (Branzei *et al.,* 2008). During these phases, the sister chromatids are available, thus providing reliable templates for the broken stands which could be repaired through a high-fidelity process resulting in error-free repair of DNA lesions (Sung and Klein, 2006). Therefore, homologous recombination is not a mutation-inducing process. The mechanism of action of

homologous recombination, when DNA lesion is caused by IR, involves sensing of double-strand breaks by meiotic recombination protein-11 (MRE11), RAD50 and Nijmegen breakage syndrome protein-1 (MRN) complex. MRE11 possesses both endonuclease and exonuclease activities (Paull and Gellert, 1998; Trujillo *et al.,* 1998; Trujillo and Sung, 2001) and together with RAD50, which contains ABC-ATPase domain, binds to DNA (Hopfner *et al.,* 2001; Tsubouchi and Ogawa, 1998; Furuse *et al.,* 1998). As opposed to MRE11 and RAD50, NBS1 lacks enzymatic activity. However, it is important for DNA binding and nuclease activity of MRE11 (Paull and Gellert, 1999; Williams *et al.,* 2009). MRN complex activates ATM kinase and recruits it to the double-strand break (Lee and Paull, 2005). The recruitment of inactive ATM dimers results in its activation by dissociation and autophosphorylation (Harper and Elledge, 2007). The activated ATM kinase participates in phosphorylation of histone variant H2AX at serine 139, resulting in γH2AX, which is regarded as a highly specific and sensitive molecular marker of DNA damage (Mah *et al.,* 2010). The mediator of DNA damage checkpoint 1 (MDC1) is then recruited to MRN complex and γH2AX which results in spreading of H2AX phosphorylation along damaged DNA (Zeman and Cimprich, 2014). ATM is also known to phosphorylate CHK2 kinase which leads to its activation (Ahn *et al.,* 2002; Oliver *et al.,* 2006; Cai *et al.,* 2009). Following phosphorylation, CHK2 acts on its substrates which are involved in cell cycle progression, apoptosis and gene transcription (Lukas *et al.,* 2003). Subsequently, the MRN complex, which is the ATM substrate *per se*, initiates the DNA resection (Ciccia and Elledge, 2010).

DNA resection is crucial for committing cells to the homologous recombination pathway as the resected DNA ends cannot be directly ligated via NHEJ machinery

(Dupré *et al*., 2008; Shibata *et al*., 2014). It has been shown that DNA end resection is a two-stage process (Zhu *et al*., 2008; Mimitou and Symington, 2008). The initial part of the resection is slow and is catalysed by MRN complex together with CtIP in human cells (Zhu *et al.,* 2008; Anand *et al.,* 2016). It is known that MRE11 component of MRN complex has exonuclease activity and is able to digest DNA with 3'-5' polarity (Paull and Gellert, 1998). However, this is in opposition to the double-strand break repair model according to which 3' ssDNA tails are generated by degradation of 5'-terminated DNA (White and Haber, 1990; Sun *et al.,* 1991; Zhu *et al.,* 2008). This paradox can be explained by the fact that MRE11 has also endonuclease activity on hairpin structures (Paull and Gellert, 1998; Trujillo *et al.,* 1998; Cannavo and Cejka, 2014). Therefore, MRE11 is able to make incisions through its endonuclease activity approximately 200−300 nucleotides away from the double-stand break and then MRE11 exonuclease degrades the DNA towards the DNA end with 3'-5' polarity (Gravel et al., 2008; Mimitou and Symington, 2008; Zhu et al., 2008; Shibata et al., 2014; Zakharyevich et al., 2010). MRE11 may be joined in the degradation of DNA by another exonuclease, i.e. EXD2, which digests DNA in 3'-5' direction as well. EXD2 has also been shown to interact with CtIP and its depletion sensitised cells to the DNA damage (Broderick *et al*., 2015). The reason why cells employ two exonucleases with the same polarity is unknown. However, it has been suggested that it might accelerate the double-stand break resection and ensure efficient generation of 3' ssDNA overhangs (Broderick *et al*., 2015). After the initial resection has taken place, the long-range resection commences. The creation of incisions by MRE11 makes space for the entry of resection machinery which digests DNA in 5'-3' direction away from double-stand breaks (Nimonkar *et al*., 2011; Mimtou and Symington, 2008; Niu *et al*., 2010; Anand

*et al*., 2016; Gravel *et al*., 2008). The long-range resection is attained by two machineries which consist of BLM−DNA2−RPA−MRN and EXO1−BLM−RPA−MRN (Nimonkar *et al*., 2011). The BLM−DNA2−RPA−MRN complex acts in an ATP-dependent manner. MRN complex recruits BLM helicase to the DNA which, in turn, unwinds the double helix. DNA2 exonuclease resects DNA and RPA enforces the cleavage in 5'-3' direction. The EXO1−BLM−RPA−MRN machinery acts by recruitment of EXO1 by MRN to DNA and utilising its exonuclease activity which works with 5'-3' polarity. BLM functions in enhancing the binding of EXO1 to DNA (Nimonkar *et al.,* 2011). It has also been demonstrated that DNA2 helicase/nuclease can act in long-range resection of DNA with conjunction with WRN helicase *in vivo* (Sturzenegger *et al.,* 2014; Pinto *et al.,* 2016). Both of these long-range resection mechanisms can resect thousands of nucleotides (Nimonkar et al., 2011). The 3' ssDNA overhangs which result from resection are coated by RPA. Subsequently, the RAD51 replaces RPA on ssDNA by a process mediated by BRCA2 (Sung and Klein, 2008). The RAD51-coated ssDNA invades the sister chromatid, which serve as a template for error-free repair of a double-strand break (Farmer *et al.,* 2005).

It is also worth noting that RPA-coated ssDNA overhangs can recruit ATR-interacting protein (ATRIP) together with its partner ATR, thus leading to activation of ATR (Cimprich and Cortez, 2008). As a consequence, RAD17/RFC2-5 complexes associate with the lesion and participate in loading of RAD9-RAD1-HUS1 (9-1-1) complex (Branzei and Foiani, 2008). 9-1-1 with topoisomerase-binding protein-1 (TopBP1) stimulates the ATR kinase activity which, in turn, phosphorylates CHK1. In this way, CHK1 can act in regulating the cell cycle delays in S and G2 phases (Sørensen *et al.*, 2005).

### 1.1.3 Non-homologous end joining

The alternative pathway which acts in repair of double-strand breaks is known as non-homologous end joining (NHEJ) (Chapman *et al.,* 2012). This type of repair does not require the presence of an intact sister chromatid which might be used as a template for damaged DNA. Instead, broken ends of DNA are directly ligated. Therefore, this type of repair is regarded as error-prone. As sister chromatid is not required for this pathway, NHEJ can function in all phases of the cell cycle (Liber, 2010; Daley *et al.*, 2015). The mechanism of action of NHEJ can be divided into three phases, i.e. double-strand break recognition, double-stand break processing and ligation (Yang *et al.,* 2016). The double-stand break recognition is performed by Ku70/80 heterodimer which has affinity towards various DNA molecules containing nicks (Mimori and Hardin, 1986; Voets *et al.*, 2004) and has a toroidal structure with a hole enabling the loading onto damaged DNA (Dolan *et al.,* 2013). In this way, Ku70/80 forms a complex with DNA which restricts the mobility of DNA and keeps both DNA ends in the vicinity to one another (Downs and Jackson, 2004). At the same time, the conformation of Ku70/80 changes in order for it to serve as a scaffold for downstream repair proteins (Yang *et al*., 2016). Subsequently, Ku70/80 recruits and activates DNA-PKcs (DNA-dependent protein kinase catalytic subunit) through C-terminus of Ku80 (Walker *et al*., 2001; Falck *et al*., 2005). The activated DNA-PKcs, in turn, phosphorylates a number of NHEJ proteins, e.g. ARTEMIS (Davis *et al*., 2014). DNA-PKcs can be phosphorylated itself in ATM-dependent manner, which helps in recruitment of ARTEMIS, whereas DNA-PKcs autophosphorylation leads to destabilisation of its interaction with DNA and enabling the ligation of DNA ends (Jiang *et al*., 2015). DNA-PKcs phosphorylates ARTEMIS at its C-terminus and induces its endonuclease activity (Ma *et al*., 2002). Moreover, it

recruits ARTEMIS to Ku/DNA. The newly formed DNA-PKcs-ARTEMIS complex is known to perform endonucleolytic cuts, thus processing complex double-strand breaks prior to ligation (Ma *et al*., 2005; De Ioannes *et al*., 2012). Moreover, the processing of complex double-stand breaks requires the stabilisation of DNA end alignment before ligation. For this reason, XRCC4 (X-ray cross-complementing protein 4), XLF (XRCC4-like factor) and PAXX are required (Yang *et al*., 2016; Ochi *et al*., 2015). It was shown that XLF and XRCC4 form filaments and it has been speculated that they play a role in facilitation of the ligation process. The newly identified PAXX was shown to bind Ku/DNA complex directly through its C-terminus. This novel component of the NHEJ pathway was demonstrated to act epistatically with XRCC4 and XLF in resolution of IR-induced genotoxic lesions (Ochi *et al*., 2015). After processing of DNA ends, the ligation process may commence. This is achieved by the XRCC4-XLF complex which brings LIG 4 to Ku-DNA-PKcs and stimulates its activity (Modesti *et al*., 1999; Lu *et al*., 2007).

### 1.1.4 Base excision repair

Base excision repair (BER) pathway is utilised by cells when removal of base mismatches as well as oxidised/reduced, alkylated or deaminated bases is necessary (Parsons and Dianov, 2013). These types of lesions usually result from action of reactive oxygen substances (ROS) or endogenous hydrolysis. The removal of damaged base(s) is achieved by the action of specific glycosylases which result in the formation of an abasic (AP) site. Depending on the number of removed bases, various molecular mechanisms are utilised (Petermann *et al.*, 2006). When one nucleotide needs to be

removed, i.e. short stretch, APE1 endonuclease is recruited and cleaves the phosphodiester bond 5' to the AP site. Subsequently, Pol β is recruited in order to fill in the lesion and the ligation by Lig3/XRCC1 follows. When 2-10 bases need to be removed, i.e. long stretch, the APE1 is also recruited. Afterwards the RFC/PCNA-Polδ/ε complex performs repair synthesis and nick translation. As the final steps, the FEN1 nuclease removes the flap structure and ligation is carried out by Ligase 1 (Parsons and Dianov, 2013).

### 1.1.5 Nucleotide excision repair

Nucleotide excision repair (NER) pathway plays a role is removal of bulky DNA adducts, such as cyclobutane pyrimidine dimmers (CPD) or 6-4 pyrimidine-pyrimidone photoproducts (6-4PPs) (Goodsell, 2001). This type of lesions can be caused by ultraviolet radiation and if left unrepaired they may result in a blockage of DNA polymerases. Moreover, NER is important in repair of endogenous DNA damage. Defects in this pathway may cause Xeroderma pigmentosum or Cockayne syndrome (Lehmann, A. R. 2003).

Depending on the type of DNA-damage detection mechanism, NER can be divided into global genome NER (GG-NER) or transcription-coupled NER (TC-NER) (Marteijn *et al*., 2013). The mechanism of lesion recognition in GG-NER scanning the genome and recognition of distortions with XPC, RAD23B, CENT2 together with UV-DDB proteins which function together in a complex (Shuck *et al.,* 2008). Following this step, XPG endonuclease either with or without TFIIH is recruited to the lesion. TFIIH helicase unwinds double-helix in the vicinity of the lesion in the complex with XPD, XPB and

XPA. Subsequently, RPA binds to the undamaged DNA strand and recruits XPF-ERCC1 heterodimer which, in turn, makes 5' incision to the lesion (Marteijn *et al*., 2013). The 3' incision is made by the activity of XPG. After DNA incision by XPF-ERCC1, PCNA is recruited onto DNA. PCNA recruits Pol δ, Pol κ or Pol ε in order to fill in the DNA gap. The process of DNA repair by NER is completed by ligation of DNA nicks with ligase 1 or ligase 3 (Moser *et al*., 2007).

### 1.1.6 Translesion synthesis

Translesion synthesis (TLS) pathway together with template-switch (TS) pathway constitute post-replication repair mechanisms (Mailand *et al*., 2013). Through these repair machineries, the cells are able to repair DNA lesions during replication in an error-prone manner (TLS) or error-free manner (template-switch). TLS employs non-replicative Y-family of DNA polymerases, namely: Pol η, Pol κ, Pol ι, Pol ξ or Rev1 (Ohmori *et al*., 2001). These, in turn, do not possess the 3'-5' proofreading activity as opposed to B family replicative polymerases (Sale *et al*., 2012). They also have the ability to bypass damaged DNA due to their less constrained active site, as compared with high-fidelity replicative DNA polymerases (Kim and D'Andrea, 2012).

The mechanism of TLS pathway involves monoubiquitination of PCNA at lysine 164 by the action of E2-ubiquitin conjugating enzyme, RAD6, and E3 ubiquitin ligase RAD18 (Sale *et al.*, 2012). PCNA is a polymerase processivity factor which serves as a moving platform in DNA synthesis (Moldovan *et al*., 2007). After the replication is arrested, the RAD6-RAD18 complex binds to RPA-coated ssDNA present at the DNA damage site (Kim and D'Andrea, 2012). Moreover, the RAD18 activity becomes

stimulated by this association. Following, the monoubiquitination of PCNA, TLS polymerases are recruited to the damage site and are able to bypass the lesion, thus preventing the replication fork collapse (Ulrich, 2009).

The alternative mechanism of damage tolerance is known as a template-switch. It encompasses the polyubiquitination of PCNA through an addition of K63-linked ubiquitin chains on PCNA which is already monoubiquitinated on lysine 164 (Cohn *et al.,* 2008). This ubiquitination is performed by the activity of E2-E3 complex: UBC13, MMS2 and RAD5 (Welchman *et al.,* 2005). The template-switch utilises the intact DNA on the newly synthesised sister chromatid as a template for the lesion bypass by temporary replacement of damaged DNA *via* fork reversal or D-loop formation, therefore resulting in the error-free repair process (Chang and Cimprich, 2009).

### 1.1.7 Fanconi anemia pathway

Fanconi anemia DNA repair pathway functions in the resolution of the interstrand crosslinks which form covalent bonds between two DNA strands, thus preventing replication or transcription (Ceccaldi *et al.,* 2016). The mechanism of action of this crucial DNA repair pathway is discussed in detail in the next section (see, 1.2 Fanconi anemia DNA repair pathway).

## 1.2 Fanconi anemia DNA repair pathway

### 1.2.1 Fanconi anemia background

Fanconi anemia (FA) is an autosomal and X-linked recessive disorder (Mirchandani and D'Andrea, 2006). It was first described by the Swiss paediatrician, Guido Fanconi in 1927, who depicted the condition based on a study of three brothers afflicted with this disease. Fanconi anemia is classified as a rare disease and its prevalence in population is 1 in 100,000 (Walden *et al*., 2014). Furthermore, clinical manifestations of Fanconi anemia include bone marrow failure, hearing impairment, limb deformities and susceptibility in development of leukaemias as well as solid tumours (Kim and D'Andrea 2011). Patients suffering from this disorder also exhibit sensitivity to various genotoxic agents, such as mitomycin C, diepoxybutane (DEB) or cisplatin (Walden *et al*., 2014). The rise in chromosome aberrations, proneness to deletions and increased G2/M arrest are common occurrences in patient-derived cells (Kee and D'Andrea, 2010). Mitomycin C and DEB are used in widely utilised diagnostic test for the Fanconi anemia (Kim and D'Andrea, 2011).

The mutations in FA genes are more prevalent in core complex proteins. 75% of mutations alone are present in FANCA and FANCC. Mutations in downstream proteins are less abundant. However, they result in more severe phenotypical manifestations (Walden *et al.,* 2014). This indicates the importance of the FA downstream effectors in maintaining the genome stability (Howlett *et al.,* 2002).

### 1.2.2 Molecular mechanism of the Fanconi anemia pathway

The FA pathway constitutes a crucial tool for resolving ICLs (Figure 1). 21 proteins have been identified so far as its components which are known to form at least three groups, i.e. core, FANCD2/FANCI and downstream effector proteins (Mamrak *et al.*, 2016).

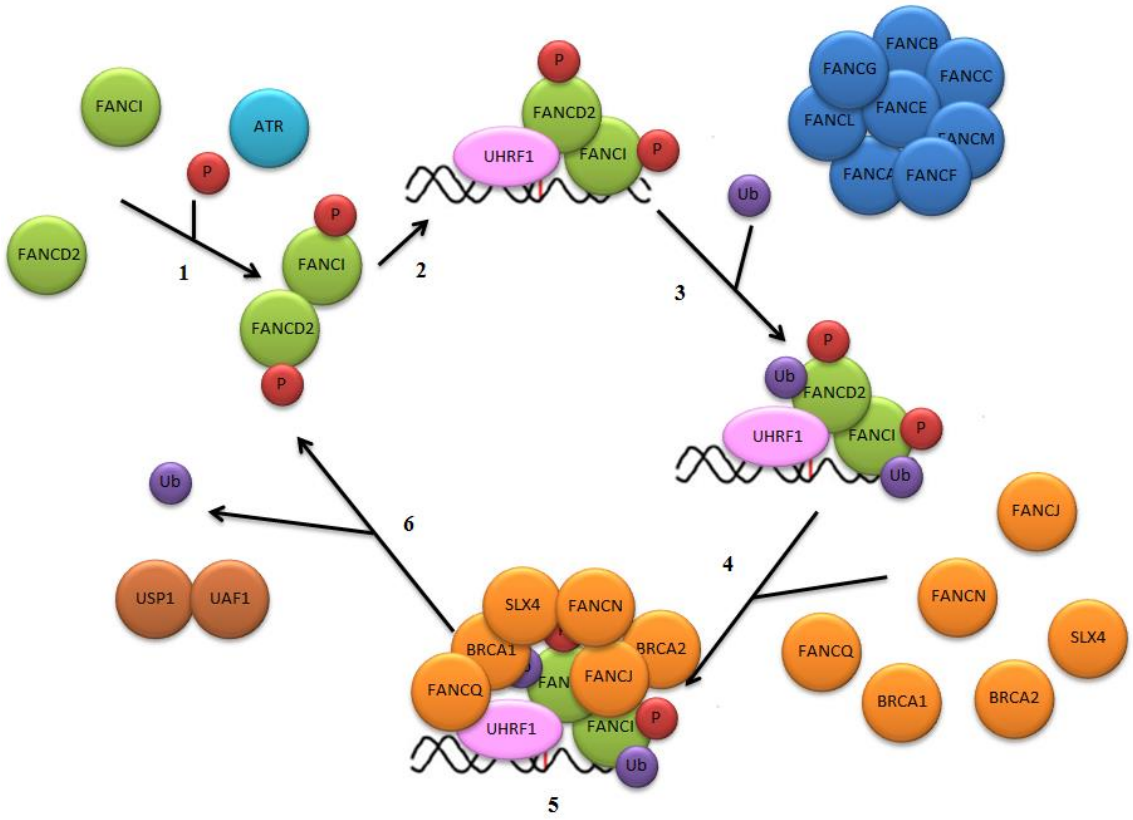



**Figure 1. Simplified diagrammatic representation of the Fanconi anemia ICL-repair pathway** 1) Phosphorylation of FANCD2 and FANCI by ATR. 2) Sensing of ICL by UHRF1 and localisation of FANCD2/FANCI complex to ICL. 3) Monoubiquitination of FANCD2 and FANCI at lysine 561 and lysine 523, respectively, by E3 ligase activity of FANCL. 4) Recruitment of downstream effector proteins to ICL. 5) Assembly of DNA repair machinery at the ICL. 6) Deubiquitination of FANCD2 and FANCI by USP1/UAF1 complex and disassembly of the DNA repair machinery. Not all known components of the Fanconi anemia pathway are included in this model.

The monoubiquitination of FANCD2 and FANCI is recognised as a hallmark of the Fanconi anemia pathway activation and platform for recruitment of proteins which resolve the ICLs (Cohn *et al.,* 2008; Kottemann and Smogorzewska, 2013). The core complex consists of eight proteins (FANCA, FANCB, FANCC, FANCE, FANCF, FANCG, FANCL, FANCM) and three Fanconi anemia-associated proteins (FAAP20, FAAP24 and FAAP100). Table 2 and Table 3 contain a complete list of Fanconi anemia and Fanconi anemia-associated, respectively. The function of core complex is to monoubiquitinate FANCD2 and FANCI by E3 ligase activity of FANCL (Meetei, *et al.,* 2004; Longerich *et al.,* 2009). The *in vitro* experiments demonstrated that FANCL alone is capable of FANCD2 monoubiquitination (Alpi *et al.,* 2008). Rajendra *et al*. (2014) successfully reconstituted whole core complex *in vitro* and identified the minimal subcomplex capable of FANCD2 monoubiquitination, i.e. FANCB, FANCL and FAAP100. The two remaining groupings within the context of the core complex were identified as: FANCA-FANCG and FANCC-FANCE-FANCF. The loss of any core complex component was shown to decrease the FANCD2 monoubiquitination. It was also demonstrated that monoubiquitinations of FANCD2 and FANCI are dependent on each other (Smogorzewska *et al.,* 2007).

The FANCD2/FANCI complex was shown to be multiphosphorylated by ATM and ATR kinases (Matsuoka *et al.,* 2007). The phosphorylation of FANCI was shown to influence the ubiquitination of FANCD2 (Ishiai *et al*., 2008). FANCD2 is known to be monoubiquitinated at lysine 561 and FANCI is monoubiquitinated at lysine 523. The monoubiquitination is regarded as an activation step of the FA pathway (Kottemann and Smogorzewska, 2013). However, it remains elusive how ubiquitin entities access both of these lysines as they have been shown to be buried within FANCD2/FANCI interface

(Joo *et al.* 2011). The crystal structure of murine FANCD2/FANCI complex, uncovered this surprising revelation. Therefore, it remains unclear how FANCL acting in accord with other core complex proteins would be capable of accessing these sites to be post-transcriptionally modified. It is probable that FANCD2/FANCI complex needs to undergone a conformational alteration in order to accommodate this critical post-translational modification. Alternatively, FANCD2 and FANCI would need to be monoubiquitinated before forming a complex, thus eliminating the problem of FANCL entry into the FANCD2/FANCI interface.

Based on the recent study the FANCD2/FANCI complex is first targeted to chromatin and undergoes ubiquitination later (Liang *et al.*, 2016). Subsequently, downstream effector proteins are recruited to the damage site where DNA is repaired (Kottemann and Smogorzewska, 2013). However, it remains elusive how FANCD2/FANCI complex is recruited to the damaged chromatin and how resolution of ICLs is performed (Cohn and D'Andrea, 2008). The recent study performed by Liang *et al*. (2015) shed some light on this issue by demonstrating that UHRF1 may act as a sensor of ICL and plays a role in recruitment of FANCD2 to the DNA damage site. However, there might be other factors involved in the recruitment of FANCD2/FANCI, either directly or indirectly, in response to the DNA damage. FANCM was also implicated in the recognition of ICLs. This 2,048 amino acid-long protein is known to possess two DNA binding domains which may facilitate that interaction (Walden *et al.*, 2014). Moreover, FANCM is known to localise constitutively to chromatin through FAAP10 (MHF2) and FAAP16 (MHF1) (Walden *et al*., 2014).

The monoubiquitinated FANCD2/FANCI complex helps to recruit downstream effector proteins which function in the unhooking of ICLs during S-phase of the cell cycle

(Knipsheer *et al*., 2009). FANCD1, FANCJ, FANCN, FANCO and FANCP are well-known downstream effector proteins and they function after monoubiquitination of FANCD2/FANCI. It was shown by *in vitro* analysis that two DNA forks are required to converge in order to trigger the ICL repair process (Zhang *et al.,* 2015). A single fork does not support the CMG dislocation, which is necessary to initiate the ICL resolution process (Zhang *et al.,* 2015). Therefore, the ICL-unhooking process involves two forks converging and pausing at -20 to -40 nucleotides (nt) before the ICL (Knipscheer *et al.*, 2009). BRCA1 promotes the unloading of CMG helicase (Long *et al.,* 2014). Subsequently, one leading strand approaches the site of damage and stalls at -1 nucleotides from the ICL. Following this, the incisions on the other parental strand are performed and they uncouple the ICL. The nucleases suggested to be involved in the ICL resolution include: MUS81-EME1, SLX1-SLX4, XPF-ERCC1, FAN1, SNM1A and SNM1B) (Zhang and Walter, 2014). XPF-ERCC1 was proposed to act as a primary 3' incision endonuclease as it shows preference for cutting at the 3' arm of a splayed arm structures and XPF depletion abrogates ICL repair (Klein Douwel *et al.*, 2014). XPF-ERCC1 itself contains ERCC4 endonuclease domain and a Helix-hairpin-Helix DNA binding domain and was shown to be recruited to ICLs by SLX4, which, in turn, is recruited to ICLs by FANCD2 (Yamamoto *et al.,* 2011; Klein Douwel *et al*., 2014). The endonuclease which makes the incision at the 5' side of ICL is currently being disputed (Zhang and Walter, 2014). It has been proposed that XFP-ERCC1 also makes an incision at the 5' side of the ICL, thus acting on both sides of the crosslink (Klein Douwel *et al.,* 2014). However, this function may also be fulfilled by an alternative DNA endonuclease. As SLX1 nuclease showed preference towards cutting 5' flap substrates, it was suggested that it could cut at the 5' side of the ICL (Zhang and Walter,

2014). Although, MUS81-EME1 prefers cutting at 3' flap structures, the mutations in MUS81-EME1 do not sensitise cells to ICL to the same extent as in the case of XPF-ERCC1 (Ciccia *et al.*, 2003; Ciccia *et al.*, 2008; Crossan *et al.*, 2011; Wang *et al.*, 2011). Moreover, the depletion of MUS81-EME1 did not result in abrogation of ICL repair as opposed to XPF depletion (Klein Douwel *et al.*, 2014). Therefore, MUS81-EME1 might play a secondary role in ICL unhooking process. SLX4 acts as a scaffold protein for the assembly of said nucleases (Svendsen *et al.*, 2009). Another endonuclease which might play a role in making incisions at the 5' side of ICL is Fanconi Associated Nuclease 1 (FAN1). FAN1 is recruited to DNA damage site by monoubiquitinated FANCD2 (MacKay *et al.*, 2010) and shows preference towards 5' flap structures as well as possesses exonuclease activity (MacKey *et al.*, 2010; Kratz *et al.*, 2010). However, the sensitivity of FAN1-depleted cells is not as pronounced as in the case of the *bone fide* Fanconi anemia pathway proteins (Trujillo *et al.*, 2012). Indeed, it has been shown that depletion of FAN1 does not abrogate ICL repair (Klein Douwel *et al.*, 2014). Therefore, it has been suggested that SLX 1 cleaves DNA on the 5' side of ICL and XPF-ERCC1 makes incision at the 3' side of ICL (Klein Douwel *et al.*, 2014) (Figure 2).

After successful unhooking of the crosslinked bases, the lesion bypass is conducted by insertion of nucleotide across the DNA damage site and the strand is extended in the TLS DNA polymerase REV1-polζ complex-dependent manner (Budzowska *et al.*, 2015; Ceccaldi *et al.*, 2016). The FA core complex regulates the recruitment of REV1-polζ (Budzowska *et al.*, 2015). Subsequently, monoubiquitinated FANCD2 recruits CtIP to the incision-generated double-stand break, where CtIP resects DNA together with MRN complex (Murina *et al.*, 2014; Unno *et al.*, 2014). The following long-range

resection of DNA is performed by BLM-DNA-RPA-MRN and EXO1-BLM-RPA-MRN machineries (Nimonkar *et al.*, 2011). The RAD51-coated ssDNA invades the sister chromatid and uses it as a template for error-free repair of double-stand break (Farmer *et al.*, 2005) Subsequently, SLX4-associated nucleases MUS81-EME1 and SLX1 resolve Holliday junctions (Garner *et al.*, 2013). The concluding step of ICL repair involves a removal the unhooked lesion, which is performed by nucleotide excision repair through yet undefined mechanism (Mouw and D'Andrea, 2014; Wood, 2010) (Figure 2 and 3).

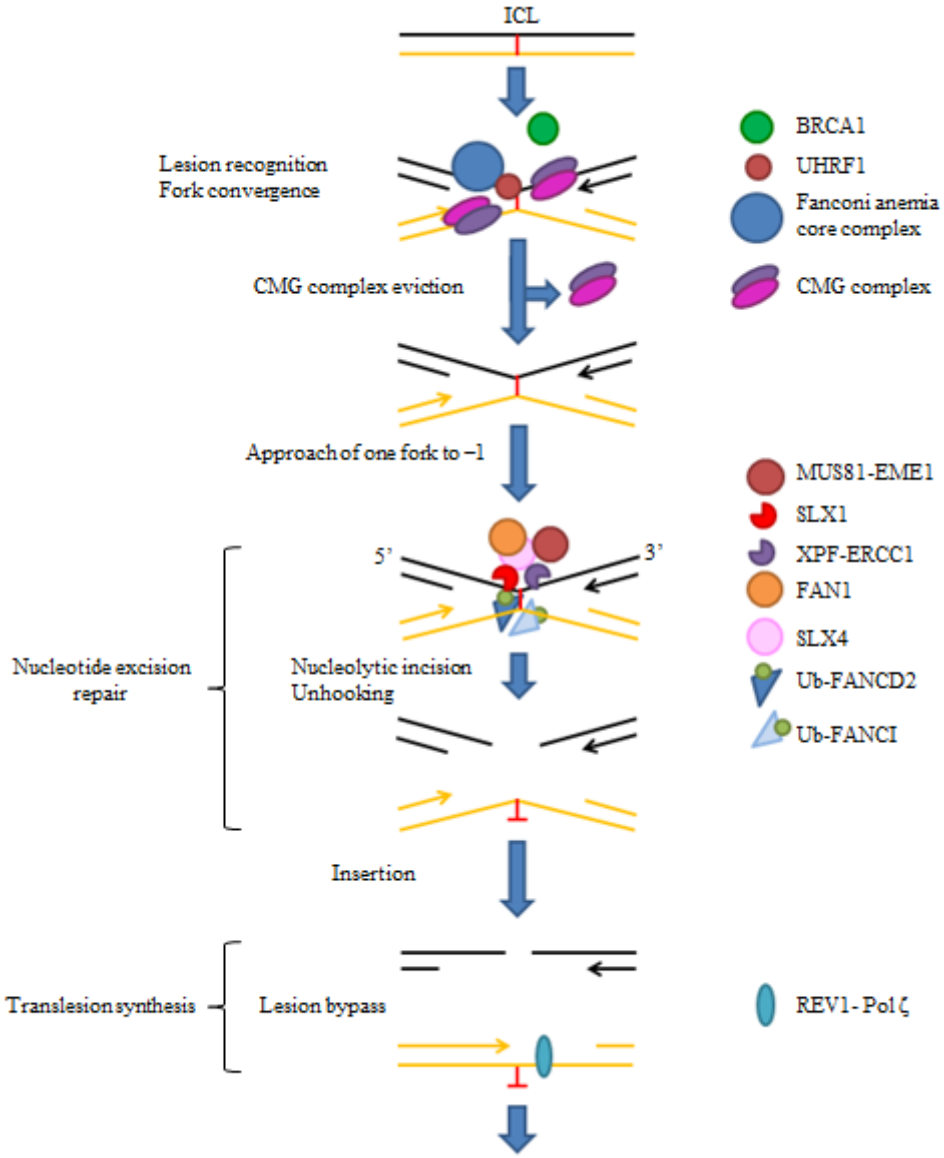



**Figure 2. Diagrammatic representation of the Fanconi anemia pathway-dependent mechanism of DNA ICL resolution during DNA replication and the proteins involved in this process (Part 1).** The graphical abstract is adapted from Knipscheer *et al.* (2009), Zhang and Walter (2014), Ceccaldi *et al*. (2016) and Lopez-Martinez *et al*. (2016).

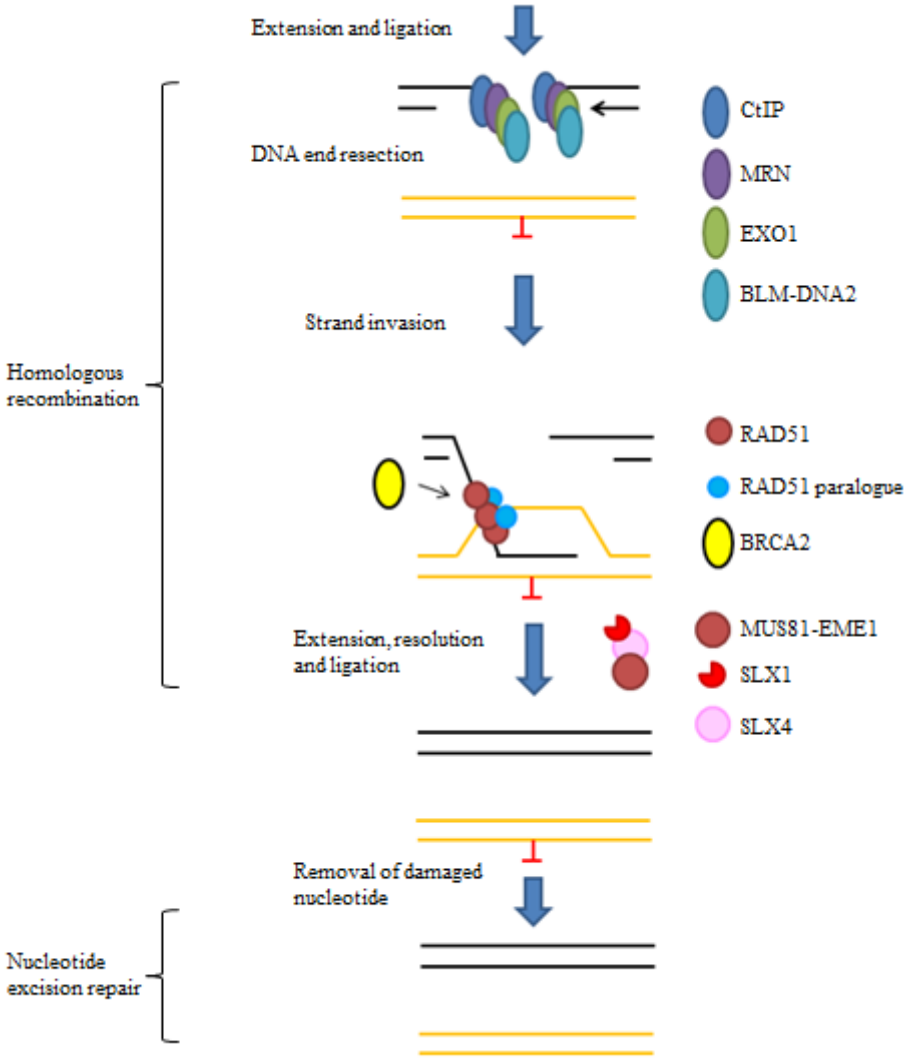



**Figure 3. Diagrammatic representation of the Fanconi anemia pathway-dependent mechanism of ICL resolution during DNA replication and the proteins involved in this process (Part 2).** The graphical abstract is adapted from Knipscheer *et al*. (2009), Zhang and Walter (2014), Ceccaldi *et al*. (2016) and Lopez-Martinez *et al*. (2016).

### 1.2.3 Ubiquitination and ubiquitin-binding domains in the Fanconi anemia pathway

Ubiquitination is a post-translational modification which plays various functions within the cell (Ulrich and Walden, 2010; Garner and Smogorzewska, 2011). Proteins can be monoubiquitinated when one 8.5 kDa ubiquitin binds to its target or multiubiquitinated when single ubiquitin molecules bind separately to the same protein. Furthermore, ubiquitin is also capable of forming versatile chains with itself (known as polyubiquitination) linked through the lysine residues which can also be attached to various protein targets (Garner and Smogorzewska, 2011). Ubiquitin it is best known for its role in targeting proteins for the 26S proteasome degradation after marking them with K48 chains. However, the ubiquitin modifications which are associated the most with DNA repair include: monoubiquitination or polyubiquitination through K63 chains (Ulrich and Walden, 2010).

Attachment of ubiquitin is a multienzyme process which requires three classes of proteins, i.e. E1 ubiquitin-activating enzymes, E2 ubiquitin-conjugating enzymes and E3 ubiquitin ligases (Huang and D'Andrea, 2006). Other proteins which participate in ubiquitin metabolism are deubiquitinating (DUB) enzymes and proteins containing ubiquitin binding domains or UBDs (Bish and Myers, 2007). In the Fanconi anemia pathway, monoubiquitination of FANCD2 and FANCI is of fundamental importance as it is regarded as an activation step of an ICL repair (Walden and Deans, 2014). The ubiquitination of these proteins is performed by UBE2T (FANCT) which acts as E2 and FANCL E3 ubiquitin ligase. It must be noted that deubiquitination of both of these proteins through the activity of USP1-UAF1 complex is also crucial as uncontained

ubiquitination leads to ineffective ICL resolution and increase in genomic instability (Kim and D'Andrea, 2012; Cohn *et al*., 2009).

There are more than 20 ubiquitin-binding domains which interact with various ubiquitin modifications (Dikic *et al.,* 2009). The interesting class of UBD are ubiquitin-binding zinc-finger domains or UBZs. Proteins which contain this type of functional conformation tend to participate in the FA or TLS DNA repair pathways (Kim and D'Andrea, 2012). Two types of UBZ domains are especially relevant for restoration of damaged DNA, namely: UBZ3 and UBZ4. UBZ3 is characterised by a conserved C2H2 motif, whereas UBZ4 contains C2HC conserved motif. Polymerase η, which participates in error-prone TLS DNA repair pathway, has UBZ3 domain (Crosetto *et al*., 2008). On the other hand, the FA proteins and FA-associated proteins such as FAN1, SLX4 or FAAP20 possess UBZ4 domain(s) (Kim and D'Andrea, 2012).

**Table 2. A list of genes mutated in Fanconi anemia patients.** This table has been partially adapted from Wang, A. T. and Smogorzewska, A. (2015), Ceccaldi *et al*. (2016) and Mamrak *et al.* (2016).

| Gene | Name | Protein function |
|---|---|---|
| FANCA | - | Subunit of FA core complex (Kupfer *et al*., 1999) |
| FANCB | - | Subunit of FA core complex (Fei *et al*., 2005) |
| FANCC | - | Subunit of FA core complex (Kupfer *et al*., 1997) |
| FANCD1 | BRCA2 | Functions in homologous recombination (Howlett *et al*., 2002) |
| FANCD2 | - | Forms heterodimeric complex with FANCI; monoubiquitinated by FANCL after DNA damage (Timmers *et al*., 2001) |
| FANCE | - | Subunit of FA core complex (Pace *et al*., 2002) |
| FANCF | - | Subunit of FA core complex (de Winter *et al*., 2000) |
| FANCG | - | Subunit of FA core complex (de Winter *et al*., 1998) |
| FANCI | - | Forms heterodimeric complex with FANCD2; monoubiquitinated by FANCL after DNA damage (Smogorzewska *et al*., 2007) |
| FANCJ | BRIP1 (BACH1) | 5'-3' helicase; functions in homologous recombination |
| FANCL | - | Subunit of FA core complex; E3 ubiquitin ligase (Meetei *et al*., 2004) |
| FANCM | - | Subunit of FA core complex; DNA translocase; important for ATR activation in ICL repair (Meetei *et al*., 2005) |
| FANCN | PALB2 | Functions in homologous recombination (Reid *et al*., 2007) |
| FANCO | RAD51C | Functions in homologous recombination (Vaz *et al.,* 2010) |
| FANCP | SLX4 (BTBD12) | Scaffold and coordinator for nucleases: XPF-ERCC1, MUS81-EME1/2, SLX1 (Stoepker *et al*., 2011) |
| FANCR | RAD51 | Functions in homologous recombination and fork stabilization (Wang *et al.,* 2015) |
| FANCQ | ERCC4 (XPF) | Associates with ERCC1 to form a SLX4-dependent ICL unhooking nuclease; participates in NER independently of SLX4 |

| | | |
|---|---|---|
| | | (Bogliolo *et al*., 2013) |
| FANCS | BRCA1 | Functions in homologous recombination; removes CDC45-MCM-GINS complex during ICL repair; inhibits NHEJ (Sawyer *et al.*, 2014) |
| FANCT | UBE2T | E2 ubiquitin-conjugating enzyme; works with FANCL (Rickman *et al.*, 2015) |
| FANCU | XRCC2 | Functions in homologous recombination and maintenance of genome integrity (Park *et al.*, 2016) |
| FANCV | REV7 (MAD2L2) | Functions in translesion synthesis (Bluteau *et al.*, 2016) |

**Table 3. A list of Fanconi anemia-associated genes.** This table has been partially adapted from Wang, A. T. and Smogorzewska, A. (2015) and Ceccaldi et al. (2016))

| Gene | Name | Protein function |
|---|---|---|
| FAAP100 | C17orf70 | Subunit of FA core complex (Ling *et al.*, 2007) |
| FAAP24 | C19orf40 | Subunit of FA core complex (Collis *et al*., 2008) |
| FAAP20 | C1orf86 | Subunit of FA core complex (Leung *et al.*, 2012) |
| FAAP16 | APTD1 (MHF1, CENPS) | Subunit of FA core complex (Singh *et al*., 2010) |
| FAAP10 | STRA13 (MHF2, CENPX) | Subunit of FA core complex (Yan *et al*., 2010) |
| FAN1 | (MTMR15, KIAA1018) | Nuclease; interacts with monoubiquitinated FANCD2 (Liu *et al*., 2010) |
| BOD1L | | Functions in RAD51 nucleofilament stabilization and fork stabilization (Higgs *et al.*, 2015) |
| UHRF1 | | Functions in lesion recognition (Liang *et al.*, 2015) |
| USP1 | | Functions in FANCD2/FANCI deubiquitylation (Nijman *et al.*, 2005) |
| UAF1 | | Functions in FANCD2/FANCI deubiquitylation (Cohn *et al.*, 2007) |

## 1.3 Werner helicase interacting protein 1 (WRNIP1)

### 1.3.1 Werner helicase interacting protein 1

Werner syndrome (WS) is a rare autosomal recessive disorder which results in a premature aging phenotype as well as genomic instability (Cox and Mason, 2013). The mutation in *WRN* was identified to be an underlying cause of WS. The protein product of *WRN*, Werner helicase, belongs to the RecQ family and is implicated in playing a role in DNA repair. In an effort to find WRN interacting partners, Kawabe *et al*. (2001) performed a study which led to identification of WHIP which was later renamed as WRNIP1. Werner helicase-interacting protein 1 (WRNIP1) was first identified as an interacting partner of mouse Werner helicase by yeast two-hybrid assay (Kawabe *et al*., 2001). The human WRNIP1 is a 665 amino acid long $AAA^+$ ATPase which is known to be highly conserved from *E. coli* to humans (Kawabe *et al*., 2001). The *Saccharomyces cerevisiae* orthologue of WRNIP1, Mgs1, has been identified by two independent studies (Kawabe *et al*., 2001 and Hishida *et al*., 2001) and it has been suggested to play a role in bypass of stalled replication forks. On the other hand, the role of WRNIP1 has remained elusive. WRNIP1 also shares homology with replication protein C (RFC) which functions as a clamp-loader (Nomura *et al*., 2012).

WRNIP1 is known to contain ubiquitin-binding zinc-finger (UBZ) domain at the N-terminus, ATPase domain in the middle of the protein and two leucine zippers at the C-terminus (Figure 4).

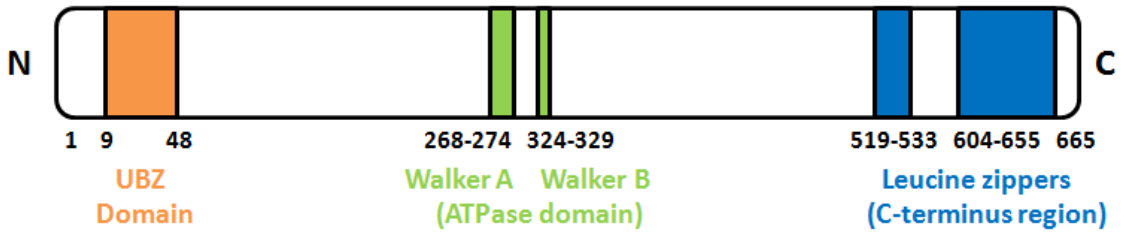



**Figure 4. Diagrammatic representation of the Werner helicase interacting protein 1 (WRNIP1).** Ubiquitin binding zinc finger domain (UBZ) is represented in orange, Walker A and Walker B motifs of ATPase domain are shown in green and two leucine zippers at the C-terminus of WRNIP1 are shown in blue. This diagrammatic representation is not to scale.

UBZ of WRNIP1 has been reported to bind both mono- and polyubiquitin (Crosetto *et al*., 2008), whereas Walker A motif of ATPase domain is responsible for interaction with WRN (Kawabe *et al*., 2006). Previous research has shown that WRNIP1 can interact with WRN, Rad18 (Yoshimura *et al.*, 2009) and DNA polymerase delta (Tsurimoto *et al*., 2005). In addition, WRNIP1's budding yeast orthologue (Mgs1) has been found to bind PCNA (Saugar *et al*., 2011). Mgs1 has been implicated in bypass of stalled replication forks (Saugar *et al*., 2011), whereas function of WRNIP1 remains elusive. It is known, however, that it can bind to forked DNA fragments which mimic stalled replication forks (Yoshimura *et al*., 2009). Moreover, it has been demonstrated that upon laser micro-irradiation WRNIP1 accumulates to the chromatin damage sites (Nomura *et al*., 2012).

### 1.3.2 Post-translational modifications of WRNIP1

Ubiquitination is a multienzyme process which plays a role in various DNA repair processes as well as it serves to target proteins for proteasome degradation (Ulrich *et al.*, 2010). This 8.5 kDa protein plays a role in signal amplification and recruitment of proteins to the DNA lesions (Dikic *et al.,* 2009). So far, various types of protein ubiquitination which have been identified, i.e. monoubiquitination, where one molecule of ubiquitin is conjugated to the substrate, multiubiquitination, during which several molecules of ubiquitin are attached to the substrate and finally polyubiquitination, where a few ubiquitin molecules form chains *via* lysines (Huang and D'Andrea, 2006). The polyubiquitin chains associated with targeting proteins for proteasomal degradation form through K48 lysine linkages. K29-linked polyubiquitin chains are also known to target substrates for proteasomal degradation (Bish *et al.*, 2008). Another type of ubiquitin chains is K63-linked polyubiquitin chains. This type of polyubiquitination is associated with DNA repair as well as inflammation (Ulrich and Walden, 2010). It is also known that K6-linked polyubiquitination leads to DNA repair signalling (Bish *et al.*, 2008).

WRNIP1 is known to have a ubiquitin zinc finger (UBZ) domain which is located at its N-terminal end. This type of domain has been identified so far to be associated with proteins which play roles in translesion synthesis and the Fanconi anemia DNA repair pathways, such as: RAD18, FAN1, polymerase η or polymerase κ (Hofmann, 2009). WRNIP1 was identified to bind polyubiquitin through its UBZ domain (Bish and Myers, 2007) as well as monoubiquitin (Crosetto *et al.*, 2008). It was also observed that WRNIP1 was monoubiquitinated, polyubiquitinated and sumoylated (Bish and Myers,

2007). The ubiquitination of WRNIP1 as well as its binding to ubiquitin were completely inhibited after deletion of UBZ domain or an introduction of D37A mutation in its UBZ domain (Bish and Myers, 2007; Bish *et al*., 2008). The aspartic acid residue of WRNIP1 (D37) is known to interact *via* noncovalent interactions with arginine residue (R42) of ubiquitin (Figure 5).

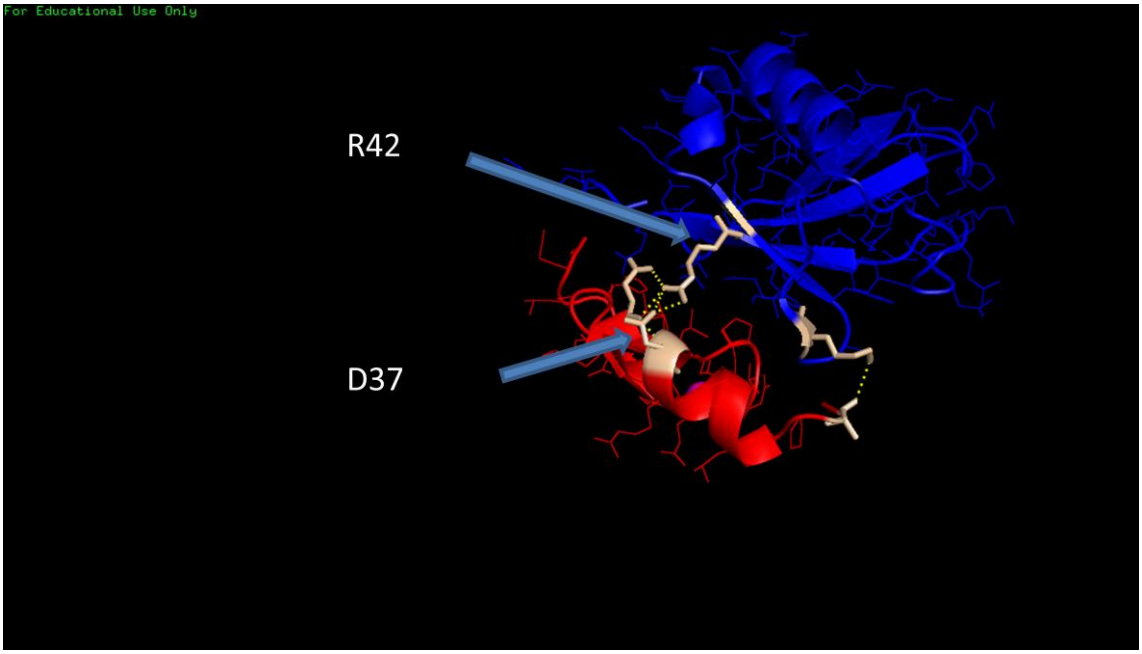



**Figure 5. Interactions between WRNIP1's UBZ domain and ubiquitin.** UBZ domain of WRNIP1 is indicated in red and ubiquitin is shown in blue. Aspartic acid residue (D37) of UBZ domain is shown to interact with arginine (R42) of ubiquitin. D37 and R42 are shown in white.

### 1.3.3 WRNIP1 and its interacting partners

WRNIP1 was identified as a binding partner of WRN by performance of yeast two-hybrid assay which demonstrated the interaction between mouse WRN and three other proteins: Ubc-9, SUMO-1 and WRNIP1 (Kawabe *et al*., 2001). The physical interaction between two proteins was confirmed in the same study. WRNIP1 was demonstrated to bind to WRN in a ATP-dependent manner. The interaction between WRNIP1 and WRN raised a question of a possibility of their interaction in the same pathway. However, a study by Kawabe *et al*. (2006) disproved this hypothesis. Furthermore, WRNIP1 was found to bind E3 ligase RAD18 which is known to play a role in a translesion synthesis pathway (Yoshimura *et al*., 2009). WRNIP1 was shown to bind three of four subunits of polymerase δ and stimulate its activity. Finally, WRNIP1 was shown to interact with polymerase eta. Most recently, WRNIP1 was demonstrated to interact with ATM cofactor – ATMIN (ATM Interactor) (Kanu *et al.*, 2015). WRNIP1 is also known to bind DNA in an ATP-dependent manner. It was shown to display the highest affinity towards forked DNA fragments which mimic stalled replication forks as well as short and long DNA fragments bound together which emulate template-primer pair (Kanamori *et al*., 2011).

### 1.3.4 WRNIP1's role in DNA repair

WRNIP1 was shown to interact with various types of DNA. The highest affinity was demonstrated by performance of EMSA experiments for DNA structures which mimicked the stalled replication forks as well as template-primer pair (Kanamori *et al*., 2011). Moreover, it was shown that WRNIP1 was binding three out of four subunits of

replicative polymerase δ and was able to stimulate its activity (Tsurimoto *et al*., 2005). The budding yeast orthologue of WRNIP1, Mgs1, was also shown to bind polymerase δ and was suggested to function in a bypass of stalled replication forks. Furthermore, WRNIP1 could interact with RAD6B-RAD18 complex and was able to interfere with binding of RAD18 to DNA (Yoshimura *et al*., 2009). RAD6B-RAD18 complex is known to be recruited to the stalled replication forks and act in monoubiquitination of PCNA which, in turn, functions in the recruitment of polymerase η to the site of DNA damage. Polymerase η was demonstrated to bind to WRNIP1 (Yuasa *et al*., 2006). Together with the ability of WRNIP1 to bind polymerase δ (Tsurimoto *et al*., 2005), these results suggested that WRNIP1 might play a role in translesion synthesis DNA repair pathway. According to that study the mechanism of WRNIP1's action would involve the recruitment of WRNIP1 by RAD18 E3 ligase to the stalled replication forks. There, WRNIP1 would be able to participate in polymerase exchange by replacing translesion synthesis polymerase for replicative polymerase δ. In this way, WRNIP1 could play a role in a restart of stalled replication forks, after the error-prone bypass of the DNA lesion. However, the mode of WRNIP1/Mgs1 recruitment to the sites of replication stress by RAD18 is not completely clear as it was shown that ubiquitinated PCNA targets Mgs1 to the DNA lesions (Saugar *et al.*, 2011).

Further evidence that WRNIP1 acts in DNA damage was provided by the study performed by Crosetto *et al.* (2008), where WRNIP1 was shown to form DNA repair foci after treatment of cells with various genotoxic agents which stall replication forks, i.e. UVC, topotecan or hydroxyurea. The appearance of WRNIP1 foci was limited to the nucleus and was independent of the cell cycle. However, the foci were mostly enlarged during S phase.

Most recently, WRNIP1 was shown to promote ATM signalling in response to replication stress with RAD18 and ATMIN (Kanu *et al*., 2015). In that study, it was demonstrated that WRNIP1 forms DNA damage foci upon introduction of replication stress by α and δ DNA polymerases inhibition with aphidicolin. The foci formation was shown to be dependent on monoubiquitination of PCNA by RAD18. In conclusion, WRNIP1 was suggested to act together with ATMIN and RAD18 in ATM signalling pathway which is activated by replication stress as opposed to ATM activation in response to introduction of DNA double-strand breaks and resolved by MRN (Kanu *et al.*, 2015).

A study performed by Nomura *et al*. (2012) demonstrated that WRNIP1 may also act in the repair of double-strand breaks. It was shown that WRNIP1 is recruited to the cells which were subjected to laser micro-irradiation without application of any other genotoxic agent. The laser introduced single-stranded and double-stranded DNA breaks. WRNIP1 was shown to accumulate to both types of DNA lesions, thus suggesting its role in the DNA repair.

The recruitment of WRNIP1 to the DNA damage sites was suggested to be led by its UBZ domain located at its N-terminus. Moreover, the appearance of WRNIP1 foci was also linked to both UBZ domain as well as its C-terminus, which contains two leucine zippers.

## 1.4 Possible interaction between FANCD2 and WRNIP1

As FANCD2 is a well-established member of the Fanconi anemia pathway and its monoubiquitination is a recognised signal of the Fanconi anemia pathway activation, proteins which might bind to monoubiquitinated FANCD2 were searched using mass spectrometry. In order to prepare samples for mass spectrometry, the Flag-tagged FANCD2 was expressed in HeLa cells (Chih-Chao Liang, Dr Martin Cohn's laboratory). After treatment of cells with MMC, the Flag-tagged FANCD2 was purified using α-Flag M2 agarose chromatography. The immunoprecipitate was analysed by mass spectrometry by the same method as described by Liang, C.-C. *et al.* (2015) resulting in 21 peptides from WRNIP1 protein (Chih-Chao Liang, Dr Martin Cohn's laboratory). WRNIP1 is known to have a UBZ domain which binds both mono- and polyubiquitin (Bish and Myers, 2007; Bish *et al.*, 2008). Proteins containing ubiquitin-binding zinc finger domains (UBZs) have been known to bind various ubiquitin chains (Dikic *et al*., 2009). Furthermore, proteins which have UBZ domains have been identified to be members of DNA repair mechanisms, i.e. Fanconi anemia pathway or translesion synthesis, such as FAN1, SLX4 or polymerase η (Jackson and Durocher, 2013). In the Fanconi anemia pathway, FAN1 is also known to interact with monoubiquitinated FANCD2 (Liu *et al.*, 2010). WRNIP1 is known to have a mono- and polyubiquitin-binding UBZ domain at its N-terminus. Moreover, it was implicated to localise into nuclear foci as a consequence of cell treatment with replication fork stalling agents (Crosetto *et al*., 2008). Finally, WRNIP1 accumulated at laser irradiation sites which introduced single- and double-strand DNA breaks. This result indicated that WRNIP1 might be involved in the DNA repair. The results of mass spectrometry experiment together with the outcomes of literature search, which proposed that

WRNIP1 is a ubiquitin-binding protein with possible DNA repair activity, led us to hypothesise that WRNIP1 might interact with either monoubiquitinated or non-uniquitinated FANCD2 and thus play a role in the Fanconi anemia pathway.

## 1.5 Aims of the thesis

WRNIP1 was identified through mass spectrometry as a possible binding partner of either monoubiquitinated FANCD2, non-ubiquitinated FANCD2 or proteins that interact with any of the aforementioned species under the conditions of genotoxic stress which are known to activate the Fanconi anemia pathway. The previous studies have suggested that WRNIP1 might play a role in the DNA repair and that it may interact with ubiquitinated proteins through its UBZ domain. Therefore, it has been hypothesised that WRNIP1 might have a yet unidentified function in the Fanconi anemia DNA repair pathway possibly via interaction with FANCD2. This interaction, if present, might occur through the UBZ domain of WRNIP1. As FANCI forms a heterodimeric complex with FANCD2, the possible interaction of WRNIP1 might also be extended to FANCI.

The specific aims of this project were as follows:

1. To determine whether WRNIP1-depleted cells replicate the sensitivity phenotype of cells lacking established Fanconi anemia pathway proteins when they are exposed to the conditions of ICL-inducing genotoxic stress.
2. To investigate whether there is a functional link between WRNIP1 and FANCD2 under the conditions of ICL-inducing genotoxic stress.
3. To investigate whether WRNIP1 is a binding partner of the established components of the Fanconi anemia pathway, i.e. FANCD2 and FANCI *in vitro* and, if interaction is established, identify the domains responsible for this interaction.

4. To examine the type of ubiquitin modification of WRNIP1 and to determine if ubiquitination pattern of WRNIP1is dependent on any of its domains.

Chapter 1 has provided the background information about the DNA repair machinery which is present in mammalian cells. The information on DNA repair pathways is introduced. This chapter discussed WRNIP1 and its possible functions.

Chapter 2 has provided information about materials used during the course of this doctoral study as well as described experimental methods used in this project.

Chapter 3 has addressed the first aim of the thesis by investigating whether WRNIP1's depletion from cells influences their survival. The deficiency of any *bone fide* Fanconi anemia protein is known to predispose cells to be more sensitive to crosslinking agents such as MMC and results in their diminished survival as compared to healthy cells. Hence, the clonogenic survival assays were performed to examine whether WRNIP1's deficiency from the cells influenced their sensitivity and, in this way, to examine if WRNIP1's depletion resulted in a similar phenotype to the deficiency of other *bona fide* Fanconi anemia proteins under the genotoxic conditions.

Chapter 4 has addressed more specifically the question whether WRNIP1's deficiency would result in a similar phenotype as deficiency of the established members of the Fanconi anemia pathway by determining if there was a functional link between WRNIP1 and FANCD2 (the second aim of the thesis). It is known that FANCD2 forms DNA repair foci under the conditions of ICL-inducing genotoxic stress, therefore any protein in the Fanconi anemia pathway, which acts upstream of FANCD2, might influence the formation of FANCD2 repair foci. Moreover, it was shown that the cells deficient in proteins acting in the Fanconi anemia pathway upstream of FANCD2

impact its ubiquitination levels. Therefore, drawing comparisons between WRNIP1-deficient cells and normal cells under ICL-inducing genotoxic stress could help in testing whether WRNIP1 has the same phenotype as other established Fanconi anemia proteins and whether there was a functional link between WRNIP1 and FANCD2. Moreover, comparing the ubiquitination levels of FANCD2 in healthy and WRNIP1-depleted cells under ICL-inducing genotoxic stress could also help in establishing a potential connection between WRNIP1 and the Fanconi anemia pathway by examining the functional link to FANCD2.

Chapter 5 has addressed the third aim of the thesis and attempted to answer the question of whether WRNIP1 could interact directly with non-ubiquitinated FANCD2. This chapter also investigated how various WRNIP1 deletion mutants influence binding with FANCD2 and tested the hypothesis that WRNIP1 might interact with FANCD2 through its UBZ domain. This chapter also investigated whether WRNIP1 could interact directly with non-ubiquitinated FANCI as well as an entire FANCD2/FANCI heterodimeric complex.

Having investigated the role of WRNIP1 in the Fanconi anemia pathway and its interactions with FANCD2 and FANCI *in vitro*, we decided to characterise WRNIP1's ubiquitination patterns in chapter 6 (the forth aim of the thesis). Ubiquitination is known to be important in signal transduction and the fate of ubiquitinated proteins is dependent on the type of ubiquitination linkage present. Therefore, we aimed to investigate whether WRNIP1 was modified by monoubiquitination that is associated with DNA repair, as opposed to ubiquitin linkages which target proteins for degradation by the proteasome. We closed this chapter by determining which domains influenced ubiquitination of WRNIP1.

Chapter 7 has discussed the experimental results obtained from this study and described the main conclusions.

Chapter 8 has provided information about the suggested future directions of the experimental work.

Chapter 9 has provided the research literature which was used during the course of this study.

# 2 Materials and Methods

## 2.1 Materials

### 2.1.1 Reagents and solvents

**Table 4. List of buffers and solutions used in this project.**

| Buffer/Solution Name | Buffer Composition |
|---|---|
| Mitomycin C (MMC) | 1 mg/ml (2.99 mM) in 50% EtOH |
| Cisplatin | 2.5 mg/ml in $H_2O$ |
| 4,5',8-trimethylpsolaren (TMP) | 1 mg/ml in DMSO |
| Basic Buffer | 150 mM KCl<br>10% glycerol<br>20 mM Tris-HCl pH 8.0<br>0.1% Tween-20<br>0.2 mM PMSF<br>2 mM β-ME |
| Transformation Buffer | 3.52 g PIPES<br>2.2 g $CaCl_2$-2x$H_2O$<br>18.67 g KCl<br>10.88 g $MnCl_2$<br>(17.11 g $MnCl_2 \cdot 4H_2O$) |
| CSK (Cytoskeletal) Buffer | 10 mM PIPES<br>300 mM sucrose<br>1 mM $MgCl_2$<br>1 mM EDTA<br>0.5% Triton X-100 |
| NTA Purification Binding Buffer | 150 mM KCl<br>10% glycerol<br>20 mM Tris-HCl pH 8.0<br>0.1% Tween-20<br>0.2 mM PMSF<br>2 mM β-ME<br>10 mM imidazole |
| NTA Purification Washing Buffer | 150 mM KCl<br>10% glycerol<br>20 mM Tris-HCl pH 8.0<br>0.1% Tween-20<br>0.2 mM PMSF<br>2 mM β-ME<br>20 mM imidazole |
| NTA Purification Elution Buffer | 150 mM KCl<br>10% glycerol<br>20 mM Tris-HCl pH 8.0 |

| | |
|---|---|
| | 0.1% Tween-20<br>0.2 mM PMSF<br>2 mM β-ME<br>250 mM imidazole |
| StrepTactin Elution Buffer | 150 mM KCl<br>10% glycerol<br>20 mM Tris-HCl pH 8.0<br>0.1% Tween-20<br>0.2 mM PMSF<br>2 mM β-ME<br>2.5 mM desthiobiotin |
| MiniPrep Solution I | 50 mM glucose<br>25 mM Tris·Cl pH 8.0<br>10 mM EDTA pH 8.0 |
| MiniPrep Solution II | 0.2 N NaOH<br>1% SDS |
| MiniPrep Solution III | 60 ml 5 M potassium acetate<br>11.5 glacial acetic acid<br>28.5 ml $H_2O$ |
| Buffer 1 (*in vivo* binding) | 20 mM Tris-HCl pH 8.0<br>0.5% Triton X-100<br>10% Glycerol<br>50 Unit/ml Benzonase (e.g. 2 µl benzonase per 1 ml Buffer)<br>2 mM MgCl2 |
| Buffer 2 (*in vivo* binding) | 20 mM Tris-HCl pH 8.0<br>0.5% Triton X-100<br>10% Glycerol<br>2 mM MgCl2<br>150 mM KCl |

The reagents and solvents used during the course of this doctoral study were purchased from Sigma-Aldrich unless indicated otherwise.

### 2.1.2 Cell lines and antibodies

The human cervical cancer cells (HeLa), *Spodoptera frugiperda* (Sf9) insect cells and Phoenix A cells were obtained from ATCC (American Type Culture Collection). Flp-in$^{TM}$ HeLa cells were purchased from Thermo Fisher Scientific. HeLa and Phoenix A cells were grown in DMEM (Sigma, D5796) supplemented with 2.5-10% foetal bovine serum (FBS). Sf9 cells were grown in Sf-900 medium (Thermo Fisher Scientific). The HeLa cells expressing an empty pSuper.retro vector (Clontech) were used throughout this study and were referred to as HeLa.pSuper. Stable HeLa cells expressing WRNIP1 knockdown and FANCD2 knockdown plasmids were generated by shRNA using the protocol described in Cohn *et al.*, 2007. HeLa FANCD2 knockdown cells were generated by Caroline Schneider (Dr Martin Cohn's laboratory). The shRNA-mediated knockdown of WRNIP1 or FANCD2 genes was attained by expressing the target sequence 5'-GCGCAGTTCTTTCGAATAA-3 (internal communication) and 5'-GAGCAAAGCCACTGAGGTA-3' (Liang C.-C. *et al.* 2015), respectively, in the pSuper.retro vector (Clontech). The obtained DNA plasmids were transfected with the use of FuGENE6 (Promega) according to the manufacturer's instructions. The knockout of WRNIP1 or FANCD2 from HeLa or Flp-in HeLa cells was carried out with the use of CRISPR/Cas9 nickase-based gene editing technology. In order to obtain HeLa WRNIP1 knockout or Flp-in HeLa WRNIP1 knockout cell lines, the targeting sequence used in the sgRNA was: 5'-GGCGAGTTGATGTGCGCGGC-3' and was targeting the first exon of WRNIP1 (Anna Socha, personal communication). HeLa WRNIP1 knockout and Flp-in HeLa WRNIP1 knockout were generated by annealing and introducing the following primers: 5'-CACCGGCGAGTTGATGTGCGCGGC-3' and

5'-AAACGCCGCGCACATCAACTCGCC-3' into the pX459 plasmid (Addgene #48139) through its BbsI site. HeLa and Flp-in HeLa cells were transfected with 2 µg of the resultant pX458 plasmid and selected with 4 µg/ml of puromycin after 24 h. The cells were plated at low density after another 24 h and clones were picked after 2 weeks. The clones were analyzed by Western blotting analysis (Anna Socha, Dr Martin Cohn's laboratory). Sequencing of the DNA from the resultant HeLa WRNIP1 knockout and Flp-in WRNIP1 knockout cell lines is ongoing (Anna Socha and Dr Martin Cohn, personal communication). In order to obtain HeLa FANCD2 knockout, the targeting sequence used in the sgRNA was: 5'-GTTTGTCTTGTGAGCGTCTGC-3' and was targeting the forth exon of FANCD2 (David Lopez-Martinez, personal communication). HeLa FANCD2 knockout was generated by annealing and introducing the following primers: 5'-CACCGTTTGTCTTGTGAGCGTCTGC-3' and 5'-AAACGCAGACGCTCACAAGACAAAC-3' into the pX459 plasmid through its BbsI site. HeLa cells were transfected with 2 µg of the resultant pX459 plasmid and selected with 4 µg/ml puromycin after 24 h. The cells were plated at low density after another 24 h and the clones were picked after 2 weeks. The clones were analyzed by Western blotting analysis (Liang C.-C. *et al.* 2016). Sequencing of the DNA from the resultant FANCD2 knockout cells is ongoing (David Lopez-Martinez and Dr Martin Cohn, personal communication). Primary antibodies used in this project were as follows: α-WRNIP1, 1:2000 dilution (sc-376438, Santa Cruz Biotechnology); α-FANCD2, 1:100 dilution (sc-20022, Santa Cruz Biotechnology); α-Lamin B, 1:1000 dilution (sc-6216, Santa Cruz Biotechnology); α-α-Tubulin, 1:2000 dilution (5829, Millipore); α-FANCI, 1:500 dilution (Ab74332, Abcam); α-HA, 1:1000 dilution

(11583816001, Roche); FK2, 1:1000 dilution (04-263, emdmillipore); FK1, 1:1000 (04-262, emdmillipore); and α-His, 1:1000 dilution (H1029, Sigma). Secondary antibodies used in this project were as follows: α-mouse (HRP-conjugated), 1:2000 dilution (NA9310V, GE Healthcare); α-rabbit (HRP-conjugated), 1:2000 dilution (NA934V, GE Healthcare); α-goat (HRP-conjugated), 1:2000 dilution (sc-2768, Santa Cruz Biotechnology); and α-mouse (Alexa Fluor 488), 1:2000 (A21202, Life Technologies).

2.1.3 Primers

**Table 5. Primers used in this project**

| Name | Sequence |
|---|---|
| WRNIP1 Reverse Transcription primer | 5’ – CAT CCT TCT GCT GTC GTG CCC – 3’ |
| WRNIP1 PCR primer | Forward:<br>5’ – AGTC GGATCC TA GAG GTG AGC GGG CCG GAA G – 3’<br>Reverse:<br>5’ – AGTC GTCGAC TCA GCA CCT CCT CTG CTT GAA G – 3’ |
| WRNIP1ΔUBZ primer (WRNIP1 UBZ domain deletion primer) | Forward:<br>5’ – CTG CTC CAC CCG GCG GG – 3’<br>Reverse:<br>5’ – GTG CAG CTG CGA AAG GAA GGG – 3’ |
| WRNIP1ΔATPase primer (WRNIP1 ATPase domain deletion primer) | Forward:<br>5’ – CTT GAG AAG CTT CCA GTA GAG GC – 3’<br>Reverse:<br>5’ – GGC CTT GCT CTG CCC GAA G – 3’ |
| WRNIP1ΔCterminus primer (WRNIP1 C-terminus deletion primer) | Forward:<br>5’ - CAG AGG AGG TGC TGA GTC GAC – 3’<br>Reverse:<br>5’ – CCG CAT GGA CTT GTG CAG GG – 3’ |
| WRNIP1ΔUBZ-ATPase primer (WRNIP1 UBZ domain to ATPase domain deletion primer) | Forward:<br>5’ – GCC GTG GGC CAG GAT ACC – 3’<br>Reverse:<br>5’ – CAG ACA GCG GTC CAG GTG C – 3’ |
| WRNIP1ΔATPase-Cterminus primer (WRNIP1 ATPase domain to C-terminus deletion primer) | Forward:<br>5’ – GGC TCA GAC CAG AAC GCC – 3’<br>Reverse:<br>5’ – AAG AAC AAT CAC TCG ACA GCG G – 3’ |

## 2.2 Methods

### 2.2.1 Cell survival (clonogenic) assay

6-well plates were used in this experiment. 200 cells were added to wells 1 and 2. 400 cells were added to wells 3 and 4. 2000 cells were added to wells 5 and 6. MMC (Sigma, M0440) was added to the wells in the following concentrations: 0 ng/ml ($1^{st}$ well), 1 ng/ml ($2^{nd}$ well), 2 ng/ml ($3^{rd}$ well), 4 ng/ml ($4^{th}$ well), 8 ng/ml ($5^{th}$ well) and 16 ng/ml ($6^{th}$ well). When cisplatin clonogenic assay was performed, the same cell numbers were added to the wells as during MMC treatment. Cisplatin (Sigma) was added to the wells in the following concentrations: 0 µM ($1^{st}$ well), 0.5 µM ($2^{nd}$ well), 1 µM ($3^{rd}$ well), 1.5 µM ($4^{th}$ well), 2 µM ($5^{th}$ well) and 4 µM ($6^{th}$ well). When TMP-UVA clonogenic assay was performed, 500 cells were added into each well and the cells were treated with 50 ng/ml TMP (Sigma) for 30 min and subsequently irradiated with indicated UVA dosages. After treatment with any ICL-inducing agent, the 6-well plates were left in the incubator for two weeks and medium was not changed during that time. After two weeks the 6-well plates were recovered from the incubator and were subsequently stained. In order to stain the colonies, the plates were placed on their lids. The medium was aspirated from all wells. Subsequently, PBS was added gently into each well in order to remove any remaining medium. PBS was aspirated and the cells were fixed in 10% MeOH/10% acetic acid/water for 10 minutes at RT. The plates were placed on the blue towels. The fixing solution was aspirated. The colonies were stained with 1% (w/v) crystal violet in methanol for 5 minutes. In the meantime, the plastic container was filled with tap water for washing the crystal violet off the plates. After 5-minute staining was finished, the crystal violet was poured off the plates. The plates were washed in the tap water from the container. The wash was repeated with a fresh

tap water. The plates were placed upside down in the heater to dry. After recovery from the heater, the colonies present in each well were counted and plotted as cell survival graphs.

### 2.2.2 Immunofluorescence microscopy (IF)

The cells were grown in the Petri dishes. The cells were washed with PBS. The cells were subjected to trypsinisation (with 1:5 trypsin/PBS dilution) from the Petri dishes and were the trypsin was neutralised with 2.5% FBS (Sigma, F7524) in DMEM (Sigma, D5796). Afterwards, the cells were transferred into the 15 cm Falcon tube and were spun down in the centrifuge at 1000 rpm for 5 minutes. Following the centrifugation, the medium was removed and the resultant pellet was resuspended in a new medium. Sterile round cover slips were washed in 70% (v/v) EtOH. The decontaminated cover slips were placed in wells of 24-well plates. The cover slips were not used until EtOH evaporated in the hood. Subsequently, the cells were subjected to counting as an optional step. The counting involved pipetting 10 µl of cells in the medium into the haemocytometer. The cell numbers were adjusted so that the cells reached 50-70% confluency the following day. Following the counting, 500 µl of the cells resuspended in the medium were loaded into each well of 24-well plate. The cells were inspected under the microscope. The cells were grown in the incubator overnight. The cells were recovered from the incubator the following day. The stock solution of MMC was recovered from the freezer and diluted with DMEM. The resultant MMC was added to the wells at the various time points to a final concentration of 160 ng/ml and were left in the incubator. The cells were recovered from the incubator and the medium was

removed from each well. The cells were washed once with 1 ml of room temperature PBS supplemented with 0.1% Tween-20. The cells were pre-extracted on ice with cold pre-extraction buffer (PBS supplemented with 1% Triton-X100) for 10 minutes. The cells were washed with room temperature PBS. The cells were fixed in 4% (w/v) of paraformaldehyde dissolved in PBS at room temperature for 10 minutes. After completion of fixing, the cells were washed three times for five minutes in PBS supplemented with 0.1% Tween-20 on a well-by-well basis, so the cells did not dry out. The cells were blocked with 5% BSA/PBS/0.1% sodium azide/0.1% Tween-20 for 1 h at room temperature. The parafilm was placed at the bottom of the transparent plate and was rubbed to its surface until it adhered to it. The round cover slips were recovered from the 24-well plates. The cover slips were leaned to the side in order to remove excess liquid. Care was taken not to touch the cover slips with a tissue in order to avoid cell detachment. Afterwards, the cover slips were placed upwards on the parafilm. A drop of primary antibody in 5% BSA/PBS/0.1% sodium azide/0.1% Tween-20 was placed on the cover slips containing cells. The cells were incubated overnight at 4°C in the fridge. The tissue was placed in the container as well in order to prevent cells from drying. The cover slips were recovered from the fridge and were washed five times on a rocker for five minutes with PBS/0.1% Tween-20 at room temperature. After washing, the cover slips were leaned to the side in order to remove excess PBS/0.1% Tween-20. Care was taken not to touch cells with a tissue in order to avoid their detachment. The round cover slips were placed on the parafilm. The drops of the secondary antibody (Alexa Fluor; 1:1000 dilution) in 5% BSA/PBS/0.1% sodium azide/0.1% Tween-20 were placed on the cover slips and were incubated at room temperature for one hour. From that moment on, the cover slips were kept under the foil. The cells were washed

five times on the rocker for five minutes with PBS/0.1% Tween-20 at room temperature. As an optional step, the cells were fixed with 4% (w/v) paraformaldehyde in PBS at room temperature. Subsequently, the cells were washed quickly three times in PBS/0.1% Tween-20 at room temperature. The cells in wells were stained with 0.5 µg/ml of DAPI for five minutes. The cover slips were taken from the wells with tweezers and were washed with MQ water. The round cover slips were placed on 7 µl of Vectashield drops (there was no DAPI in Vectashield) with the cells facing downwards. The cover slips were left in Vectashield for a few minutes in order to allow DAPI to stain the nuclei. Pressing the cover slips to remove excess Vectashield was avoided during that time. After incubation with Vectashield, the excess Vectashield was removed with a tissue. The round cover slips were sealed with a nail polish to a glass slides. The glass slides were stored in the fridge or were taken for an immunofluorescence analysis straightaway. The slides were protected from light at all times. Immunofluorescence imaging was conducted by DeltaVision System installed with Resolve 3D SoftWoRx-Acquire Version 4.0.0. 60X optic objective (Olympus 60X/1.42, PlanApo, N) was used for the experiments and the images were captured by the camera (CoolSNAP_HQ/ICX285).

### 2.2.3 Cell transformation

The competent TOP10 cells were taken from the freezer. The cells were transformed by addition of 1 µl pFastBac1-SHT plasmid DNA to 20-100 µl previously prepared competent cells. The cells were heat-shocked at 42°C for 45 seconds. The cells were cooled down on ice for 5-10 minutes. 400 µl of chilled and sterile LB was added to the cells (LB was poured under the flame to avoid contamination). The cells were incubated

at 37°C on a shaker for 30-60 min. Subsequently, the cells were spun down at 3000 rpm for one minute. After spinning, 300 µl of supernatant was discarded and the cells were resuspended in the remaining 200 µl. The serial dilutions were made (1 original concentration and 2 dilutions). The cells were plated on the LB agar plates and incubated at 37°C overnight. After recovery of plates from the incubator, a few colonies were picked and each colony was transferred into a 15 ml tube containing 3 ml LB supplemented with antibiotic(s). The tubes containing colonies were incubated at 37°C overnight.

### 2.2.4 Restriction enzyme digestion

The restriction enzyme digestion mixture was prepared in a 1.5 ml Eppendorf tube. All the reaction components were kept on ice. The 50 µl restriction enzyme reaction was prepared. Two restriction enzyme mixtures were made: one for cutting insert and one for cutting vector. 1 µg of insert DNA (or 2 µg of vector) were added to the mixture. Subsequently, 5 µl of 10X NEBuffer 3 was added. BSA was added so that its final concentration in the mixture was 100 µg/ml. The water was added to the mixture. 1 µl of each restriction enzyme (equivalent of 10 units) was added to the mixture as the last component. The components were mixed together by pipetting up and down or by flicking the reaction tube. The components were not vortexed. The tube was spun down quickly in the centrifuge. Afterwards, the reaction mixture was incubated at 37°C for 1 h. The restriction enzymes were inactivated at 65°C for 20 minutes on the heating block if necessary.

### 2.2.5 Plasmid fragment dephosphorylation

Add 10X NEBuffer 3 (0.5 µg/10 µl) to the digested DNA, so that buffer's final concentration is 1X. Add 0.5 units of CIP/µg vector DNA. Incubate the reaction mixture at 37°C for 1 h. Inactivate CIP by adding 500 mM EDTA to a final concentration of 10 mM. Remove CIP from dephosphorylated ends of DNA by heat-treatment at 65°C for 20 min.

### 2.2.6 Ligation

The ligation reaction was set up on ice in the 1.5 ml Eppendorf tube. Vector DNA as well as insert DNA were added, so that the vector-to-insert ratio was 1:3. If 20 µl ligation reaction was used, 2 µl of 10X T4 DNA ligase buffer was added. The T4 ligase buffer was thawed and resuspended first at room temperature. Moreover, nuclease-free water was applied in order to top up the reaction volume to 20 µl. 1 µl of T4 ligase was added as a last to the reaction mixture. After addition of all the aforementioned components, the ligation reaction was mixed by pipetting up and down. Moreover, the reaction was briefly centrifuged. Finally, the reaction was incubated at 16°C overnight in the waterbath. The ligation reaction was recovered the following day from the waterbath and 20 µl of reaction were used to transform 200 µl of competent cells.

### 2.2.7 *In vitro* binding assay

Flag-HA-FANCD2 in Flag peptide eluate and His-Strep(II)-WRNIP1 in desthiobiotin eluate were used in this experiment. 0.1 µg to 0.8 µg of WRNIP1 and FANCD2 were combined in the Eppendorf tube. FANCD2, WRNIP1, 1 µl BSA and binding buffer

(150 mM KCl, 20 mM Tris-HCl pH 8.0, 0.2 mM PMSF, 2 mM β-ME) were added to the Eppendorf to the final volume of 10 µl. The sample was mixed by vortexing and brief spinning. 1 µl from each Eppendorf was taken for WB analysis. The sample was incubated at 4°C or 30°C (depending on the experiment) for one hour. Afterwards, Tween-20 was added to the binding buffer to the final concentration of 0.1% (v/v). α-HA bead slurry was recovered from the fridge and the beads were washed two times in binding buffer/0.1% Tween-20 at 2000 rpm for five minutes. 10 µl of α-HA bead slurry was added into each Eppendorf tube. The samples were vortexed gently and spun down quickly. The Eppendorfs were incubated for half an hour on the rotor in the cold room. Following half hour incubation, the Eppendorfs were recovered from the cold room and all the contents were added to the purification column. 0.5 ml of binding buffer with 0.1% (v/v) Tween-20 was added into each Eppendorf. The Eppendorf tubes were placed in the centrifuge and spun down for a few seconds. The washing was repeated five more times. After finished washing, 50 µl of 1X loading buffer were added to the column. The column was span down at 1000 rpm for 2 min. The samples were heated at 70°C for 10 min. The samples were analysed on WB with α-WRNIP1 and α-FANCD2 antibodies.

### 2.2.8 Fractionation of HeLa cells (Intact nuclei method)

The cells were plated in 15 cm dishes and were grown until they reached confluency. The cells were scraped off with the spatula and were pipetted into 50 ml Falcon tube. Afterwards, the cells were spun at 3000 rpm for 5 minutes in order to remove the medium. The resultant cell pellet was resuspended in 1 ml cold PBS. The cells were spun down at 3000 rpm for five minutes in order to remove the supernatant. The

hypotonic buffer was taken from the fridge, poured into Falcon tube and supplemented with PMSF and β-ME to the final concentrations of 0.2 mM PMSF and 2 mM β-ME respectively. The pellet was resuspended in 1 ml hypotonic buffer in order to wash the cells. The cells were spun down at 3000 rpm for 5 minutes and the supernatant was discarded. The cell pellet was resuspended in twice pellet volume of hypotonic buffer. Subsequently, the suspension was incubated on ice for 10 min. 5 µl of cells were taken and placed on a glass slide for analysis on a microscope. The other cells were transferred to the glass press and were homogenised by pressing 30 times. 5 µl of homogenised cells were transferred with a loading tip and placed on the glass slide for analysis. Both samples covered with the cover slips. The homogenised sample should have contained round nuclei separated from cytoplasm. The homogenised cells were taken out of the glass press with a loading tip and transferred to a new Eppendorf tube. The press and pestle were washed with deionised or MQ water. The tubes were spun at 4000 rpm for 15 minutes. The resultant supernatant represented cytoplasmic and plasma membrane fraction of the cell. The pellet was representing the nuclear fraction. The pellet sample was prepared for WB with benzonase as done previously. The cytoplasmic fraction was transferred to a new tube and 11% of the volume of the cytoplasmic fraction was added to it as 10X S-100 buffer. Both nuclear and cytoplasmic factions were vortexed and spun down. The WB samples were prepared. The WB sample of cytoplasmic fraction was prepared by making an assumption that nuclei to cytoplasm ratio was 1:1.

### 2.2.9 Fractionation of HeLa cells

The HeLa (HeLa.pSuper) cells were plated in the 9 cm dishes and grew over night to confluency. The following day, MMC was added to the final concentration of 160 ng/ml at 0h, 3h, 6h and 9h time intervals. The cells were recovered from the incubator. The cells were scraped off with a spatula. The cells in the medium were transferred to the 15 ml Falcon. The cells were spun down at 1000 rpm for 5 minutes. The medium was removed from the Falcon tube, leaving the cell pellet at the bottom of the tube. The cells were resuspended in 1 ml cold PBS and were moved into 1.5 ml Eppendorf tube. The sample was kept on ice from that moment on. Afterwards, the cells were spun down for 10 seconds at maximum speed. 900 µl of PBS was removed from the Eppendorf and fresh 900 µl of cold PBS was added to the tube. The cells were spun down again for 10 seconds at maximum speed. The PBS was aspirated from the Eppendorf, so that only cell pellet was left. The volume of the pellet was estimated. Five times the volume of the pellet of CSK buffer containing 0.5% (v/v) Triton was added to the Eppendorf tube. The cell pellet was resuspended by pipetting up and down. In order to ensure complete resuspension of the pellet, the cells were vortexed briefly. Afterwards, the resuspended pellet was kept on ice for 10 minutes. The cells were spun down at 3000 g for 5 minutes. The supernatant was carefully transferred into another tube and it was spun down for 1 min at maximum speed. The resultant supernatant was gently transferred again into another tube. Care was taken not to mix any cell pellet with the supernatant. This supernatant constituted a cytoplasmic fraction of the cells. 1 µl of the cytoplasmic fraction was mixed at this point with 1 ml of Bradford solution and the protein concentration was measured by spectrophotometer. Afterwards, the volume of the pellet, which remained in the original Eppendorf tube, was estimated. 1 µl of benzonase

was mixed with 100 µl benzonase buffer in an alternative Eppendorf tube. The equal volume of benzonase buffer containing benzonase was added to the pellet. The pellet was resuspended in the benzonase buffer by pipetting and vortexing. The resultant suspension was kept on ice for 10 minutes. Afterwards, 2% (v/v) SDS was added to the suspension. The volume of added SDS was equal to the volume of cell pellet resuspended in the benzonase buffer. The resultant solution was pipetted and vortexed. Following the mixing, the sample was heated up at 70°C for 10 minutes on the heating block. After recovering the Eppendorf tube from the heating block, the sample was spun down in the room temperature centrifuge at maximum speed for 1 minute in order to avoid any SDS precipitation. If any pellet was visible at this point, the sample was vortexed again and the heating was repeated. The sample was kept at room temperature from now on. The sample was vortexed well and 1 µl was taken for the Bradford assay analysis, where 1 µl sample was mixed with 1 ml of Bradford solution. The vortexing of the sample was optional. The tube was inverted several times. The absorbance of the sample was measured with the spectrophotometer and the protein concentration of the sample was calculated. Following the calculations, the supernatant, LDS and reducing agent were mixed together in an Eppendorf tube by pipetting, vortexing and briefly spinning down in the centrifuge. Finally, the sample was heated at 70°C for 10 minutes. The sample was either used straightaway for the Western blotting analysis or stored in the freezer.

### 2.2.10 Reverse transcription reaction

All the reaction components were thawed on ice. The reagents were centrifuged briefly before the experiment was started. The concentration of total RNA was measured. All the reagents: 1.4 µl of total RNA (equivalent of 1 µg), 4 µl (concentration of 10 µM) and 7.6 µl water were mixed in the Eppendorf tube. Two additional reactions were prepared as negative the controls: the first without reverse transcriptase, the second without cDNA. The samples were incubated at 65°C for 10 minutes. The reaction mixtures were cooled down on ice for 2 min. Subsequently, 4 µl of reverse transcriptase buffer (5X concentrated), 2 µl (concentration of 10 mM) dNTP, 0.5 µl RNase inhibitor and 0.5 µl reverse transcriptase were added. The reaction components were mixed by vortexing and the tube was spun down briefly in the centrifuge. Afterwards, the sample was incubated at 55°C for 1 h. After recovery of the sample, the reverse transcriptase was inactivated by heating to 85°C for 5 min. The tube was placed on ice. The tube was stored at 2-8°C for 1-2 h or at -15− -25°C for longer periods. The resultant cDNA was used directly for PCR.

### 2.2.11 Polymerase chain reaction (PCR)

The reagents were added to the thin-walled PCR tube. The total volume in the tube was 50 µl. First, water was mixed with 1.5 µl (100%) DMSO at room temperature to avoid crystallisation of DMSO. After, careful mixing by pipetting up and down, the remaining components were added, i.e. 2 µl DNA template, 2 µl forward and 2 µl reverse primers (both at 10 µM concentration), 1.25 µl of 10 mM dNTP, 5 µl of 10X buffer, 2 µl of 10 mM $MgSO_4$. 1 µl Pfu polymerase was added last to the reaction mixture. The PCR

reaction mixture was pipetted up and down followed by quick vortexing and spinning down to ensure that all the reaction components were at the bottom of the PCR. The Thermocycler was switched on and the PCR tubes were placed inside after the temperature was reached 90°C in order to ensure a hot start. The PCR tubes were placed in the Thermocycler and set the cycles as indicated. The number of cycles and temperatures were changed depending on the experiment.

**Table 6 The example of conditions applied during Polymerase Chain Reaction (PCR).**

| Time [s] | Temperature [°C] | No. of cycles |
|---|---|---|
| 60 | 95 | 1 |
| 30 | 95 | 35 |
| 30 | 62 | 35 |
| 300 | 68 | 35 |
| 300 | 68 | 1 |
| ∞ | 4 | 1 |

The PCR tubes were recovered from the Thermocycler. The resultant PCR samples were prepared to be run on an agarose gel by mixing, e.g. 5 µl of PCR sample with 6X BPB solution. The DNA fragments were run on an 1% agarose gel (50 ml 1X TBE buffer supplemented with 2.5 µl ethidium bromide) to check whether PCR reaction was successful.

### 2.2.12 Lysis of the Sf9 insect cells

The Sf9 insect cells infected with 10 µl of P2 baculovirus were recovered from an incubator. The virus-containing supernatants were pipetted into the Eppendorf tubes. The tubes were spun down at 3000 rpm for five min in order to remove any remaining cells. The supernatants were transferred into the fresh tubes and FBS was added to the

final concentration of 2%. Three 1.5 ml tubes of virus-containing supernatants were frozen in liquid nitrogen and were kept in the freezer for the future use. The remaining virus-containing supernatant was either kept in the fridge for more immediate use. 15 cm plates were taken and Sf9 insect cells were seeded in them to near confluency. The cells were mixed with medium in a Falcon tube in order to achieve an even distribution of cells in the dish. The cells were allowed to adhere by being left in the flow-bench for five minutes. 50 µl of baculovirus was added into each plate and mixed well by rocking the plate. The dishes were incubated at 27°C for two (or three) days. The dishes were taken from the incubator and medium was aspirated from each plate. The cells were washed with room temperature PBS carefully. Each dish was tilted in order to aspirate PBS. PBS was aspirated from the dishes on a one-by-one basis and PBS was left in the dishes while aspirating PBS from the previous ones in order not to allow cell to dry out. One dish at a time was placed on ice and 3 ml of previously prepared lysis buffer were added into each dish. The cells were scraped off with a spatula and were pipetted into 15 ml Falcon tube. The Falcon tube was kept on ice. The lysis for two remaining dishes was repeated and the cells were pipetted into the same 15 ml Falcon. The Falcon tube containing the cell lysates was incubated on ice for 15 minutes. The Falcon tube was inverted up and down several times during the incubation period. After incubation, the resultant cell lysate was transferred into 2 ml Eppendorf tubes. The cells were centrifuged at maximum speed for 10 minutes. The supernatant was transferred into the fresh Eppendorf tubes and was spun down again for 10 minutes. The supernatants were pooled together in a fresh 15 ml Falcon tube. The supernatants were used for purification of proteins straightaway or were snap frozen in liquid nitrogen and stored in -80°C freezer.

### 2.2.13 Western blot (WB) sample preparation

The cells were grown in 9 $cm^2$ plates in an incubator overnight. Afterwards, the cells were scraped off into the medium with a clean spatula. The medium with the scraped off cells was transferred to a Falcon tube. The cells were span down at 1000 rpm for five minutes. The medium off was taken off from the Falcon tube. The cells were washed with 1 ml cold PBS and the sample was kept on ice from this moment on. The cells were transferred into an Eppendorf tube and were spun down at 10,000 rpm for 10 seconds in the centrifuge. 900 µl of PBS was taken out from the Eppendorf. The sample was spun down at 10,000 rpm for 10 s. PBS was aspirated. The volume of the pellet was estimated and an equal volume of benzonase buffer with benzonase was added. The cells were resuspended completely by pipetting and vortexing. The sample was placed on ice for 10 minutes. 2% SDS was added to the cell pellet with benzonase, so that the SDS volume was equal to that of cell pellet combined with benzonase buffer. The sample was vortexed briefly. The sample was heated at 70°C for 10 minutes on the heating block. After recovering the tube from the heating block, the sample was spun down in the room temperature centrifuge at maximum speed for 1 min. If any pellet remained visible at that stage of a sample preparation, the sample was vortexed and heated again. The sample was kept at room temperature from this moment on. The 2 µl of the resultant sample were mixed with 40 µl water. The sample was vortexed well. 21 µl of the sample were removed from the Eppendorf tube, so that only 21 µl remained. 1 ml of 1X Bradford solution was added into the Eppendorf. The tube was inverted several times in order to mix all the components. The concentration of the sample was measured on the spectrophotometer. The previously prepared sample was mixed with NuPAGE LDS sample buffer and NuPAGE sample reducing agent (Thermo Fisher

Scientific). The sample was heated at 70°C for 10 minutes. The resultant sample was used for Western blotting straight away or was stored in the freezer.

### 2.2.14 Transformation of cells

10 µl ligase reaction was added to an Eppendorf tube containing 100 µl competent TOP10 cells. The tube was flicked several times in order to ensure that the components were well mixed. The tube was incubated on watery ice for 30 minutes. Subsequently, the cells were subjected to heat-shock at 42°C for 45 seconds. Afterwards, the tube was cooled on ice for two minutes. Subsequently, 90 µl LB medium was added to the tube. The resultant cells in LB medium were pipetted out from the tube on a LB-agar plate under the flame. The cells were spread evenly on a plate and were incubate at 37°C overnight.

### 2.2.15 Transfection

The two 1.5 ml Eppendorf tubes were prepared. In the first Eppendorf tube, 100 µl of DMEM which did not contain neither FBS nor antibiotics, was mixed with 1 µg construct, 0.5 µg pG+P and 0.5 µg pEnv. In the second Eppendorf tube, 100 µl of DMEM without FBS nor antibiotics was mixed with 6 µl of FuGENE 6. The contents of the two Eppendorf tubes were mixed separately by inverting them multiple times or by gentle vortex. The Eppendorf tubes were spun down gently. Subsequently, the components of the two tubes were combined in one Eppendorf tube and were mixed by inverting them or by gently vortexing. The Eppendorf tube was incubated for 30 minutes. Simultaneously, 6 cm plate containing Phoenix A cells in 5 ml of DMEM

containing 10% (v/v) FBS, which was prepared a day before, was recovered from the incubator. The confluency of the Phoenix A cells was around 50% of the surface of the plate. After 30-minute incubation of the transformation mixture, it was added in a drop-wise manner to the 6 cm dish containing Phoenix a cells. The cells were left in the incubator overnight. The following day, change the medium in a 6-well dish and repeat the whole procedure. After 2 or 3 days of incubation of the 6-well dish, 50 µl of 4 µg/ml polybrin solution was added to the cells. Simultaneously, the medium was removed from the cells which were about to be transfected. These cells were grown in 6 cm dish and were grown to around 50% confluency. Subsequently, the virus-containing supernatant was collected with a syringe and filtered through 0.45 µm filter onto the cells of choice. The 6 cm dish with the cells of choice was left in the incubator overnight. The following day, the medium was changed to the fresh DMEM with 2.5% (v/v) FBS and without polybrin. The cells were allowed to recover for 24 hours. Afterwards, the resultant cells were transferred into 9 cm dish. Finally, the cells were subjected to selection by addition of 50 µl of puromycin in 10 ml, so that the final concentration of puromycin was 10 µg/ml.

### 2.2.16 $Ni^{2+}$-NTA Purification

The $Ni^{2+}$-NTA beads (Qiagen) were taken out from the fridge and prepared for the purification of the chosen proteins. A stand for columns was taken from a cold room. A small plastic column was taken and the opening of the column was enlarged by cutting it off with a razor blade. A 50 ml Falcon tube was taken and a blue ring which could hold the column was placed on top of the Falcon tube. The column was placed on the blue ring. Subsequently, the column was filled up with MQ water in order to clean it

from any contamination. The $Ni^{2+}$-NTA solution containing beads was taken from the fridge and was swirled gently until the $Ni^{2+}$-NTA beads were properly mixed with a solution to make the NTA beads slurry. The pipette tip was cut in order to avoid any interruption in the uptake of beads with the pipette and 500 µl of the $Ni^{2+}$-NTA slurry was loaded on the column. It was noted that $Ni^{2+}$-NTA beads counted for 250 µl of the overall slurry volume which was loaded on the column. The beads were washed with 10 ml of MQ water. After the MQ water was run through the column, 1 ml of basic buffer containing 0.2 mM PMSF and 2 mM β-ME was loaded on the column and was allowed to flow through it. The buffers were kept on ice at all times. The column was closed after the basic buffer run through the column. The pipette tip was enlarged by cutting it off with the scissors. 250 µl of the basic buffer which contained 10 mM imidazole was added to the column. Simultaneously, the 15 ml Falcon tube containing Sf9 insect cell lysate was thawed and centrifuged. Moreover, imidazole was added to the cell lysate to the final concentration of 10 mM. Subsequently, 500 µl of the NTA bead slurry was added to the 15 ml Falcon tube with lysate. The Falcon tube with lysate was incubated on the rotor in the cold room for one or two hours. While the beads were incubated, basic buffer was added to the closed column in order to keep the remaining beads wet. After incubation was complete, the 15 ml Falcon tube containing cell lysate was placed on ice. In the meantime, the column was opened and the basic buffer run through it. After the column was emptied, the lysate containing beads was transferred on the ml-by-ml basis to the column. Care was taken not to touch the top of the column with the pipette tip and to keep the column as clean as possible. 50 µl of flow-through were taken for an analysis. Subsequently, two ml of basic buffer containing 20 ml imidazole were added to the column in order to remove any proteins which bound unspecifically

to the $Ni^{2+}$-NTA beads. The washing was repeated two more times. Subsequently, washing buffer was carefully added to the top of the column and was allowed to flow through it. After the washing was complete, the column was brought to the cold room and 250 µl of basic buffer containing 250 mM of imidazole was added to the column in order to elute the desired protein. The $Ni^{2+}$-NTA beads inside the column were resuspended by flicking and gently vortexing the column. Subsequently, the column was opened and the eluate was collected in the Eppendorf tube. The elution was repeated two more times. After the elution was complete, the three Eppendorf tubes containing three eluates were vortexed and centrifuged quickly. The samples were taken from the resultant eluates for protein analysis. Subsequently, the three eluates were combined together in one Eppendorf tube and the tube was centrifuged at maximum speed for 10 minutes.

### 2.2.17 StrepTactin Purification

50 ml Falcon tube was placed on ice and blue ring was put on top of it. The column was placed in the blue ring. Subsequently, the column was washed with the MQ water. The vial containing StrepTactin beads (Sigma) was taken from the fridge. The beads were swirled and fully resuspended in the vial, so that the bead slurry formed. 100 µl of bead slurry were loaded on the open column with a pipette. The StrepTactin beads constituted 50% of the StrepTactin bead slurry. A few ml of MQ water were run through the column in order to wash the beads. One ml of the basic buffer was loaded on the column and it was allowed to flow through the column. If the StrepTactin beads were sticking to the pipette tip, they were removed by washing the pipette tip with an

arbitrary volume of a fresh basic buffer, which was loaded on the column. Subsequently, the column was closed and 50 µl of basic buffer were added to the beads. The beads were resuspended carefully in the buffer in the column with a pipette. The beads were transferred with a pipette into the Eppendorf tube containing NTA-pooled eluates. The Eppendorf tube was incubated in the rotor in the cold room for two hours. After the incubation was complete, the Eppendorf tube containing NTA eluates with beads was spun down at 1000 rpm for one min in order to separate the beads from the flow-through. At this point, 50 µl of the flow-through were taken for protein analysis. The flow-through was taken out from the Eppendorf tube but 200 µl were left inside and the StrepTactin beads were resuspended in that volume. 800 µl of the fresh basic buffer were added to the Eppendorf containing beads and the tube was centrifuged at 1000 rpm for one minute in order to wash the beads. After spinning, the washing of the beads was repeated. Following the washing, 800 µl of the buffer from the Eppendorf tube were removed and the StrepTactin beads were resuspended in the remaining 200 µl of basic buffer. The resuspended beads were loaded carefully on the column. The column was closed. Simultaneously, five µl of desthiobiotin were added to the 200 µl of basic buffer in order to make a 2.5 mM desthiobiotin elution buffer. The StrepTactin beads were washed three times with one ml of the fresh basic buffer. Afterwards, the column was filled up to the top with the washing buffer which was allowed to flow through the column. The column was closed and brought into the cold room. 50 µl of desthiobiotin elution buffer were added to the beads. The column was flicked and vortexed gently in order to resuspend the beads. The beads were incubated for five minutes. Following the incubation, the column was opened and the proteins were eluted into the Eppendorf tube. Two more 50 µl elutions were conducted into two separate Eppendorf tubes. The

eluates were vortexed and centrifuged briefly. Each eluate was taken for protein analysis.

### 2.2.18 Preparation of the desthiobiotin stock

Desthiobiotin was added to the 2 ml Eppendorf tube. DMSO was added to the desthiobiotin to the final concentration of 100 mM. The desthiobiotin was dissolved in DMSO by vortexing and spinning briefly. The desthiobiotin stock was kept in -20°C freezer.

### 2.2.19 Preparation of 4% (w/v) paraformaldehyde

Between 70 to 80 ml of MQ water was poured into a beaker. A regular laboratory glassware was not used for making paraformaldehyde. A bottle with solid paraformaldehyde (Sigma-Aldrich) was taken from the cold room. Four grams of paraformaldehyde were weighed out on a top loading balance. The weighed-out paraformaldehyde was added into a beaker containing MQ water. The beaker was placed on the heat/stir plate in the fume hood and the stirring was begun while heating simultaneously at 55-60°C. The thermometer was placed directly in the beaker in order to monitor whether the temperature stayed between 55-60°C. A few drops of NaOH were added to the paraformaldehyde until the solution became clear. Once the paraformaldehyde dissolved, it was allowed to cool down to the room temperature. The pH of the solution was checked with pH strips and it was adjusted to 7.4 (HCl was used if it became necessary). 10 ml of 10X concentrated PBS was added to the paraformaldehyde and the solution was topped up with MQ water to reach a final

volume of 100 ml. The solution was mixed and pH was checked again. The 4% (w/v) paraformaldehyde was filtered through 0.45 µm filter. The paraformaldehyde was aliquoted into 2 ml tubes and stored at -20°C.

### 2.2.20 Cell competency

The cells were streaked out on the plate so that the single colonies formed. A single colony was inoculated in 2 ml medium overnight. The following day, 250 ml culture was inoculated in a flask at 25°C and the culture was allowed to grow until OD reached 0.6-1.0. Simultaneously, 50 ml Falcon tubes, 1.5 ml Eppendorf tubes and TB buffer were pre-cooled on ice/water slurry. The flask was incubated on ice/water slurry for 10 minutes. The culture was poured into five pre-cooled 50 ml Falcon tubes. The Falcon tubes were spun down at 2500 *g* at 4°C for 10 minutes. After spinning, the supernatant was discarded and the cells were resuspended by addition of five ml of TB buffer into each tube with pastette in the cold room. The resuspended cells were swirled gently on ice/water slurry. It was ensured that the cells were fully resuspended. 11 ml of TB buffer were added per tube to the resuspended cells (the final volume in all Falcon tubes should have reached 80 ml). The cells were pooled into two Falcons and were incubated for 10 minutes. The tubes were spun down at 2500 *g* for 10 minutes. The supernatant was discarded and the cells were resuspended in 5 ml TB buffer in each tube. The cell suspensions from the two Falcons were pooled together and 10 ml TB buffer was added. 1.4 ml of DMSO was added to a final concentration of 7% (v/v). 200 µl of cell suspension was aliquoted in pre-chilled Eppendorf tubes. The Eppendorf tubes were snap frozen in liquid nitrogen. The competency of the cells was tested.

### 2.2.21 Collection of baculovirus particles and harvesting of Sf9 insect cells for WB

The baculovirus-containing supernatants were collected from 6-well plates and were pipetted into 2 ml Eppendorf tubes. Subsequently, the supernatants were spun down at 3000 rpm for five minutes in order to remove any remaining Sf9 insect cells. The supernatants were transferred into the fresh Eppendorf tubes and FBS was added to the final concentration of 2% (v/v). The Eppendorf tubes could be stored at 4°C at that point. The 6-well plates were taken and the cells were washed in room temperature PBS once. Subsequently, the PBS was aspirated and 6-well plates were placed on ice. The 500 µl of basic buffer was added into each well. The cells were scraped off the bottom of each well with a plastic spatula. The cells in basic buffer were transferred into the Eppendorf tubes. The tubes were incubated on ice for five minutes. The cells were centrifuged at maximum speed at 4°C for 15 minutes. After the spinning, the supernatants were transferred into the new tubes. The samples were taken for the protein analysis by Bradford assay.

### 2.2.22 FANCD2/FANCI heterodimeric complex purification

Each of four 15 cm plates containing Sf9 insect cells was infected with both 50 µl of Flag- and HA-tagged FANCD2 and 50 µl of His- and Strep(II)-tagged FANCI simultaneously. The plates were incubated in the 27°C incubator for 72 hours. After that time, the cells were recovered from the incubator and were washed with room temperature PBS. 3 ml of basic buffer supplemented with 0.2 mM PMSF and 2 mM β-ME (Sigma) was poured into each plate and the cells were scraped off with the spatula into 15 ml Falcon tube. The cells were incubated on ice for 10 minutes in order to lyse

the cells. Following the lysis, the solution was pipetted into 2 ml Eppendorf tubes and was centrifuged at 4°C at maximum speed for 20 minutes. The cell lysate was collected into the fresh 15 ml Falcon tube and was incubated with 400 µl of pre-equilibrated α-Flag M2 agarose beads slurry for two hours in the cold room.

### 2.2.23 Gene knockdown

The Phoenix A cells were grown in 6 cm dish containing DMEM supplemented with 10% (v/v) FBS. The cells were grown to the 50% of dish capacity. The two Eppendorf tubes were prepared. The first one contained 100 µl of DMEM without FBS nor antibiotics. 1 µg of the desired plasmid was added to the tube as well as 0.5 µg pG+P and 0.5 µg pEnv. The second Eppendorf tube contained 100 µl DMEM without FBS nor antibiotics. 6 µl of FuGENE 6 were added to the tube. The components of the both Eppendorf tubes were mixed separately. The first Eppendorf tube was vortexed gently. The second Eppendorf tube was inverted several times. The tubes were centrifuged at 1000 rpm for a few seconds. Subsequently, the contents of both tubes were combined and were mixed thoroughly. The Eppendorf was incubated in the flow cabinet for 30-45 minutes and was spun down at 1000 rpm for a few seconds subsequently. The Phoenix A cells were trypsinised and 10-15% of Phoenix A cells were seeded in 5 ml DMEM in a 6 cm dish. 200 µl of the prepared transfection solution was transferred in a drop-wise manner into the dish with the Phoenix A cells. The 6 cm dish was placed in the incubator for two days. Once the cells reached the confluency, the supernatant was collected with a 10 ml pipette and was transferred into a syringe with an attached 0.45 µm filter. 50 µl of 4 µg/µl polybrin was added into the syringe. In the meantime, a dish

with 50% confluent HeLa cells was recovered from an incubator. Medium was discarded from HeLa cells. Subsequently, the contents of the syringe were filtered through 0.45 µm filter onto the HeLa cells. The HeLa cells were allowed to grow for a minimum of six hours. After that time, a fresh medium was added (DMEM supplemented with 2.5% FBS) and the cells were allowed to recover for 24 hours. Subsequently, the cells were trypsinised and transferred into a 9 cm dish. The cells were selected with the addition of 50 µl puromycin in 10 ml medium, resulting in a final concentration of 10 µg/ml.

### 2.2.24 Heat inactivation of FBS

The bottle with FBS was taken from the fridge. Subsequently, the FBS bottle was placed into 37°C waterbath and the temperature was allowed to equilibrate. The temperature of the water bath was increased to 55°C and FBS was kept at that temperature for 20 minutes. After completion of heat inactivation of FBS, the bottle was labelled accordingly.

### 2.2.25 *In vivo* α-Flag binding assay

A few cell lines were grown to confluency in 15 cm dishes. Two dishes of cells were used for each cell line. The cell lines used in this experiment were: HeLa and HeLa with Flag- and HA-tagged FANCD2. MMC was added into a dish containing each of the cell line to the final concentration of 160 ng/ml. All the dishes were incubated overnight. The cells were harvested the following day. The cells were washed in the room

temperature PBS. After aspiration of PBS from the tube, the resultant cell pellet was resuspended in equal volume of buffer 1 and transferred into 15 ml Falcon tube. The cells were incubated on ice for 30 minutes. Afterwards, five times volume of buffer 2 was added to the resuspended pellet. The sample was incubated on the rotor in the cold room for 30 minutes. After the incubation was complete, the sample was transferred into the Eppendorf tubes. The tubes, in turn, were centrifuged at 17,000 x *g* for 10 minutes at 4°C. At that point, the supernatant was taken for protein concentration measurement by Bradford assay. The supernatants from the Eppendorf tubes were combined in a 15 ml Falcon tube. Subsequently, the purification column and M2 agarose beads were taken. The column and α-Flag M2 agarose beads were prepared as before. Moreover, the α-Flag M2 agarose beads were washed in a few ml of buffer 2. 40 µl of the resultant α-Flag M2 agarose bead slurry was added to the supernatant and the sample was incubated n a rotor in the cold room for three hours. After incubation, the sample was transferred into the Eppendorf tubes. The tubes were centrifuged at 500 x *g* at 4°C for five minutes. The α-Flag M2 agarose beads were washed two times with 1 ml of buffer 2. The buffer was removed every time by aspiration with syringe and needle. The Flag-tagged protein was eluted from the α-Flag M2 agarose beads by addition of 40 µl 1X LDS buffer with 1X reducing agent into an Eppendorf tube. The sample was vortexed for a few seconds and centrifuged afterwards. Subsequently, the sample was heated up for 10 minutes at 70°C. The eluate was separated from the beads with syringe and needle and was transferred into the fresh Eppendorf tube.

### 2.2.26 Preparation of X-gal Luria Agar (LB) plates for baculovirus selection

20 g of LB agar (Sigma-Aldrich) were weighed out and put into red-capped bottle. The bottle was filled with 500 ml of the MQ water. The LB agar was mixed with water by swirling the bottle. The LB agar was autoclaved. The LB agar bottle was kept in the 55°C waterbath for 1 hour in order to avoid setting of agar. The flame was lit to avoid contaminating the LB agar. The following components were added to the chilled LB agar: kanamycin (50 µg/ml), gentamicin (7 µg/ml), tetracycline (10 µg/ml), IPTG (40 µg/ml) and X-gal (300 µg/ml). The bottle was swirled in order to mix all the added components. The resultant LB agar was poured into Petri dishes under sterile conditions. The dishes were closed and were placed on the bench in order to cool down. Finally, the Petri dishes were wrapped up in the foil and were left in the cold room.

### 2.2.27 α-Flag M2 agarose purification of Flag-tagged proteins

The 50 ml Falcon tube was placed on ice and the blue ring for holding columns was put on top of it. The purification column was taken, the end of the column was broken off and the column opening was enlarged with trimming it with a razor blade. Afterwards, 10 ml of MQ water were run through the column in order to remove any contamination. Simultaneously, α-Flag M2 agarose beads (Sigma-Aldrich) which immersed in a solution were taken out from the freezer. The Eppendorf tube which contained α-Flag M2 agarose beads was inverted several times in order to ensure the complete mixing of α-Flag M2 agarose beads with the solution. Afterwards, the pipette tip was cut to eliminate the possibility of ineffective uptake of beads with a pipette. 400 µl of α-Flag M2 agarose slurry was taken out from the Eppendorf tube and was loaded into the

prepared column. The beads constituted 50% of the slurry. 1 ml of the basic buffer was applied to the column and was allowed to flow through it. In the meantime, all the buffers were kept on ice. Subsequently, 1 ml of 0.1 M glycine of pH 2.5 was loaded on the column and was allowed to flow through it. Similarly, 1 ml of 1 M Tris pH 8.0 was loaded on the column was allowed to flow through it. Afterwards, 5 ml of the basic buffer were loaded on the column and were allowed to flow through. The column was capped and 200 µl of basic buffer were added to the beads. The pipette tip was cut and the beads were loaded on the column. Subsequently, the beads were added to the 15 ml Falcon tube containing a protein to be purified. The Falcon tube was left on the rotor in the cold room for two-hour incubation. A few millilitres of the basic buffer were added to the column in order to keep the trances of residual α-Flag M2 agarose beads wet. After the incubation was complete, the 15 ml Falcon tube was recovered from the cold room. The column was opened and the basic buffer flew through it. The pipette tip was cut in order to allow for uninterrupted uptake of beads from the 15 ml Falcon tube with a lysate. The lysate was transferred with the pipette on the ml-by-ml basis to the column until all the beads collected at the bottom of the column. The care was taken not to contaminate neither column nor the pipette. 50 µl of the flow-through sample was taken for the protein analysis. After all the lysate was emptied from the column, the beads were washed three times, 1 ml at a time. Subsequently, the basic buffer was carefully added to the top of the column in order to complete washing of the beads. The flow-through was aspirated in order to avoid contamination of the column. After the washing was complete, the column was brought into the cold room. The column was closed with parafilm and it was capped in order to prevent any spillage of the elution buffer. The 200 µl of elution buffer containing basic buffer with 0.5 µg/µl Flag peptide was added

to the column. The column's capped opening was additionally protected with placing the column in 2 ml Eppendorf tube. The top of the column was also closed with a parafilm. The column was incubated on a shaker at 4°C for one hour. The shaker was set to the lowest speed. After the incubation was complete, the column was opened and the sample was eluted into the Eppendorf tube. The elution was conducted one more time. The resultant eluates were vortexed gently and centrifuged quickly. The eluates were centrifuged for 10 minutes at maximum speed and were transferred into the fresh Eppendorf tubes. Moreover, the eluates were taken for protein analysis. The eluates could be snap frozen in the liquid nitrogen at that point.

### 2.2.28 SDS-PAGE gel stack preparation

The tank for making gel stacks was taken. A rectangular glass plate and a thin rectangular plastic plate were placed in the tank as the first layer. A metal rectangular plate was placed in the tank next. The metal dividers were placed on top of the metal plate and the glass plate was put on the dividers. The wax paper was taken and was placed on the glass plate. Subsequently, the metal rectangular plate was put on top of the wax paper and the procedure was repeated until the tank was full. When the tank was full, it was closed with a transparent lid and secured with plastic clamps. It was checked with the tweezers whether all the plates and dividers were put in their proper places. In the meantime, the beaker was placed on ice and the resolving gel was prepared according to the recipe. Following, the addition of all the components and ensuring that they were completely mixed, the resultant resolving gel was taken up with a 60 ml syringe and loaded into a tank into the indicated level. Subsequently, 200 µl of the MQ water were pipetted from one side of each gel and another 200 µl of MQ water

from the other side of each gel. The MQ water addition was repeated for each gel present in the tank. The resolving gel was left on the bench until it solidified. After the resolving gel solidified, the MQ water war removed from the tank by tilting the gel tank to its side. Subsequently, a 50 ml Falcon tube was taken and the stacking gel was made according to the recipe. The ready stacking gel was poured into the gel tank directly on the solidified resolving gel. The combs were placed quickly inside each space between glass and metal plates. The stacking gel was allowed to solidify. After solidification of the stacking gel, the gel tank was opened with a metal spatula. The gels were wrapped up in the cling film and were placed in the cold room.

### 2.2.29 Plasmid purification

A single bacterial colony was transferred into 3 ml of LB medium which contained 100 µg/ml of a final concentration of ampicillin. The LB medium with the bacterial colony was kept in a 14-ml loosely-capped tube. The inoculated LB medium was subjected to vigorous shaking in an incubator at 37°C overnight. The following day, the culture was pipetted into 1.5 ml Eppendorf tubes. The tubes were centrifuged at maximum speed at 4°C for 1 minute. The remaining culture (if any) could be stored at 4°C. After centrifugation, the LB medium was removed by aspiration and the bacterial pellet was left as dry as possible at the bottom of the tube. Subsequently, the lysis by alkali was conducted. 0.8 µl of RNase A at the concentration of 10 mg/ml was added into an Eppendorf containing 100 µl of Solution I. 100 µl of ice-cold Solution I were added to the Eppendorf tube containing bacterial pellet and the pellet was resuspended with the pipette. Subsequently, 200 µl of freshly prepared Solution II was added. The Eppendorf

tube was closed tightly and the components were mixed by inverting the tube rapidly several times. The sample was not vortexed. Afterwards, the Eppendorf tube was stored on ice. 150 µl of ice-cold Solution III was added to the tube. The tube was closed and vortexed gently for 10 seconds in order to mix Solution III thoroughly with the bacterial lysate. Subsequently, the tube was stored on ice for 3-5 minutes. Following the incubation, the sample was centrifuged at maximum speed at 4°C for 5 minutes. The supernatant was transferred into a fresh Eppendorf tube. Subsequently, the equal volume of phenol:chloroform:isoamyl alcohol was added to the supernatant. The resultant sample was mixed by vortexing. Afterwards, the sample was centrifuged at maximum speed at 4°C for 20 minutes. The aqueous phase was transferred into a new Eppendorf tube. The equal volume of chloroform was added into the aqueous phase. Subsequently, the sample was vortexed and centrifuged at maximum speed for 1 minute. The aqueous phase was taken out with the pipette and was transferred into a fresh Eppendorf tube. The sample was centrifuged again at maximum speed for 1 minute. The upper layer was transferred into a new tube. Afterwards, the double-strand DNA was precipitated with two volumes of room temperature absolute ethanol. The sample was mixed by vortexing. The resultant sample was incubated at -20°C for 1 hour. Following the recovery from the freezer, the sample was centrifuged at the maximum speed at 4°C for 20 minutes. The supernatant was removed from the Eppendorf tube by a gentle aspiration in order not to disturb the pellet. The Eppendorf tube containing the pellet was left in an inverted position for a few minutes on a paper towel in order to allow any remaining fluid to drain away. Afterwards, the pellet of double-strand DNA was washed with 1 ml of 70% (v/v) of 4°C ethanol. The sample was centrifuged at the maximum speed for 10 minutes. Subsequently, the supernatant

was aspirated carefully and the pellet was allowed to dry in the air for 10 minutes. The pellet was dissolved in 50 µl of TE buffer at pH 8.0. Finally, the sample was vortexed briefly and stored at -20°C.

### 2.2.30 Mycoplasma detection protocol

The cells, which were suspected to be contaminated, were plated in the 9 cm dishes. The plates were placed in the incubator for three days, until which point they should have reached confluence. Between 0.5 to 1 ml of cell culture supernatant was transferred into the 1.5 ml Eppendorf tube. The cell debris were pelleted by brief centrifugation at 250 x *g*. Subsequently, the supernatant was transferred into the new sterile Eppendorf tube and was centrifuged at the maximum speed for 10 minutes in order to sediment mycoplasma. The resultant supernatant was carefully decanted and the pellet was kept. Subsequently, the pellet was resuspended in 50 µl PBS and was mixed thoroughly with pipette. Afterwards, the sample was heated to 95°C for three minutes. The sample could be stored at that stage at -20°C for later use. Subsequently, the PCR reaction mixture was prepared as shown in the Table 7. PBS was used as a negative control.

**Table 7. The reagents and their volumes used for polymerase chain reaction (PCR) in order to detect mycoplasma.**

| Component | Volume [µl] |
|---|---|
| 10X Taq buffer | 1 |
| MGSO primer (10 µM) | 0.2 |
| GP0-3 primer (10 µM) | 0.2 |
| dNTP mix (10 mM) | 0.2 |
| Taq polymerase | 0.1 |
| Sample | 1 |
| Water | 7.3 |

The ready PCR samples were placed in the thermocycler and were subjected to the following PCR cycle protocol.

**Table 8. The polymerase chain reaction (PCR) conditions used for mycoplasma detection.**

| Temperature [°C] | Time [s] | Number of cycles |
|---|---|---|
| 94 | 30 | 1 |
| 94 | 30 | 35 |
| 60 | 120 | 35 |
| 72 | 60 | 35 |
| 72 | 300 | 1 |
| 4 | ∞ | 1 |

After completion of PCR, the samples were run on 2% agarose gel. The 100 bp was used as a ladder.

2.2.31 PCR-based colony screening

A single colony was taken with a pipette tip from a dish. The whole colony was not taken as it was going to be used for the future experiment. The colony was transferred in to the empty PCR tube. The 10 µl of Taq polymerase mix was made as given in Table 9.

**Table 9. Components and their volumes used in the PCR-based colony screening.**

| Component | Volume [µl] |
|---|---|
| Taq polymerase buffer (10X) | 1 |
| dNTP mix (10 mM) | 0.2 |
| M13 Forward primer (10 µM) | 0.2 |
| M13 Reverse primer (10 µM) | 0.2 |
| Taq polymerase | 0.05 |
| MQ water | 8.35 |

(The given components were necessary for one reaction only)

The 10 µl of the Taq polymerase mix was added to the PCR tube containing the colony. All the components were mixed with the pipette. The PCR tube was transferred into a thermocycler. The thermocycler PCR conditions were set as provided in Table 10.

**Table 10. Conditions used for polymerase chain reaction (PCR)-based colony screening.**

| Time [s] | Temperature [°C] | No. of cycles |
|---|---|---|
| 300 | 95 | 1 |
| 30 | 95 | 25 |
| 60 | 55 | 25 |
| 300 | 68 | 25 |
| 300 | 68 | 1 |
| ∞ | 4 | 1 |

10 µl of the PCR reaction was loaded into agarose gel for analysis.

2.2.32 Transfection of Sf9 insect cells

The cells were recovered from the liquid nitrogen. Sf900 medium was warmed up in an incubator, so that it reached a room temperature. 15 ml of Sf900 medium was poured into a red-capped flask. The contents of the cryotube containing Sf9 insect cells were pipetted into the Sf900 medium. The flask was placed in a shaking incubator set to 26°C. The cap of the flask was left loosened in order to keep the cells aerated. The Sf9 insect cells were left in the incubator overnight. The number of Sf9 insect cells was kept around 2-8 million. The cells were recovered from the incubator the following day. The flask was stirred in order to ensure an even distribution of the cells and the cells were counted with haemocytometer. After counting, 9 x $10^5$ cells were seeded in 2 ml of Sf900 medium in a 6-well plate. The cells were allowed to attach to the 6-well plate in the 27°C incubator for one hour. Subsequently, the solutions used for transfection of Sf9 insect cells were prepared. 5 µl of 1 µg of previously purified bacmid DNA was mixed

by pipetting with 100 µl Grace medium without antibiotics in an Eppendorf tube. The diluted bacmids were vortexed and were centrifuged briefly. The Grace medium was pre-heated prior to being used. Moreover, 6 µl of CellFECTIN reagent was mixed with 100 µl of Grace medium without antibiotics in the second Eppendorf tube. The vial containing CellFECTIN was flicked and inverted before use. The contents of both Eppendorf tubes were combined together in a fresh Eppendorf tube. The resultant solution was mixed by inverting the tube several times. The bacmid DNA with CellFECTIN were added to the cells. The cells were left for 72 hours in the incubator. The cells were checked every day in order to observe any signs of infection.

### 2.2.33 Infection of Sf9 insect cells with a baculovirus

6 cm plate was taken and 5 ml of Sf900 medium. Subsequently, the Sf9 insect cells were added to the plate from the red-capped flask. The Sf9 cells fell quickly to the bottom of the plate and were observed under the microscope in order to observe whether the cells were in good condition for the experiment. Moreover, the cells should have covered 50-70% surface of the plate. Subsequently, the two 9 cm plates were taken and 10 ml of Sf900 medium was added into each of them. The Sf9 insect cells were added into each plate. The tubes containing baculovirus were recovered from the fridge. 10 µl of baculovirus were loaded into the 9 cm plate containing Sf9 insect cells. 20 µl of baculovirus were loaded into another 9 cm plate. Both 9 cm plates containing cells infected with baculovirus as well as non-infected 6 cm negative control plate were placed in the 27°C incubator. The size of cells was observed for next 24 hours. The infected Sf9 insect cells should have become larger in size than the control insect cells.

### 2.2.34 TMP-UVA cell treatment for Western blot

The 9 cm plates were prepared and the HeLa cells were seeded in them a day before an experiment. The TMP (Sigma, T6137) was recovered from the freezer and was thawed until it was completely dissolved. 10 µl of 0.5 mg/ml of TMP were added into 10 ml DMEM. The medium with TMP was added into each plate. Subsequently, the cells were incubated at 37°C for 30 minutes. After the incubation was complete, the cells were subjected to UVA irradiation at 250 J/m$^2$. The cells were incubated in the 37°C incubator for a required amount of time.

### 2.2.35 Western blot preparation

The Eppendorf tubes containing previously prepared samples were recovered from the freezer (if not used straight after preparation) and were heated at 70°C for 10 minutes on a heating block. The samples were centrifuged and vortexed before being loaded on the SDS-PAGE gel. The SDS-PAGE gels were made previously in a stack (5% and 10% gels were in the stack) or a gray tank was used for making gels which were required to be run on a different acrylamide concentration. The gel was placed in the tank and running buffer was added, so that it covered the wells of the gel. The bottom of each well was indicated with a marker in order to load the samples without cutting the gel. The 1x LDS buffer was added into each well in order to visualise the shape of each well before the sample addition. 5 µl of Mark12 marker was loaded into the first and last wells of the gel. The previously prepared samples were loaded in the wells between marker wells. The gels were run at 50 V for 30-40 minutes and the voltage was changed

afterwards to 100 V till the samples reached the bottom of the gel. The transfer buffer was poured into a container. Subsequently, sponges and Whatman papers were soaked in the transfer buffer. Two wet Whatman papers, membrane, SDS-PAGE gel and another two Whatman papers were soaked in transfer buffer and were placed together in a special cage. The cage was closed and was placed with a hinge up in the transfer container. The transfer of proteins to the membrane was conducted for 1 hour at 400 mA in the cold room. The magnetic agitator was placed within the transfer tank in order to ensure mixing of the transfer buffer. After the transfer was complete, the membrane was taken out of the tank and was washed in the MQ water. Subsequently, the membrane was stained with 1X ponceau stain and the marker bands were indicated. The labelled membrane was trimmed with a razor blade. The membrane was washed with TBST for a few minutes. Afterwards, the membrane was blocked with 5% milk (w/v) supplemented with 0.1% azide for 1 hour on a rocker. After the blocking was complete, the membrane was taken out of the milk and it was placed in a container on a parafilm. The primary antibody was mixed with the milk supplemented with azide and it was loaded on the membrane. The membrane was incubated in the fridge at 4°C overnight. The following day, the membrane was recovered from the fridge and was washed three times with TBST on the rocker. Each wash lasted five minutes. A few µl of the secondary antibody were mixed thoroughly with 5% (w/v) milk. The membrane was placed on a parafilm in a contained and the secondary antibody in milk was loaded on the membrane. The membrane was incubated for 1 hour at room temperature on a rocker. After the incubation was complete, the membrane was washed three times for five minutes in TBST on a rocker. Afterwards, the membrane was washed once in TBS. Any remaining fluid was drained from the membrane by tilting the membrane on a

tissue. The membrane was placed on a plastic sleeve. In the meantime, 1 ml of solution I and 1 ml of solution II were mixed together in the 50 ml Falcon tube. The resultant mixture was poured onto the membrane. The membrane was left at room temperature for five minutes. The plastic sleeve was swirled around, so that the solution I/II was spread evenly on the membrane. The sleeve was closed and the air bubbles were avoided. The excess of solution I/II mixture was removed with a tissue. Subsequently, the sleeve with a membrane was placed in the cassette. Finally, the membrane was analysed on the developer.

### 2.2.36 Sequencing

The vectors purified in this study by the Miniprep plasmid purification method were sequenced externally by Source BioScience.

### 2.2.37 Statistical analysis

Microsoft Excel was used to perform the statistical analyses. The Student's two-tailed t-test was applied to determine statistical significance.

Standard error was calculated with the use of the following formula:

$$Standard\ error = \frac{\mathrm{SD}}{\sqrt{n}},$$

where SD stands for standard deviation and n is a number of individual experiments (Cumming *et al.*, 2007; Vaux, 2012).

Detailed information about the experiments (number of experiments and replicates) is included in individual figure legends.

### 2.2.38 Plating efficiency calculation

In order to measure the plating efficiency, cells were counted using haemocytometer and seeded into the 6-well plates. After incubation for 2 weeks, the colonies (untreated with any genotoxic agent) were stained with 1% (w/v) crystal violet in methanol. The dried and crystal violet-stained circular colonies visible with the naked eye were counted manually. Each colony was marked separately in the middle of the colony. If the integrity of a colony was in doubt, the morphology of the colony was investigated with the use of the microscope. If the colony was lacking integrity, it was not counted. The plating efficiency of cells in each well was calculated with the use of the following formula:

$$Plating\ efficiency = \frac{\text{Number of colonies formed}}{\text{Number of cells seeded}} \times 100\%$$

Plating efficiency was calculated from data from at least 3 wells. Plating efficiencies were calculated for all cell lines based on the clonogenic survival assay data.

# 3 Analysis of WRNIP1's impact on cell survival upon exposure to genotoxic agents

## 3.1 Introduction

Various studies have suggested a role of Werner helicase-interacting protein 1 (WRNIP1) in DNA repair (Nomura *et al*., 2012; Kanu *et al.,* 2015). Crosetto *et al.* (2008) has shown that WRNIP1 forms nuclear foci after treatment with UVC and hydroxyurea indicating that it plays a role in a response to stalling of replication forks. Moreover, Nomura *et al*. (2012) showed that WRNIP1 accumulates at laser-irradiated sites which introduce both single- and double-strand breaks. However, it has not been established yet whether WRNIP1 functions in the resolution of ICLs.

It has been an aim of this study to analyse whether WRNIP1's depletion might influence the survival of cells treated with various ICL-inducing agents, i.e. MMC, TMP-UVA and cisplatin, thus demonstrating phenotypic similarity to established Fanconi anemia proteins.

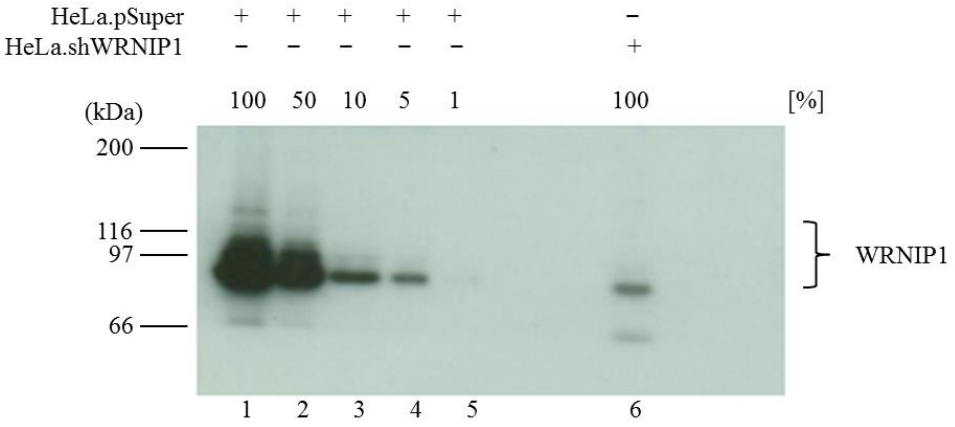
## 3.2 WRNIP1 knockdown cells exhibit lower survival than control cells

In order to establish whether WRNIP1-depleted cells exhibit the same phenotype as cells lacking established Fanconi anemia proteins, the clonogenic cell survival assay was performed using three cell lines, i.e. HeLa (HeLa.pSuper), HeLa WRNIP1 knockdown (HeLa.shWRNIP1) and HeLa FANCD2 knockdown (HeLa.shFANCD2). HeLa WRNIP1 knockdown cells were generated by establishing a HeLa (HeLa.pSuper) cell line, using hairpin RNA (shRNA), in which cellular level of WRNIP1 was only 1-

5% (Materials and Methods). The WRNIP1 knockdown level was measured by comparison to normal HeLa cells (Figure 6). HeLa FANCD2 knockdown cells were generated with shRNA by Caroline Schneider (Dr Martin Cohn's laboratory). The cells were treated with increasing concentrations of MMC and incubated for two weeks. After recovery from an incubator, the surviving colonies were stained and counted. As shown in Figure 7, the highest number of surviving colonies was found in the HeLa cells. Their resistance to increasing MMC concentrations, attributed to their ability to repair ICLs, was manifested by the highest number of surviving colonies. In comparison, FANCD2 knockdown cells, which had only minimal amount of FANCD2, resulted in a steep drop in a number of colonies after addition of MMC. The WRNIP1 knockdown was also found to influence cell survival after MMC treatment. Indeed, WRNIP1 deficiency resulted in a decreased number of surviving cells which could indicate WRNIP1's role in decreasing sensitivity to this ICL-inducing agent. However, the decrease in WRNIP1-depleted colonies was not as pronounced as in the FANCD2 knockdown cells. This result suggests that the cells in which WRNIP1 is depleted show a phenotypic similarity to the cells in which established components of the Fanconi anemia pathway are absent under the conditions of ICL-induction. Therefore, WRNIP1 might play some role in the resolution of ICL but it is not as crucial as that of FANCD2 because FANCD2-depletion resulted in more pronounced phenotype of higher cellular sensitivity to MMC.

When HeLa and HeLa WRNIP1 knockdown cells were treated with an alternative genotoxic agent, i.e. cisplatin (Figure 8), there was no observed change between in survival between these two cell lines.

**A**




**B**

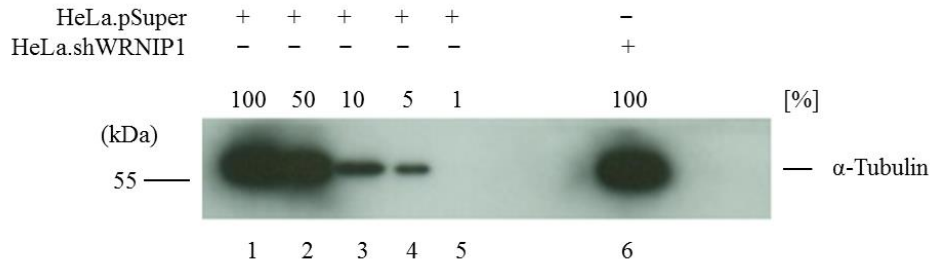
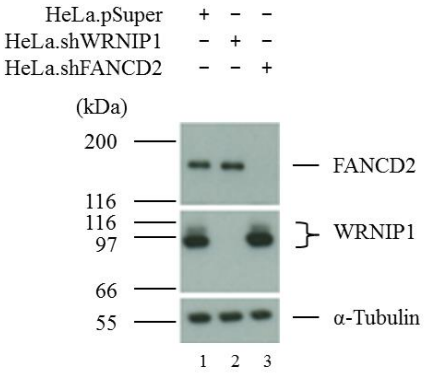



**Figure 6. Quantification of WRNIP1 knockdown in HeLa cells.** (A) Quantitative Western blot showing serial dilution of the control HeLa cells (HeLa.pSuper): lanes 1, 2, 3, 4, 5 and comparing them to HeLa WRNIP1 knockdown cells (HeLa.shWRNIP1) in which short hairpin RNA was targeting WRNIP1 (lane: 6). α-WRNIP1 antibody was used (1:2000 dilution) (B) Quantitative Western blot showing serial dilution of the control HeLa cells (HeLa.pSuper): lanes 1, 2, 3, 4,5 and comparing them to HeLa WRNIP1 knockdown cells (HeLa.shWRNIP1) in which short hairpin RNA was targeting WRNIP1 (lane: 6). α-α-Tubulin antibody was used (1:2000 dilution).

**A**




**B**

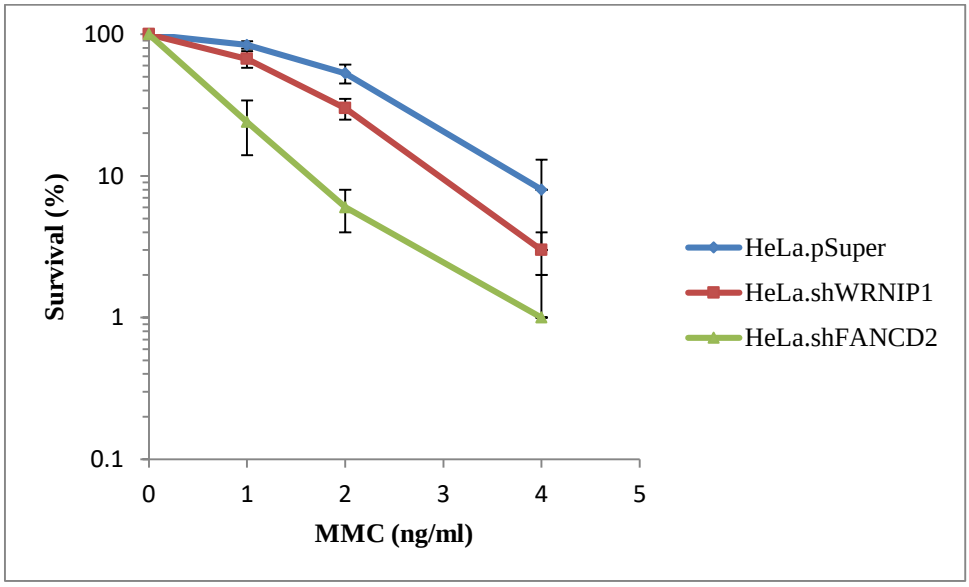
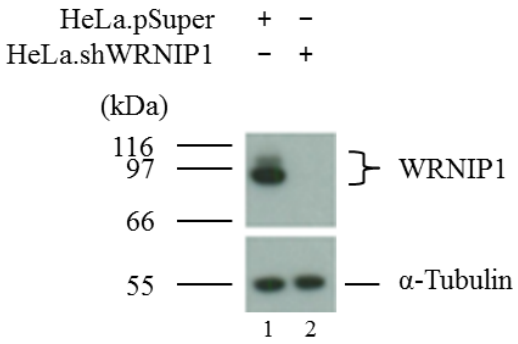



**Figure 7. WRNIP1 knockdown cells are sensitive to the treatment with MMC.** (A) Western blot showing the control HeLa cells (HeLa.pSuper), HeLa WRNIP1 knockdown cells (HeLa.shWRNIP1) and HeLa FANCD2 knockdown cells (HeLa.shFANCD2) (B) The clonogenic survival assay showing the survival of HeLa, HeLa WRNIP1 knockdown and HeLa FANCD2 knockdown which were treated with MMC. The blue curve indicates the cell survival of HeLa cells treated with MMC, green curve represents HeLa FANCD2 knockdown cells treated with MMC and red curve represents HeLa WRNIP1 knockdown cells treated with MMC. Plating efficiency of HeLa cells was 41%, plating efficiency of HeLa WRNIP1 knockdown was 45% and plating efficiency of HeLa FANCD2 knockdown was 49%. HeLa FANCD2 knockdown cells were generated by Caroline Schneider (Dr Martin Cohn's laboratory) Experiments were repeated three times with triplicates within each experiment. Error bars indicate standard error (n=3).

**A**




**B**

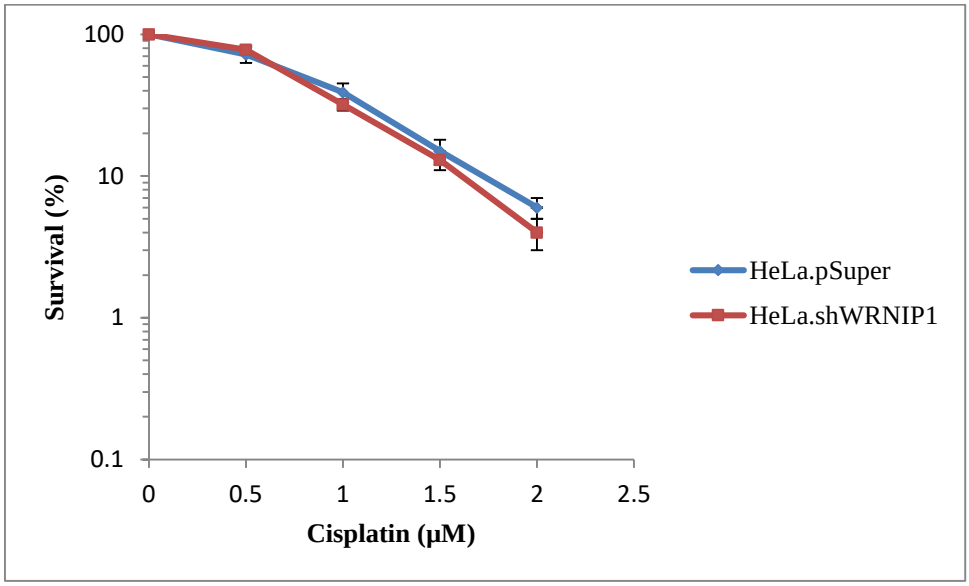



**Figure 8. WRNIP1 knockdown cells are not sensitive to the treatment with cisplatin.** (A) Western blot analysis of untreated HeLa cells (HeLa.pSuper) and HeLa WRNIP1 knockdown cells (HeLa.shWRNIP1) used in the cisplatin clonogenic assay. (B) The clonogenic survival assay showing survival of control HeLa cells (HeLa.pSuper) and HeLa WRNIP1 knockdown cells (HeLa.shWRNIP1) treated with cisplatin. The blue curve indicated the survival of HeLa cells treated with increasing concentration of cisplatin and the red curve shows the survival of the WRNIP1 knockdown cells treated with increasing concentrations of cisplatin. Plating efficiency of HeLa cells was 44% and plating efficiency of HeLa WRNIP1 knockdown was 43%. Experiments were repeated three times with triplicates within each experiment. Error bars indicate standard error (n=3).

### 3.3 WRNIP1 knockout cells show lower survival than control cells after treatment with genotoxic agents

In order to further establish whether functions in repairing ICLs, a HeLa WRNIP1 knockout (HeLa WRNIP1$^{-/-}$) cell line was generated (Figure 9). The resultant cells were treated with three ICL-inducing agents, i.e. MMC, TMP-UVA and cisplatin in three separate experiments. The HeLa WRNIP1 knockout cells were grown alongside control HeLa cells (HeLa.pSuper). Both cell lines were incubated for two weeks and stained with 1% (w/v) crystal violet in methanol.

After the recovery the clonogenic survival assays from the incubator, it was observed that WRNIP1 knockout cells showed lower survival than the control HeLa cells when treated with increasing concentrations of MMC (Figure 10). This result demonstrated that after introduction of ICLs, the cells could not repair DNA damage very well when WRNIP1 was depleted.

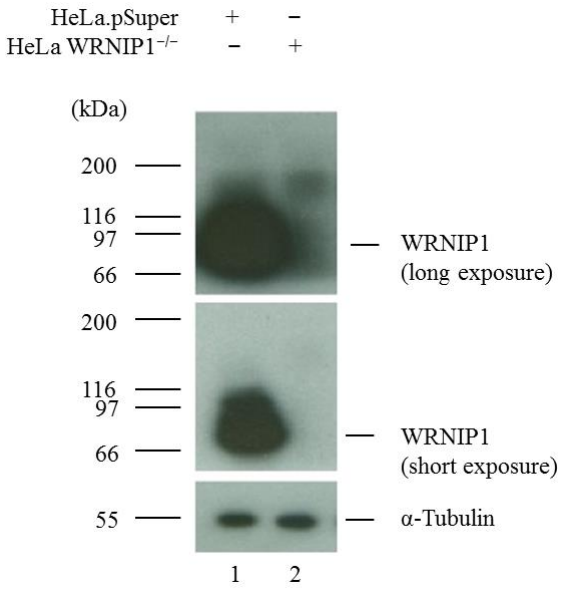
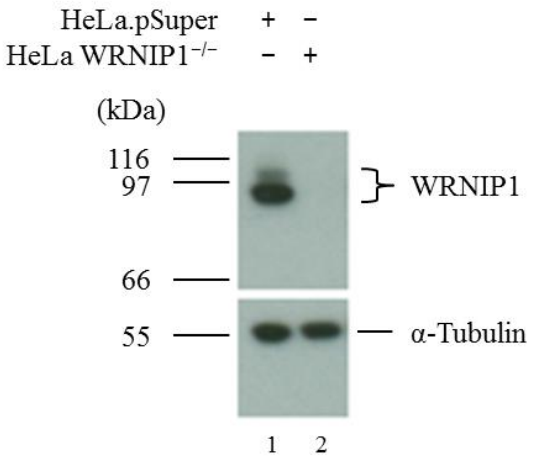



**Figure 9. Western blot of HeLa WRNIP1 knockout (HeLa WRNIP1$^{-/-}$) cells.** Lane 1 indicates control HeLa cells (HeLa.pSuper) and lane 2 indicates HeLa WRNIP1 knockout cells (HeLa WRNIP1$^{-/-}$). The HeLa WRNIP1 knockout cell line was generated with the use of CRISPR/Cas9 technology by Anna Socha (Dr Martin Cohn's laboratory).

**A**




**B**

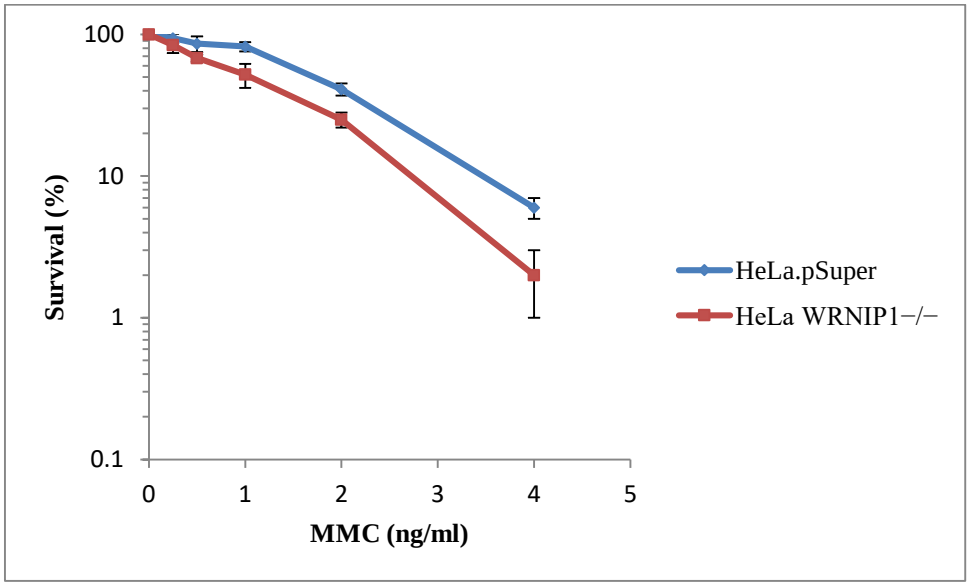
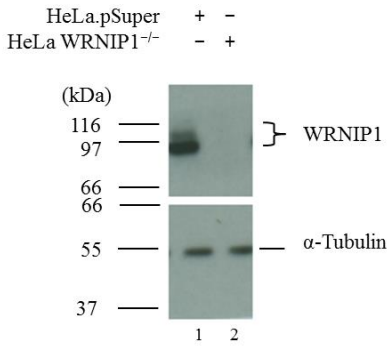



**Figure 10. WRNIP1 knockout cells are sensitive to the treatment with MMC.** (A) Western blot of untreated control HeLa cells (HeLa.pSuper) and HeLa WRNIP1 knockout cells (HeLa WRNIP1$^{-/-}$) which were used in MMC clonogenic assay. (B) Clonogenic survival assay showing survival of control HeLa cells (blue curve) and HeLa WRNIP1 knockout cells (red curve) treated with MMC. Plating efficiency of HeLa cells was 48% and plating efficiency of HeLaWRNIP1 knockout was 44%. Experiments were repeated two times with triplicates within each experiment. Error bars indicate standard errors (n=2). HeLa WRNIP1 knockout cell line was generated by Anna Socha (Dr Martin Cohn's laboratory) with the use of CRISPR/Cas9 technology.

When WRNIP1 knockout cells were treated with an alternative ICL-inducing agent, 50 ng/ml of TMP followed by irradiation with UVA (Figure 11), the cell survival mimicked the behaviour of cells treated with MMC, i.e. the WRNIP1's deficiency caused a decrease in cell survival after treatment with TMP-UVA.

In order to exclude the possibility of any secondary DNA damage caused by UVA and ensure that the damage introduced to cells was caused by combined TMP/UVA treatment (thus generating only ICLs), the control HeLa cells not treated with TMP were included in this study (Figure 11). Indeed, for the given range of UVA irradiations (10 to 320 $J/m^2$), there was no secondary damage to HeLa cells due to UVA (Figure 11). Moreover, in order to exclude a possibility of any secondary damage due to TMP or DMSO (TMP was stored in 100% DMSO), the clonogenic survival assay was performed in which control HeLa and HeLa WRNIP1 knockout cells were treated with 0, 25, 50 and 75 ng/ml TMP and were incubated for two weeks (Figure 12). No damage due to TMP treatment only was observed in both HeLa and HeLa WRNIP1 knockout cells. The final concentrations of DMSO (in which TMP was dissolved) per well were 0.0025% (when 25 ng/ml TMP added), 0.005% (when 50 ng/ml TMP added) and 0.0075% (when 75 ng/ml TMP added). Therefore, DMSO was concluded to be very diluted, thus no secondary damage to cells due to DMSO was anticipated.

**A**




**B**

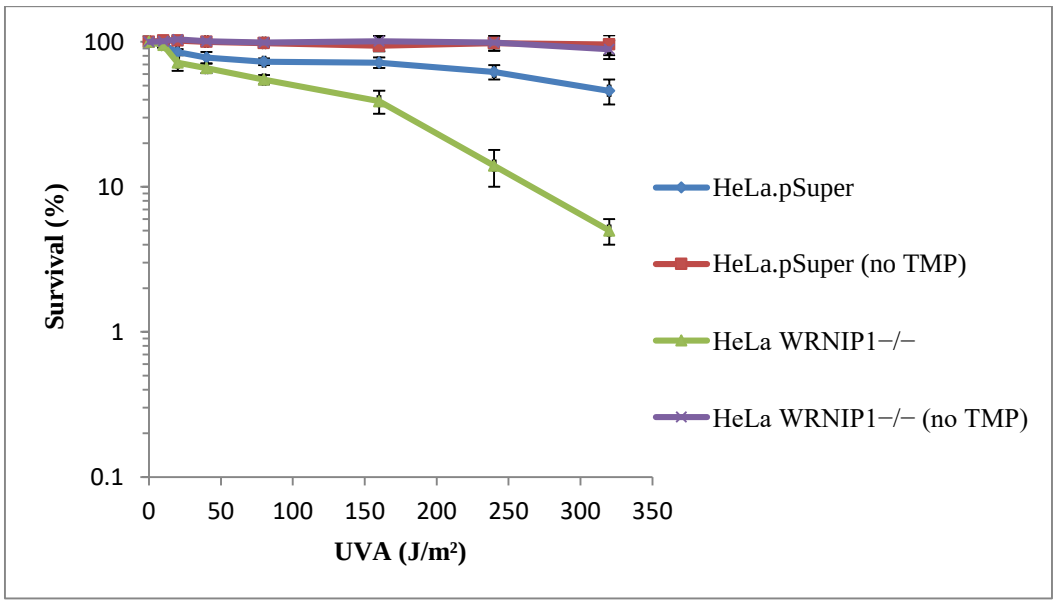
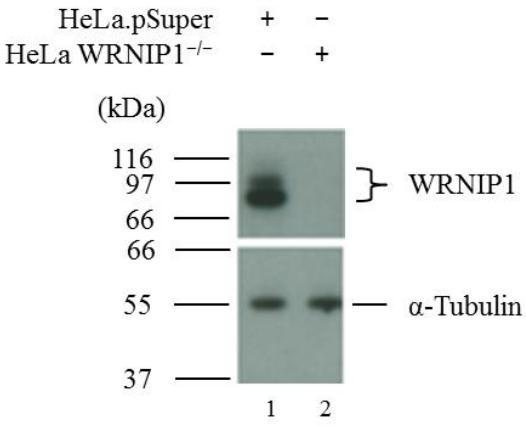



**Figure 11. WRNIP1 knockout cells are sensitive to the treatment with TMP-UVA.** (A) Western blot of untreated control HeLa cells (HeLa.pSuper) and HeLa WRNIP1 knockout cells (HeLa WRNIP1$^{-/-}$) which were used in TMP-UVA clonogenic assay. (B) The clonogenic survival assay showing survival of control HeLa cells (HeLa.pSuper) treated with 50 ng/ml TMP and UVA (blue curve), HeLa cells treated with UVA irradiation only (HeLa.pSuper (no TMP)) (red curve), HeLa WRNIP1 knockout (HeLa WRNIP1$^{-/-}$) cells treated with 50 ng/ml TMP and UVA (green curve), HeLa WRNIP1 knockout cells treated with UVA irradiation only (HeLa WRNIP1$^{-/-}$ (no TMP)) (purple curve). Plating efficiency of HeLa cells was 42% (HeLa.pSuper), 43% (HeLa.pSuper (no TMP)), 41% (HeLa WRNIP1$^{-/-}$) and 43% (HeLa WRNIP1$^{-/-}$ (no TMP)). Experiments were repeated two times with triplicates within each experiment. Error bars indicate standard error (n=2). HeLa WRNIP1 knockout cells were generated by Anna Socha (Dr Martin Cohn's laboratory) with the use of CRISPR/Cas9 technology.

**A**




**B**

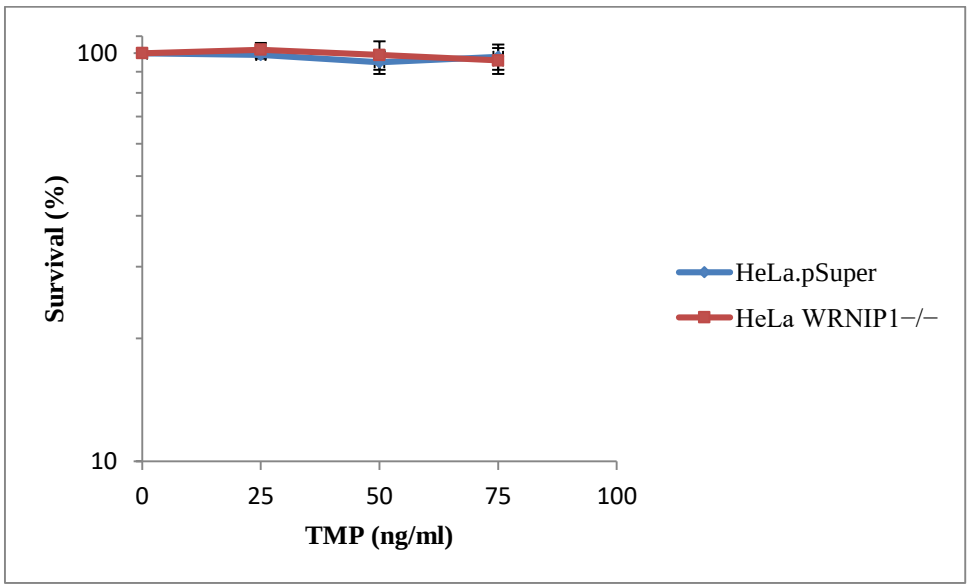
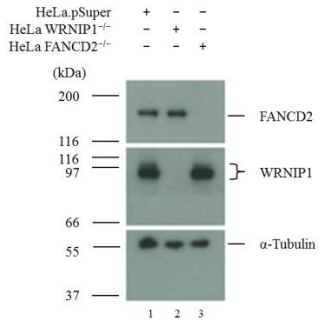



**Figure 12. WRNIP1 knockout cells are not sensitive to the treatment with TMP only.** (A) Western blot of untreated control HeLa (HeLa.pSuper) and HeLa WRNIP1 knockout (HeLa WRNIP1$^{-/-}$) cells which were used in TMP clonogenic assay. (B) Clonogenic assay showing survival of control HeLa (HeLa.pSuper) cells (blue curve) and HeLa WRNIP1 knockout (HeLa WRNIP1$^{-/-}$) cells (red curve) which were treated with TMP only. Plating efficiency of HeLa cells was 40% and plating efficiency of HeLa WRNIP1 knockout was 42%. Experiments were repeated two times with triplicates within each experiment. Error bars indicate standard error (n=2). HeLa WRNIP1 knockout cells were generated by Anna Socha (Dr Martin Cohn's laboratory) with the use of CRISPR/Cas9 technology.

The ICL-inducing TMP-UVA treatment was also investigated in a newly generated HeLa FANCD2 knockout (HeLa FANCD2$^{-/-}$) cells (Figure 13). Similarly to MMC induced-damage, the TMP-UVA treatment caused rapid decrease in the survival of cells which lacked FANCD2. Also, it was observed that WRNIP1 knockout cells showed better survival when compared with FANCD2-depleted cells (Figure 13).

**A**




**B**

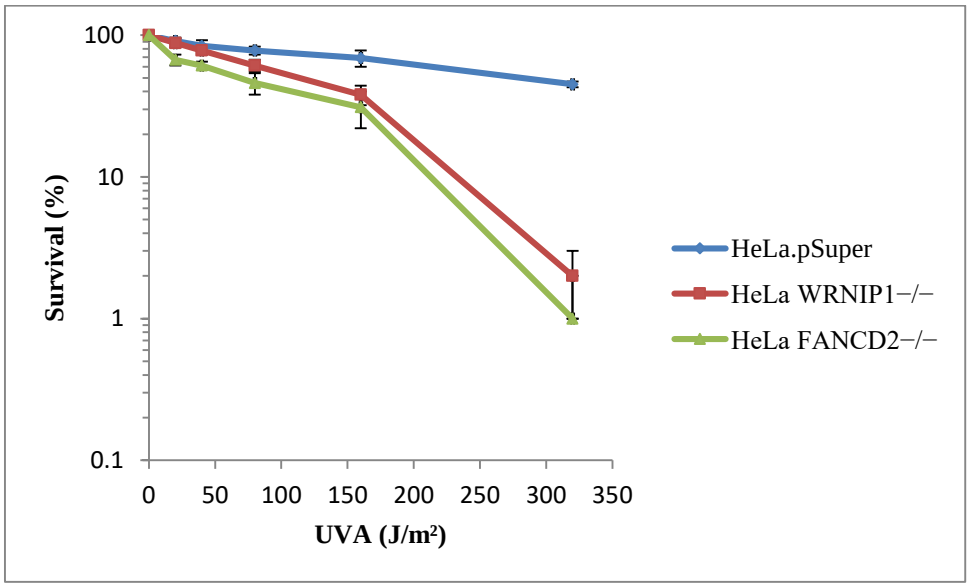
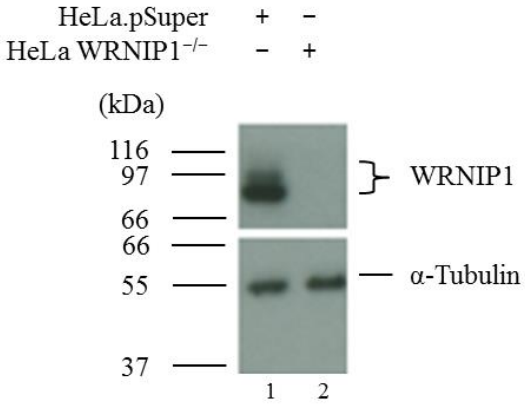



**Figure 13. WRNIP1 knockout and FANCD2 knockout cells are sensitive to the treatment with TMP-UVA.** (A) Western blot of untreated control HeLa cells (HeLa.pSuper), HeLa WRNIP1 knockout (HeLa WRNIP1$^{-/-}$) cells and HeLa FANCD2 knockout (HeLa FANCD2$^{-/-}$) cells which were used in TMP-UVA clonogenic assay. (B) The clonogenic survival assay showing survival of control HeLa (HeLa.pSuper) cells (blue curve), HeLa WRNIP1 knockout (HeLa WRNIP1$^{-/-}$) cells (red curve) and HeLa FANCD2 knockout (HeLa FANCD2$^{-/-}$) cells (green curve) treated with TMP-UVA. Plating efficiency of HeLa cells was 44%, plating efficiency of WRNIP1 knockout cells was 41% and plating efficiency of HeLa FANCD2 knockout cells was 38%. HeLa WRNIP1 knockout cells were generated by Anna Socha (Dr Martin Cohn's laboratory) and HeLa FANCD2 knockout cells were generated by David Lopez-Martinez (Dr Martin Cohn's laboratory) with the use of CRISPR/Cas9 technology. Experiment was performed once with triplicates within the experiment. Error bars indicate standard deviation.

In order to further analyse the impact of ICL-inducing genotoxic agents on the survival of WRNIP1-depleted cells, the cells were treated with cisplatin. First, the control HeLa and HeLa WRNIP1 knockout cells were treated with increasing concentrations of cisplatin. After two-week incubation, the cells were recovered, stained and counted. The results revealed that the survival of WRNIP1 knockout cells was lower than the survival of the control HeLa cells (Figure 14).

**A**




**B**

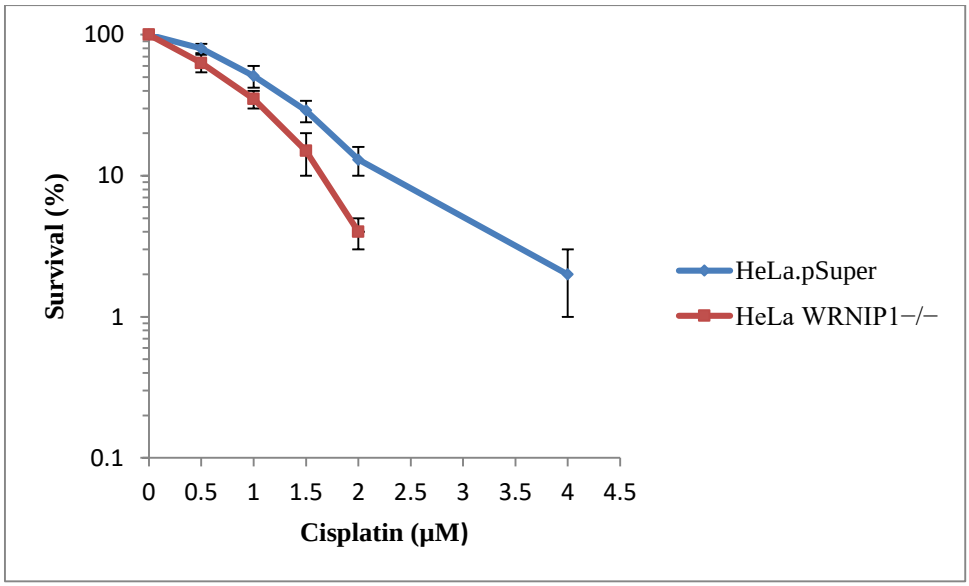
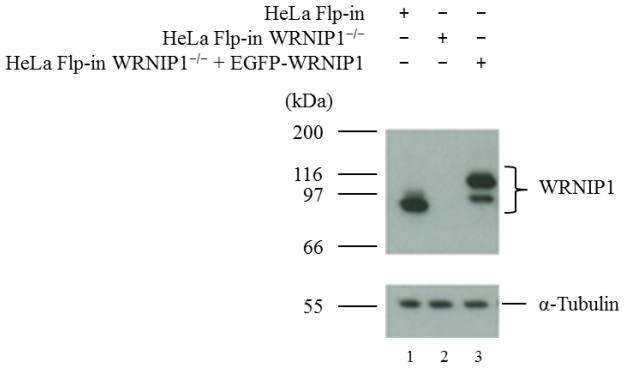



**Figure 14. WRNIP1 knockout cells are sensitive to the treatment with cisplatin.** (A) Western blot of untreated control HeLa (HeLa.pSuper) cells and HeLa WRNIP1 knockout (HeLa WRNIP1$^{-/-}$) cells which were used in the cisplatin clonogenic assay. (B) The clonogenic survival assay showing survival of control HeLa (HeLa.pSuper) cells (blue curve) and HeLa WRNIP1 knockout (HeLa WRNIP1$^{-/-}$) cells (red curve) treated with cisplatin. Plating efficiency of HeLa cells was 41% and plating efficiency of HeLa WRNIP1 knockout was 46%. HeLa WRNIP1 knockout cells were generated by Anna Socha (Dr Martin Cohn's laboratory) with the use of CRISPR/Cas9 technology. Experiments were repeated two times with triplicates within each experiment. Error bars indicate standard errors (n=2).

### 3.4 WRNIP1 partially rescues the ICL-induced DNA damage

In order to establish whether WRNIP1 showed the phenotypic similarity to more established Fanconi anemia proteins, it was investigated if WRNIP1-complemented cell line could reduce the sensitivity of cell lines to genotoxic agents, i.e. MMC (Figure 15) and TMP-UVA (Figure 16). Decreasing cell sensitivity to ICL-inducing agents after addition of WRNIP1, could imply that WRNIP1 played a role in resolving ICLs. In order to test this hypothesis, the HeLa Flp-in cells were used. WRNIP1 was depleted from these cells with the use of CRISPR/Cas9 technology. The cells were later complemented by EGFP-tagged WRNIP1. The results indicated that WRNIP1-depleted HeLa Flp-in cells were sensitive to both MMC and TMP-UVA. The WRNIP1 knockout cells which were complemented with EGFP-tagged WRNIP1 could partially rescue the sensitivity to both MMC and TMP-UVA ICL-inducing genotoxic lesions.

**A**




**B**

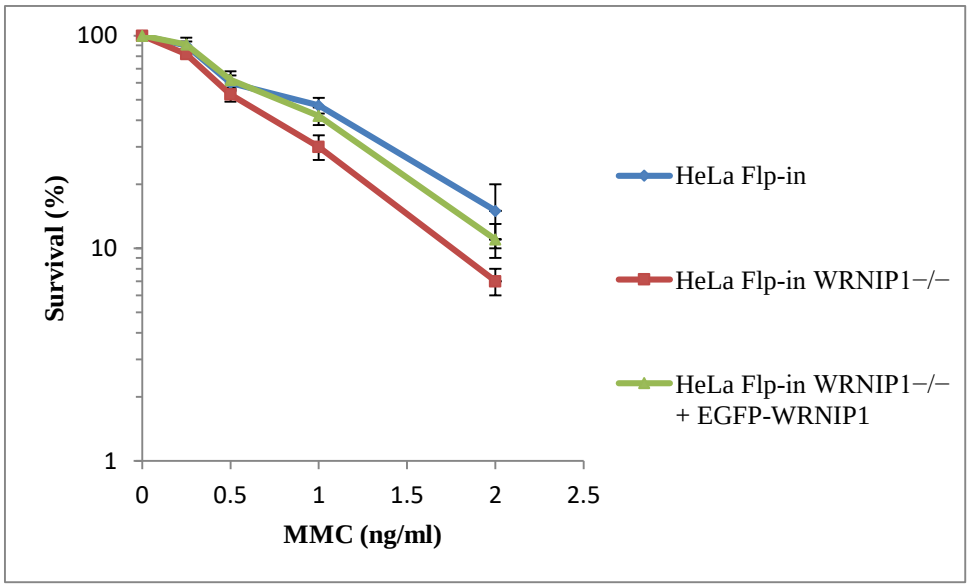
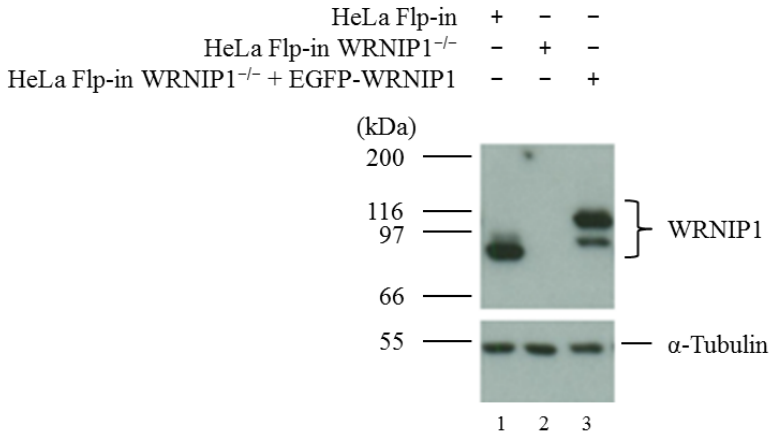



**Figure 15. WRNIP1 partially complements the cellular sensitivity to the treatment with MMC.** (A) Western blot of untreated control HeLa Flp-in cells, HeLa Flp-in WRNIP1 knockout (HeLa Flp-in WRNIP1$^{-/-}$) cells and HeLa Flp-in WRNIP1 knockout cells complemented with EGFP-tagged WRNIP1 (HeLa Flp-in WRNIP1$^{-/-}$ + EGFP-WRNIP1) which were used in the MMC clonogenic assay. (B) The clonogenic assay showing survival of HeLa Flp-in cells (blue curve), HeLa Flp-in WRNIP1 knockout (HeLa Flp-in WRNIP1$^{-/-}$) cells (red curve) and HeLa Flp-in WRNIP1 knockout cells which were complemented with EGFP-tagged WRNIP1 (HeLa Flp-in WRNIP1$^{-/-}$ + EGFP-WRNIP1) (green curve). Plating efficiency of HeLa Flp-in was 49%, 44% (HeLa Flp-in WRNIP1$^{-/-}$) and 41% (HeLa Flp-in WRNIP1$^{-/-}$ + EGFP-WRNIP1). HeLa Flp-in WRNIP1 knockout and HeLa Flp-in WRNIP1 knockout complemented with EGFP-WRNIP1 cells were generated by Anna Socha (Dr Martin Cohn's laboratory) with the use of CRISPR/Cas9 technology. Experiments were repeated three times with triplicates within each experiment. Error bars indicate standard errors (n=3).

**A**




**B**

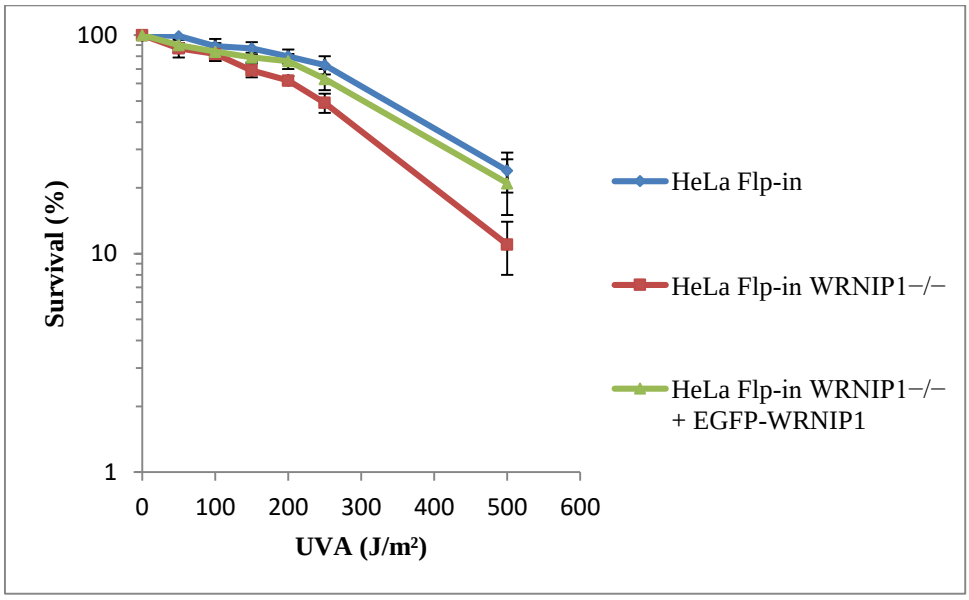



**Figure 16. WRNIP1 partially complements the cellular sensitivity to the treatment with TMP-UVA.** (A) Western blot of HeLa Flp-in cells, HeLa Flp-in WRNIP1 knockout (HeLa Flp-in WRNIP1$^{-/-}$) cells and HeLa Flp-in WRNIP1 knockout cells complemented with EGFP-WRNIP1 (HeLa Flp-in WRNIP1$^{-/-}$ + EGFP-WRNIP1). (B) The clonogenic assay showing survival of HeLa Flp-in cells (blue curve) HeLa Flp-in WRNIP1 knockout (HeLa Flp-in WRNIP1$^{-/-}$) cells (red curve) and HeLa Flp-in WRNIP1 knockout cells which were complemented with EGFP-tagged WRNIP1 (HeLa Flp-in WRNIP1$^{-/-}$ + EGFP-WRNIP1) (green curve). Plating efficiency of HeLa Flp-in was 44%, 41% (HeLa Flp-in WRNIP1$^{-/-}$) and 45% (HeLa Flp-in WRNIP1$^{-/-}$ + EGFP-WRNIP1). HeLa Flp-in WRNIP1 knockout and HeLa Flp-in WRNIP1 knockout complemented with EGFP-WRNIP1 were generated by Anna Socha (Dr Martin Cohn's laboratory) with the use of CRISPR/Cas9 technology. Experiments were repeated two times with triplicates within each experiment. Error bars indicate standard errors (n=2).

### 3.5 Discussion

The clonogenic cell survival assay experiments demonstrated that all WRNIP1 knockout cell lines showed lower survival in comparison to normal HeLa cells which were used in this study. On the other hand, WRNIP1 knockdown cell line showed sensitivity to MMC only (not cisplatin). The results of experiments where WRNIP1 knockout was used revealed that WRNIP1-depleted cells were more sensitive to all applied ICL-forming agents, i.e. MMC, TMP-UVA and cisplatin. Therefore, the lack of sensitivity of WRNIP1 knockdown cells to cisplatin could be explained by incomplete depletion of WRNIP1 from the cells. Moreover, WRNIP1-depleted cells which were complemented with EGFP-WRNIP1 partially rescued the sensitivity of cells subjected to MMC and TMP-UVA treatments. Hence, cells in which WRNIP1 was absent showed a phenotypic similarity to cells from which established members of Fanconi anemia pathway were depleted. Therefore, WRNIP1 may be necessary for repair of interstrand crosslinked and could potentially play some role of Fanconi anemia pathway due to its sensitivity to ICL-inducing genotoxic agents. However, its role may not be as pronounced as other established members of the Fanconi anemia pathway due to the mildness of the exhibited phenotypes as compared to FANCD2. This claim can be corroborated by the results of this study which demonstrated that FANCD2-deficient cells were more sensitive to both MMC as well as TMP-UVA ICL-inducing treatments as compared to WRNIP1-depleted cells. It might, thus, imply that the role of WRNIP1 in the Fanconi anemia pathway, if any, is not as significant as that of FANCD2.

# 4 An *in vivo* study of WRNIP1's response to various DNA damaging agents

## 4.1 Introduction

A study performed by Crosetto *et al.* (2008) showed that WRNIP1 was localised to the nucleus and it was demonstrated to form foci which were visible throughout the cell cycle. It was also shown that WRNIP1 itself was ubiquitinated and that WRNIP's ubiquitin chains may be linked to DNA damage response (Bish and Myers, 2007; Bish *et al.*, 2008).

The aim of this study was to investigate whether WRNIP1 was enriched in nuclear fractions after treatment with genotoxic agents, i.e. MMC or UVC, thus showing that it might function in DNA repair in the nucleus. In was also investigated whether there was a functional link between WRNIP1 and FANCD2 by examining how knockdown of WRNIP1 followed by treatment with genotoxic agent influences FANCD2 ubiquitination. It was also examined if FANCD2-depletion influenced WRNIP1's ubiquitination. Moreover, the functional link was attempted to be further established by examining the formation of FANCD2 foci after MMC treatment of WRNIP1-depleted cells. The examination of the enrichment of WRNIP1 in nuclear fraction after MMC or UVC treatment, FANCD2 and WRNIP1 ubiquitination patterns after treatment with genotoxic agents as well as WRNIP1's possible impact on FANCD2 foci formation would help in understanding whether WRNIP1 might play some role in DNA repair and if it affects FANCD2.

### 4.2 WRNIP1 is not significantly enriched in nuclear fractions after genotoxic agent treatment.

In order to establish whether WRNIP1 played a role as a DNA repair protein, the nuclear localization of WRNIP1 upon genotoxic agent treatment was investigated. HeLa (HeLa.pSuper) cells were treated with 160 ng/ml of MMC, incubated for 0, 3, 6, 9 and 24 h, and fractionated into nuclear and cytoplasmic fractions. The fractions were run on the SDS-PAGE gels and analysed with various antibodies. FANCD2 was included in this experiment as a positive control. It could be observed that the appearance of FANCD2 monoubiquitinated upper form was increasing with the length of time during which the cells were treated with MMC (Figure 17). The monoubiquitinated upper form of FANCD2 was visible in the nuclear fractions only. The amount of WRNIP1 was only very slightly increased in the nuclear fraction between 0 and 24 h (Figure 17). This gentle increase was regarded to be insignificant.

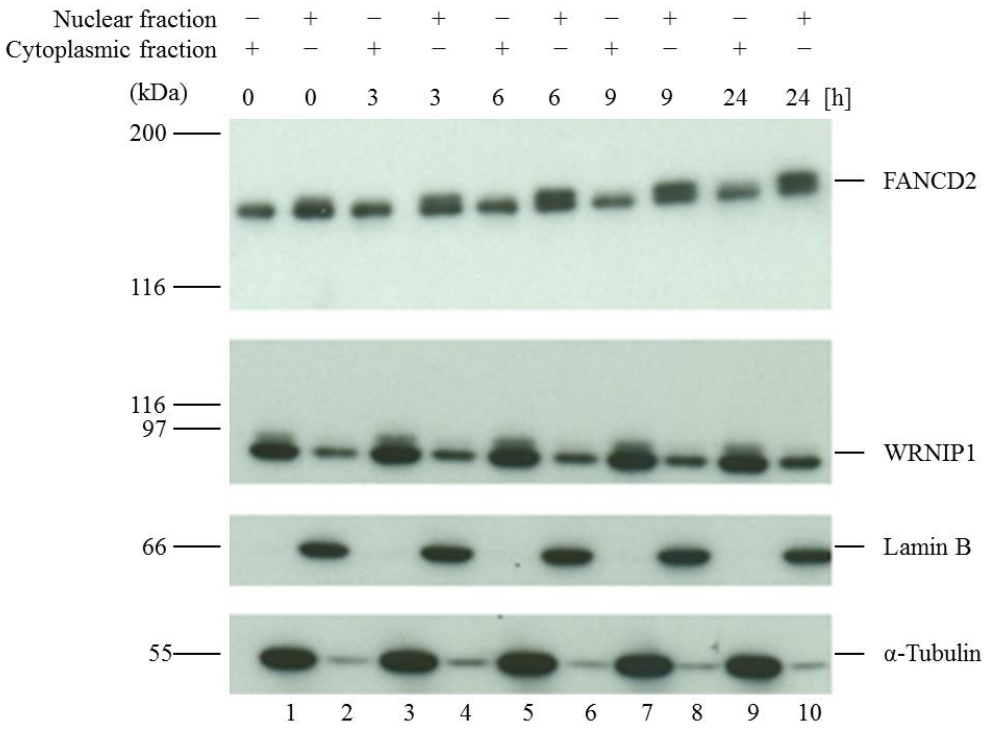



**Figure 17. Western blot analysis of MMC-treated and fractionated HeLa cells** The HeLa (HeLa.pSuper) cells were treated with MMC over a time course of 0, 3, 6, 9 and 24 h. After treatment with MMC, the cells were fractionated into nuclear and cellular fractions with cytoskeletal buffer containing 0.5% (v/v) Triton. The antibodies used in this experiment were α-FANCD2 (1:100 dilution), α-WRNIP1 (1:2000 dilution), α-Lamin B (1:200 dilution) and α-α-Tubulin (1:2000 dilution).

It was also investigated whether the amount of WRNIP1 which was present in nuclear fractions increased after treatment with UVC irradiation of 25 J/m$^2$. HeLa (HeLa.pSuper) cells were UVC-irradiated, incubated for 0, 3, 6 and 9 hours, and the resultant cells were fractionated into nuclear and cytoplasmic fractions. The fractions were run on SDS-PAGE gels and analysed with various antibodies (Figure 18). The results indicated that FANCD2 monoubiquitination was increasing with incubation time in the nuclear fraction. On the other hand, the amount of WRNIP1 in both nuclear and cellular fractions remained the same during the time course experiment.

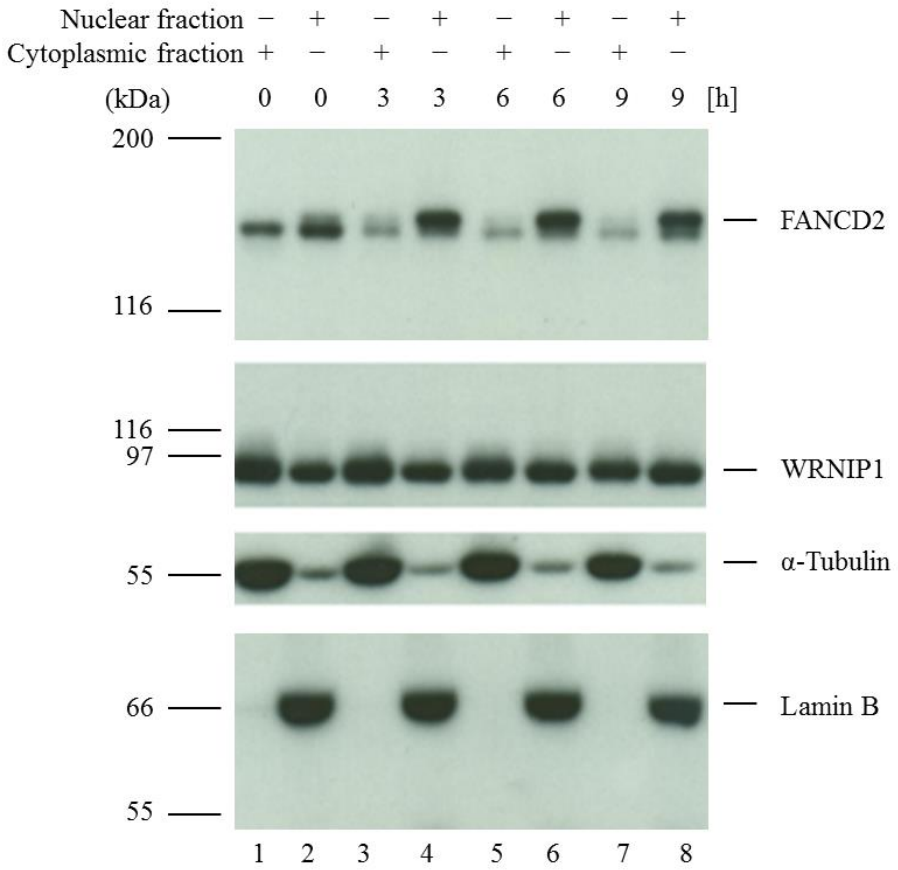



**Figure 18. Western blot analysis of UVC-treated and fractionated HeLa cells** The HeLa (HeLa.pSuper) cells were irradiated with 25 J/m2 UVC over a time course of 0, 3, 6 and 9 h. After treatment with UVC, the cells were fractionated into nuclear and cellular fractions with cytoskeletal buffer containing 0.5% (v/v) Triton. The antibodies used in this experiment were α-FANCD2 (1:100 dilution), α-WRNIP1 (1:2000 dilution), α-Lamin B (1:200 dilution) and α-α-Tubulin (1:2000 dilution).

### 4.3 FANCD2 deficiency does not influence WRNIP1's levels in the nucleus.

In order to establish whether WRNIP1 interacted with FANCD2, and therefore, was a candidate component of the Fanconi anemia pathway, the impact of WRNIP1 deficiency on FANCD2 monoubiquitination was investigated. HeLa and HeLa WRNIP1 knockdown cells were utilized in this study. Subsequently, HeLa cells were treated with various genotoxic agents, i.e. MMC and TMP-UVA. Both of these

treatments were inducing various types of ICLs (Donkert *et al.*, 2001; Lopez-Martinez *et al.*, 2016). Moreover, two fractionation methods were used in order to analyse how WRNIP1 deficiency influenced monoubiquitination of FANCD2. It was also observed how FANCD2 deficiency influenced WRNIP1 ubiquitination. First, the cytoskeletal-buffer method was used in which cells were fractionated into nuclear and cytoplasmic fractions. In this fractionation method, the integrity of the nucleus was not maintained. Second, in order to keep all the nuclear proteins inside the nucleus, an alternative fractionation method was applied in which the integrity of nucleus was maintained (Materials and Methods).

First, the cytoskeletal (CSK) buffer was used during fractionation and the integrity of the nucleus might not have been complete. Moreover, the impact of FANCD2 knockdown on WRNIP1 was examined. The HeLa, HeLa WRNIP1 knockdown cells and HeLa FANCD2 knockdown cells were treated with MMC (Figure 19) or TMP-UVA (Figure 20) and incubated for 0, 3, 6 or 9 h and 0, 1, 3 and 6 h, respectively. After incubation, the cells were fractionated into nuclear and cytoplasmic fractions. The results included nuclear fractions only and showed that FANCD2 monoubiquitination was not influenced by deficiency of WRNIP1. Similar outcomes were obtained for both MMC and TMP-UVA-treated samples (Figures 19 and 20). After investigation of the impact of WRNIP1 deficiency on FANCD2 ubiquitination, also the influence of FANCD2 knockdown on WRNIP1 ubiquitination was examined. The results indicated that for both MMC and TMP-UVA-treated samples and when FANCD2 was depleted from the cells, WRNIP1's levels were not altered in nuclear fractions (Figures 19 and 20).

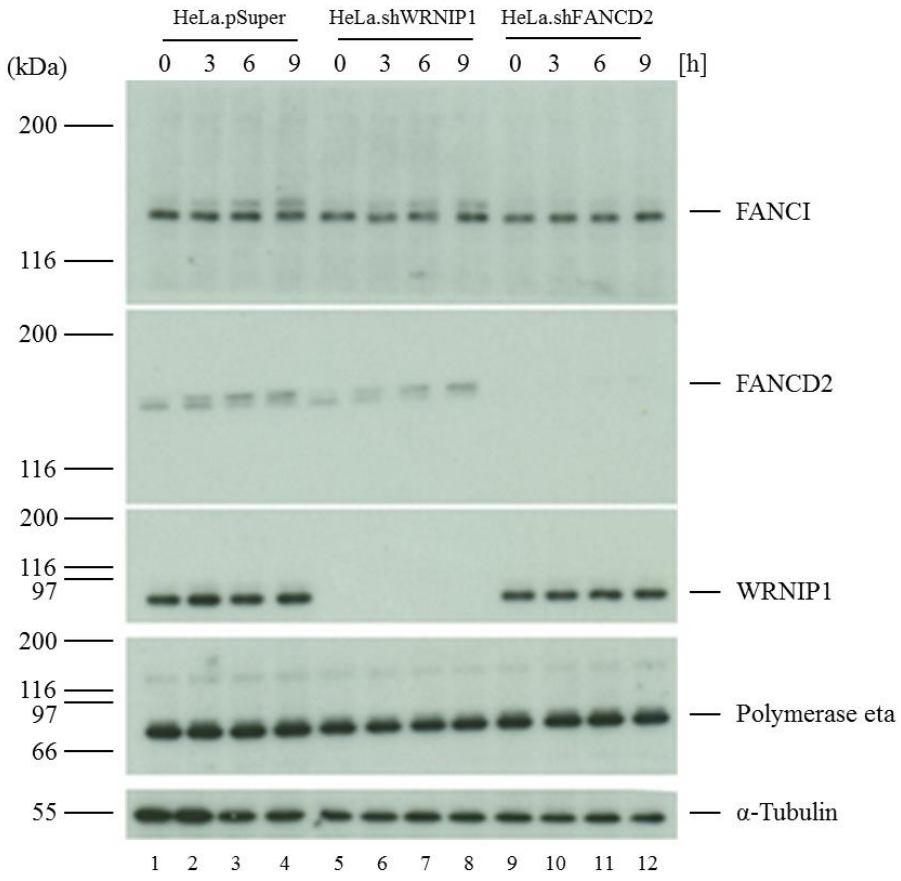



**Figure 19. Western blot analysis of MMC-treated nuclear fractions of HeLa cells** HeLa (HeLa.pSuper) cells, HeLa WRNIP1 knockdown (HeLa.shWRNIP1) cells and HeLa FANCD2 knockdown (HeLa.shFANCD2) cells were used in this experiment. The cells were treated with 160 ng/ml MMC. The cells were incubated for 0, 3 and 6 h. After incubation, the cells were fractionated into nuclear and cytoplasmic fractions. The antibodies used in this experiment were α-FANCD2 (1:100 dilution), α-WRNIP1 (1:2000 dilution), α-FANCI (1:1000 dilution), α-Lamin B (1:200 dilution), α-α-Tubulin (1:2000 dilution) and α-Polymerase eta (1:1000 dilution). The HeLa FANCD2 knockdown cells were generated by Caroline Schneider (Dr Martin Cohn's laboratory).

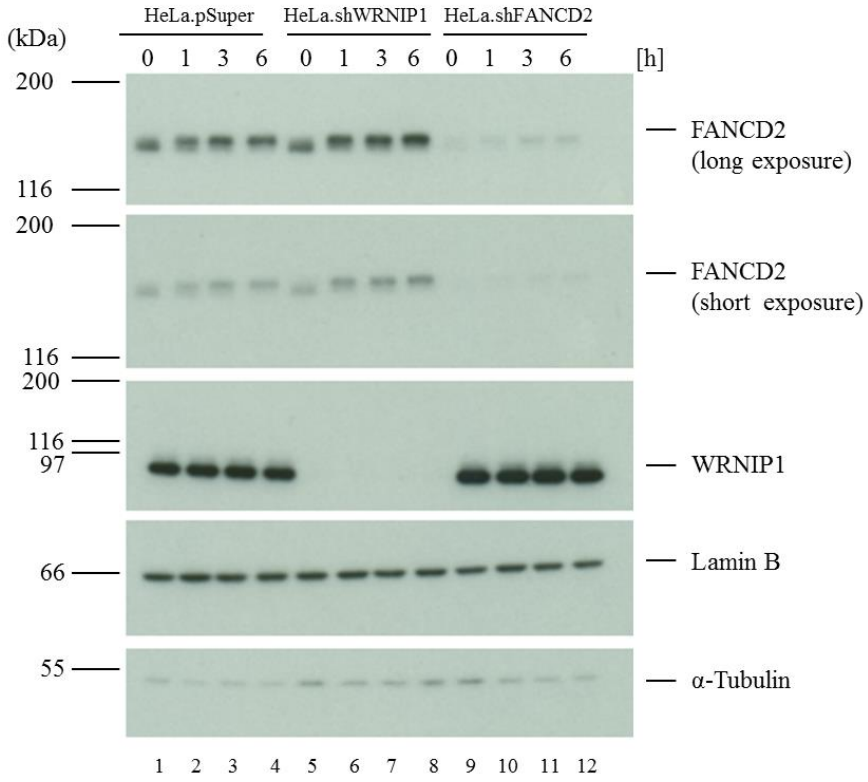



**Figure 20. Western blot analysis of TMP-UVA-treated nuclear fractions of HeLa cells.** The HeLa (HeLa.pSuper), HeLa WRNIP1 knockdown (HeLa.shWRNIP1) cells and HeLa FANCD2 knockdown (HeLa.shFANCD2) cells were used in this experiment. The cells were treated with 500 ng/ml TMP and irradiated with 250 J/m2 UVA. The cells were incubated for 0, 1, 3 and 6 h. After incubation, the cells were fractionated into intact nuclear and cytoplasmic fractions. The antibodies used in this experiment were α-FANCD2 (1:100 dilution), α-WRNIP1 (1:2000 dilution), α-FANCI (1:1000 dilution), α-Lamin B (1:200 dilution) and α-α-Tubulin (1:2000 dilution). The HeLa FANCD2 knockdown cells were generated by Caroline Schneider (Dr Martin Cohn's laboratory).

After investigating the lack of change in monoubiquitination patterns of FANCD2 and WRNIP1 after both MMC and TMP-UVA treatments, the alternative fractionation method was applied, in which the cell nuclei were kept intact. In this study, the cells were treated with MMC (Figure 21) and TMP-UVA (Figure 22) and were fractionated, so that the integrity of the nucleus was maintained. HeLa and HeLa WRNIP1 knockdown cells were used in this analysis. It was shown, however, that FANCD2

monoubiquitination did not change in WRNIP1-depleted cells which were treated with MMC (Figure 21) or TMP-UVA (Figure 22).

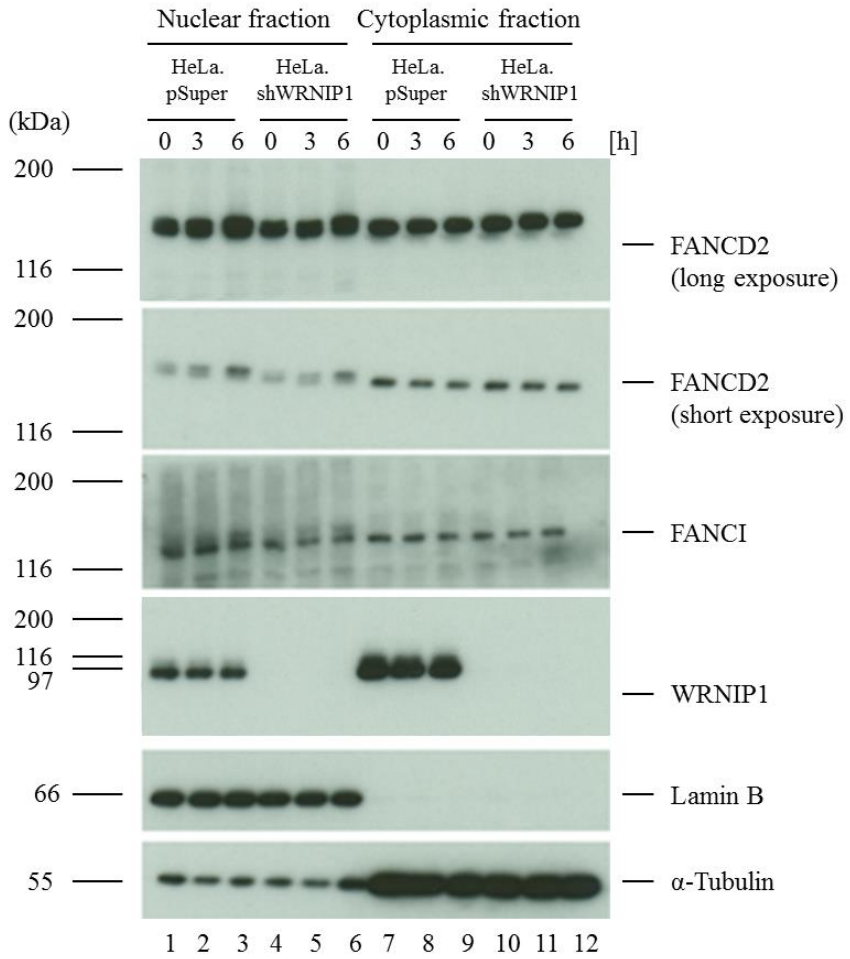



**Figure 21. Western blot analysis of MMC-treated nuclear and cytoplasmic fractions of HeLa cells.** The HeLa (HeLa.pSuper) cells and HeLa WRNIP1 knockdown (HeLa.shWRNIP1) cells were used in this experiment. The cells were treated with 160 ng/ml MMC and incubated for 0, 3 and 6 h. After incubation, the cells were fractionated into intact nuclei and cytoplasmic fractions. The antibodies used in this experiment were α-FANCD2 (1:100 dilution), α-WRNIP1 (1:2000 dilution), α-FANCI (1:1000 dilution), α-Lamin B (1:200 dilution) and α-α-Tubulin (1:2000 dilution).

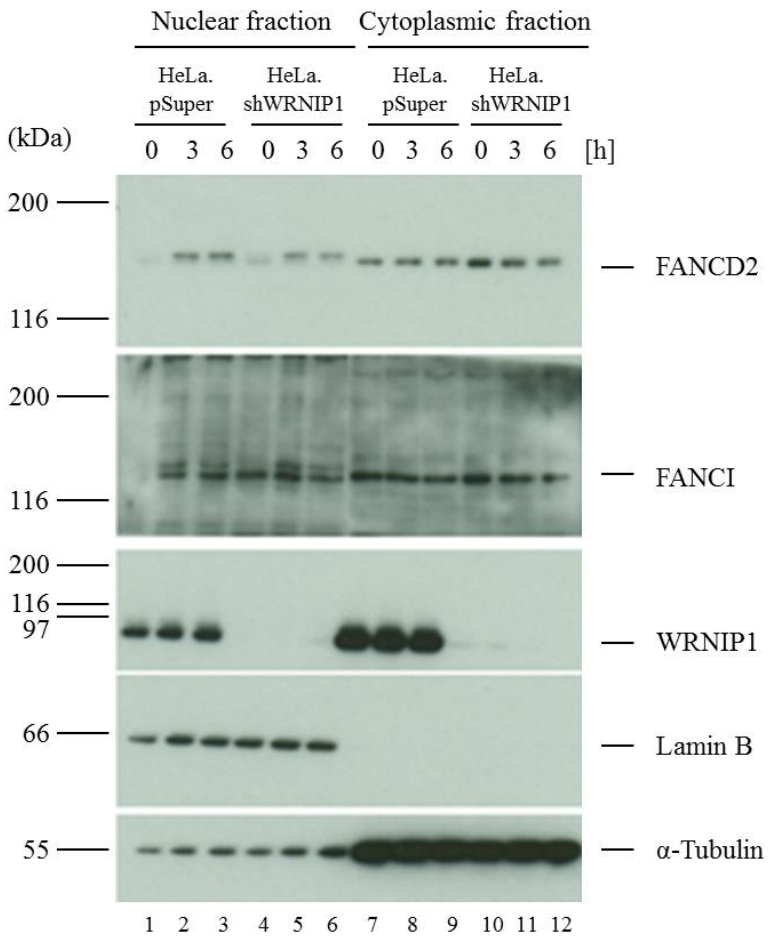



**Figure 22. Western blot analysis of TMP-UVA-treated nuclear and cytoplasmic fractions of HeLa cells.** The HeLa (HeLa.pSuper) cells and HeLa WRNIP1 knockdown (HeLa.shWRNIP1) cells were used in this experiment. The cells were treated with 500 ng/ml TMP and irradiated with 250 J/m$^2$ UVA. The cells were incubated for 0, 3 and 6 h. After incubation, the cells were fractionated into intact nuclei and cytoplasmic fractions. The antibodies used in this experiment were α-FANCD2 (1:100 dilution), α-WRNIP1 (1:2000 dilution), α-FANCI (1:1000 dilution), α-Lamin B (1:200 dilution) and α-α-Tubulin (1:2000 dilution).

### 4.4 WRNIP1 deficiency does not influence FANCD2 foci formation

In order to establish whether WRNIP1 interacts with FANCD2 and therefore could be a potential Fanconi anemia protein, the impact of WRNIP1 depletion on FANCD2 foci formation was investigated by immunofluorescence microscopy analysis. During this analysis, HeLa (HeLa.pSuper) cells (Figure 23 A) and HeLa WRNIP1 knockdown (HeLa.shWRNIP1) cells (Figure 23 B) were used. The cells were treated with 160 ng/ml of MMC at 0, 4 and 8 h time intervals in order to observe any changes in the foci formation. The FANCD2 repair foci were visualized with immunofluorescence microscopy. At least 50 cells were counted in each experiment. The nuclei, which had more than 20 FANCD2 foci, were counted in both HeLa and HeLa WRNIP1 knockdown cells (Figure 23 C). Although the number of FANCD2 foci was increasing with time, the number of cells with more than 20 FANCD2 foci for each individual time point was similar in both HeLa and HeLa WRNIP1 knockdown cells. The number of cells with more than 20 FANCD2 foci was slightly higher in HeLa cells at both 4 and 8 h time points than in HeLa WRNIP1knockdown cells. However, these differences were not significant.

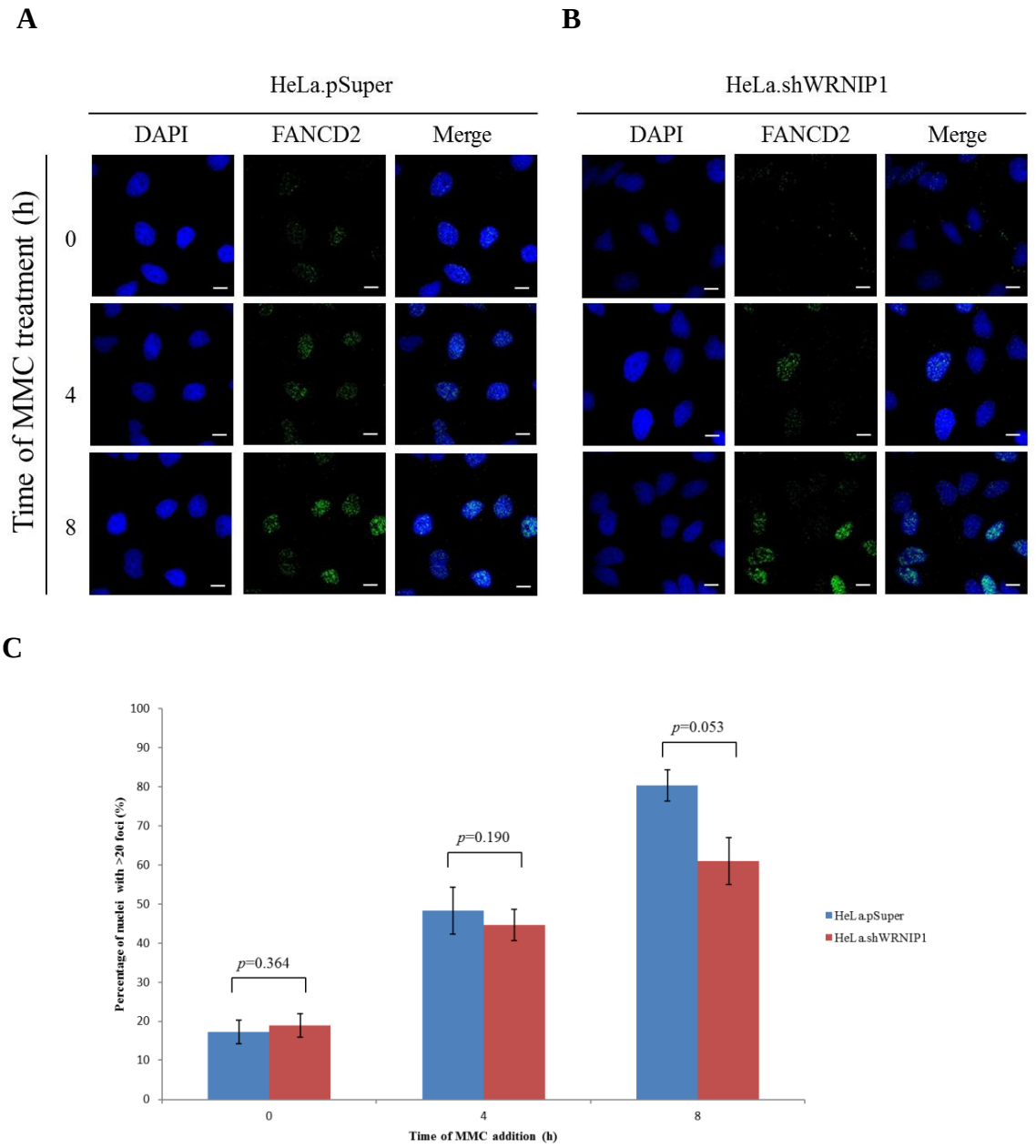



**Figure 23. WRNIP1 does not influence FANCD2 foci formation** (A) Representative images of immunofluorescence analysis of HeLa (HeLa.pSuper) cells (B) Representative images of immunofluorescence analysis of HeLa WRNIP1 knockdown (HeLa.shWRNIP1) cells. The first column of both panels A and B shows nuclei stained with DAPI. The middle column in each panel represents FANCD2 foci. The column on the right of each panel is a merge between DAPI and FANCD2 channels. The top row of each panel represents the untreated HeLa cells, a middle row shows cells treated for four hours with MMC, whereas the bottom row shows nuclei treated for eight hours with MMC. (C) Quantification of the percentage of nuclei with more than 20 foci. A minimum of 50 cells were counted for each individual experiment. Experiments were repeated three times (n=3). Error bars indicate standard errors. Student's two-tailed t-test was used to calculate significance. Scale bars represent 10 μm.

## 4.5 Discussion

It was investigated in this chapter whether WRNIP1 was enriched in the nuclear fractions after genotoxic agent treatment. It was examined whether FANCD2 monoubiquitination was influenced by WRNIP1 deficiency and *vice versa*. Furthermore, the impact of WRNIP1 deficiency on FANCD2 foci formation following DNA damage was examined as well.

The obtained results indicated that WRNIP1 was only minimally enriched in nuclear fraction when MMC treatment was applied. However, this increase was not regarded as significant. WRNIP1 was not enriched when UVC was used. MMC treatment introduced ICLs into chromatin, thus employing the Fanconi anemia pathway machinery, which repaired the induced damage. On the other hand, UVC treatment stalled replication forks and also resulted in the activation of the Fanconi anemia pathway which was indicated by monoubiquitination of FANCD2. The outcomes of this study showed that WRNIP1's presence in the nucleus did not show a significant increase after treatment with genotoxic agents.

The fractionation studies in which two fractionation methods were applied indicated that WRNIP1 was present in nuclear fractions after both MMC and TMP-UVA-treatments. Both of these treatments introduced two different types of ICLs. Upon treatment of FANCD2 deficient cell line with genotoxic agents, there was no alteration in the ubiquitination levels of WRNIP1. This result suggested that WRNIP1 might act independently of FANCD2 as a DNA repair protein or that it might act downstream of FANCD2 in the Fanconi anemia pathway. When WRNIP1 was deficient from the fractionation samples, FANCD2 monoubiquitination patterns did not change. This

outcome corroborated the previous result that WRNIP1 might act downstream of FANCD2, thus not altering the FANCD2 monoubiquitination levels.

The immunofluorescence analysis showed an increase in FANCD2 foci formation with time for both HeLa and HeLa WRNIP1 knockdown cells after treatment with MMC. Although the number of FANCD2 foci was slightly higher for HeLa cells as compared to HeLa WRNIP1 knockdown cells at 4 and 8 h time points, neither of these differences were significant. This result might suggest that WRNIP1 does not play a role in FANCD2 foci formation.

Overall, the results obtained in this study showed that WRNIP1 neither affected FANCD2 foci formation nor FANCD2 monoubiquitination and that its enrichment in nuclear faction after genotoxic agent treatment were not regarded as significant. These results would suggest that if WRNIP1 acted in the Fanconi anemia pathway, it would act downstream of FANCD2 as it did not influence its monoubiquitination levels nor the FANCD2 foci formation.

# 5 *In vitro* interactions between WRNIP1 and components of FANCD2/FANCI heterogeneous complex

## 5.1 Introduction

Werner helicase interacting protein 1 (WRNIP1) was identified by Kawabe *et al.* (2001) as an interacting partner of Werner helicase (WRN) by yeast two-hybrid assay. However, despite the interaction of both proteins both *in vivo* and *in vitro*, the role of WRNIP1 has not been established yet. WRNIP1 is a highly-conserved 665 amino acid-long protein and it is known to contain ubiquitin binding zinc finger domain (UBZ) which is located at its N-terminus. The UBZ domain of WRNIP1 was demonstrated to function in its ubiquitination, targeting WRNIP1 to the stalled replication forks (Crosetto *et al*., 2008) as well as double-strand breaks (Nomura *et al*., 2012). The second identified functional structure in WRNIP1 is ATPase domain located in the middle of the protein. It consists of two motifs, i.e. Walker A and Walker B. The Walker A motif of the ATPase domain was demonstrated to interact with WRN in an ATP-dependent manner (Kawabe *et al*., 2006). The C-terminus of WRNIP1 was shown to contain two leucine zippers which were preliminarily predicted to function in WRNIP1's oligomerization as well as to play a role in targeting WRNIP1 to the stalled replication forks (Crosetto *et al*., 2008).

WRNIP1 was demonstrated previously to interact with proteins which were suggested to function in the DNA replication or repair, i.e. WRN, Rad18 and pol η and pol δ. A budding yeast orthologue of WRNIP1, Mgs1, was also implicated in interaction with PCNA. It has been suggested *via* numerous studies that WRNIP1 might be a DNA repair protein itself. It was shown that WRNIP1 forms foci inside the cell nucleus. The

number of foci increased when the cells were treated with genotoxic agents. Moreover, Nomura *et al*. (2012) demonstrated that WRNIP1 localises to the laser-irradiated sites in mammalian cells nuclei. The level of the irradiation showed that WRNIP1 accumulated to the irradiated sites when single- as well as double-strand breaks where introduced into chromatin. Moreover, the presence of UBZ domain was linked to DNA repair proteins, e.g. FAN1, pol η or SLX4. The proteins which have this domain are associated with translesion synthesis or the Fanconi anemia DNA repair pathways. Therefore, it was suggested that WRNIP1 might be a repair protein which functions as a component of either of these DNA repair mechanisms.

The initial aim of this study to was to purify WRNIP1 from the Sf9 insect cells and examine whether it interacted with one of the main components of the Fanconi anemia pathway, i.e. FANCD2 *in vitro*. After establishing this objective, it was intended to map a domain which WRNIP1 interacted with FANCD2 by introduction of deletions into WRNIP1's DNA sequence. Subsequently, the interaction between WRNIP1 and the second component of the Fanconi anemia pathway and a binding partner of FANCD2, i.e. FANCI was investigated. FANCD2 and FANCI are known to form heterodimer complex which is recruited to the site where DNA have been affected by introduction of the ICL. Therefore, FANCI was chosen to be investigated as WRNIP1's *in vitro* binding partner as well. Finally, an interaction between all three proteins: WRNIP1, FANCD2 and FANCI was examined.

## 5.2 Cloning, expression, purification and characterization of WRNIP1

In order to determine whether WRNIP1 is a component of the FA pathway and establish if it interacts with FANCD2 or FANCI *in vitro*, it was first necessary to epitope-tag WRNIP1 and purify it as a recombinant protein. First, a full length cDNA sequence of human WRNIP1 was generated by reverse transcription PCR from total RNA obtained from HeLa (HeLa.pSuper) cells. The resultant cDNA of WRNIP1 was digested with BamHI and SalI restriction enzymes and inserted into 6xHis- and Strep(II)-tag bearing pFastBac1 vector. Both tags were located upstream of the WRNIP1 N-terminus. The resultant sequence was expressed with the use of the Invitrogen Baculovirus Expression Vector System in the Sf9 insect cells (Figure 24) and purified with $Ni^{2+}$-NTA and StrepTactin beads. SDS-PAGE gel electrophoresis followed by Coomassie staining revealed that WRNIP1 existed in two forms, i.e. more abundant fast migrating lower form which run at about 75 kDa and less abundant slow migrating upper form which run around 106 kDa (Figure 25 A). Western blotting with α-WRNIP1 antibody confirmed that both upper and lower forms represent WRNIP1 (Figure 25 B). It was further confirmed by Western blotting of StrepTactin eluates that both observed forms of WRNIP1 were His-tagged (Figure 25 C).

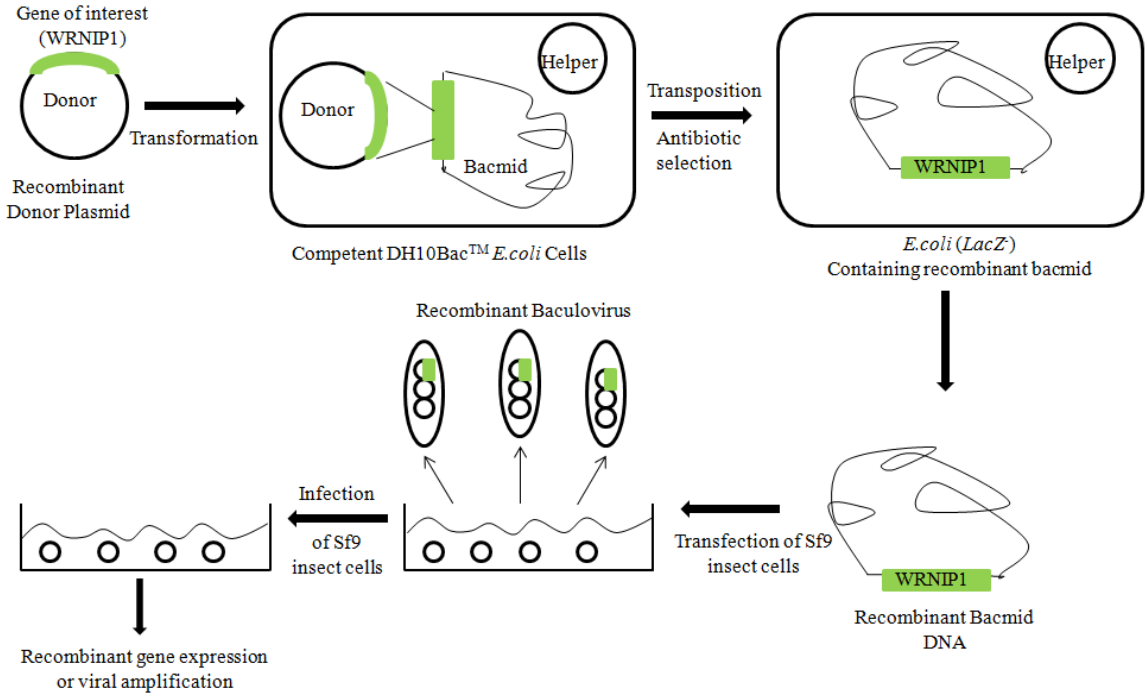
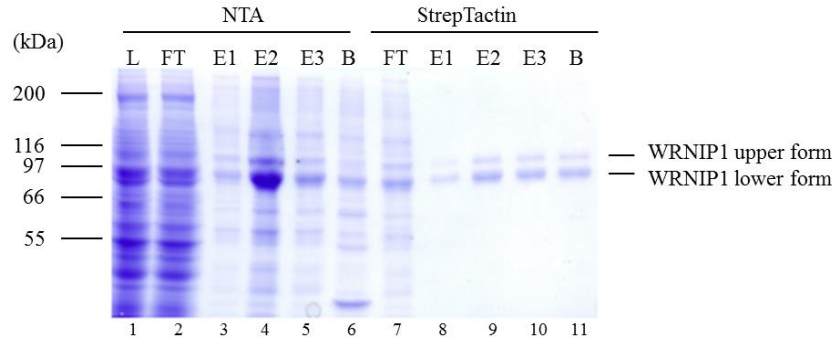
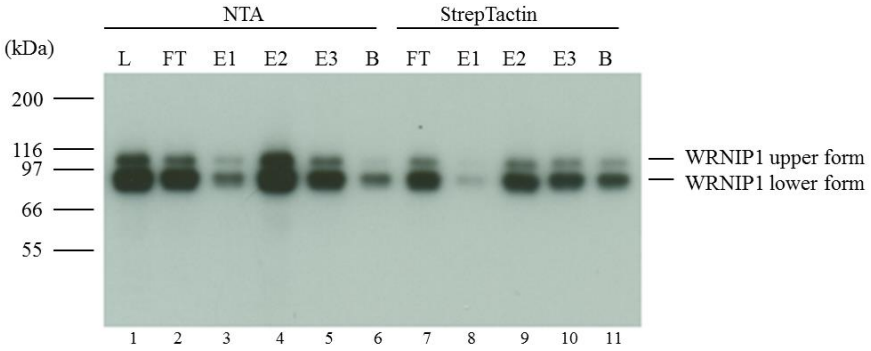



**Figure 24. Generation of recombinant baculovirus and the expression of WRNIP1 with the use of Bac-to-Bac® Baculovirus Expression System**

**A**




**B**




**C**

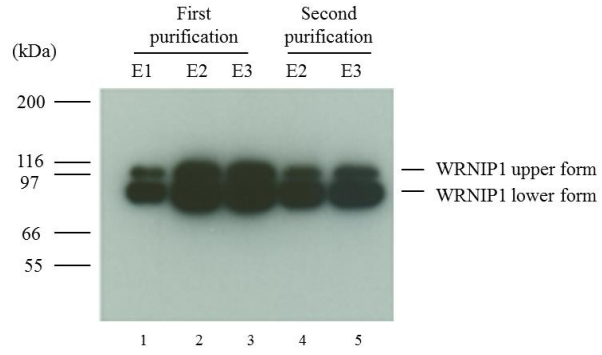



**Figure 25. Coomassie blue stain and Western blot analysis of Sf9 insect cell purified His- and Strep(II)-tagged WRNIP1** (A) SDS-PAGE followed by Coomassie staining of WRNIP1 purified from Sf9 insect cells. Order on a SDS-PAGE gel: 1) NTA L – lysate, 2) NTA FT – flow-through, 3) NTA E1 – eluate 1, 4) NTA E2 – eluate 2, 5) NTA E3 – eluate 3, 6) NTA B – beads, 7) StrepTactin FT – flow-through, 8) StrepTactin E1 – eluate 1, 9) StrepTactin E2 – eluate 2, 9) StrepTactin E3 – eluate 3, 10) StrepTactin B – beads. (B) Western blotting analysis of Sf9 purified WRNIP1. α-WRNIP1 antibody was used (1:2000 dilution). The order on the SDS-PAGE was the same as in (A). (C) Western blot analysis of Sf9 purified WRNIP1 eluates. The eluates were obtained from two NTA and StrepTactin purifications. α-His antibody was used (1:1000 dilution).

### 5.3 *In vitro* binding between WRNIP1 and FANCD2

After purification of His- and Strep(II)-tagged WRNIP1 from Sf9 insect cells, it was possible to investigate whether WRNIP1 and FANCD2 interacted with each other *in vitro*. In order to examine whether there was a possibility of interaction, an *in vitro* binding experiment was conducted. First, the Flag- and HA-tagged FANCD2 was purified from Sf9 insect cells (a recombinant FANCD2 was obtained from Chih-Chao Liang, Dr Martin Cohn laboratory). A previously prepared His- and Strep(II)-tagged WRNIP1 was used in this study as well as His-tagged MBP (His-tagged MBP was obtained from Prof. Mark Howarth laboratory). His-tagged MBP was a negative control in this experiment. Second, the *in vitro* binding experiment was conducted where FANCD2 and WRNIP1 were incubated together in the equimolar quantities for an hour at 4°C in a final volume of 10 µl. After incubation, the 10 µl of α-HA bead slurry was added to the proteins and the Eppendorf tube containing the proteins was incubated at 4°C for 30 minutes on the rotor. After the incubation was finished, the α-HA beads were recovered from the Eppendorf tube and were loaded on the column. The beds were washed on the column with 3 ml of binding buffer containing 0.1% (v/v) Tween-20. The proteins were eluted from the column with 1X LDS/loading dye. The *in vitro* binding demonstrated that Flag- and HA-tagged FANCD2 interacted with α-HA beads and WRNIP1 was pulled down with it (Figure 26). This experiment showed that FANCD2 was binding to α-HA beads as expected, whereas WRNIP1 and MBP did not. The lack of binding between WRNIP1 to the α-HA beads demonstrated that there was no unspecific binding. The His-tagged MBP negative control did not co-immunoprecipitate with FANCD2, thus corroborating the finding that WRNIP1 interacts with FANCD2 (Figure 26).

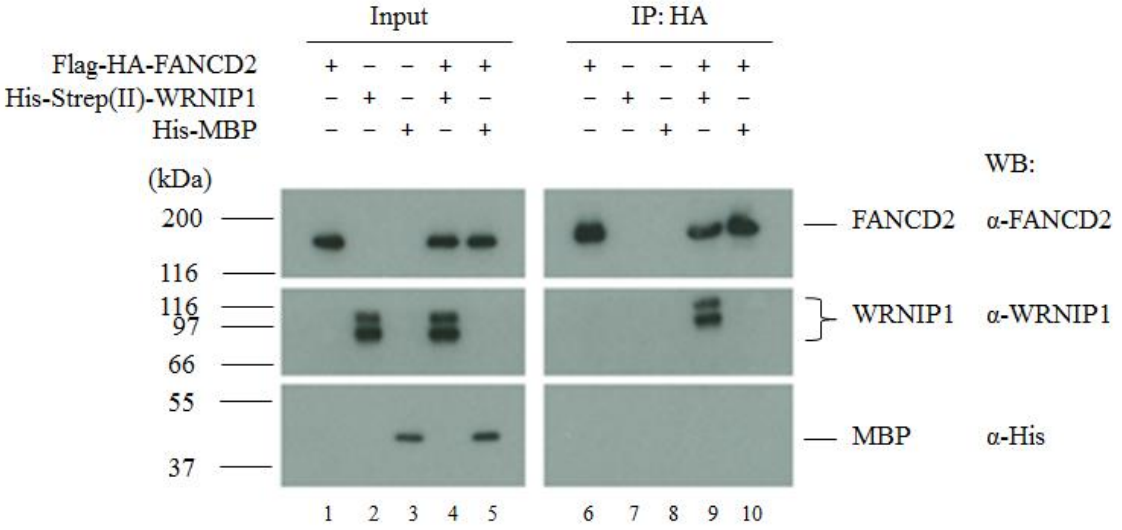



**Figure 26. WRNIP1 interacts with FANCD2 *in vitro*** Western blot analysis showing *in vitro* binding between His-Strep(II)-tagged WRNIP1 and Flag-HA-FANCD2. His-MBP was used as a negative control and did not interact with FANCD2 (His-MBP was obtained from Prof. Mark Howarth's laboratory). WB indicates Western blot. Antibodies used in this experiment were α-FANCD2 (1:100 dilution), α-WRNIP1 (1:2000 dilution) and α-His (1:1000 dilution).

### 5.4 *In vitro* binding between FANCD2 and WRNIP1 deletion mutants

In order to investigate which amino acid sequence of WRNIP1 (Figure 27 A) interacted with FANCD2 *in vitro*, three WRNIP1 deletion mutants were generated, i.e. UBZ deletion (Figure 27 B), ATPase deletion (Figure 27 C) and C-terminus deletion (Figure 27 D) mutants. The WRNIP1 mutants with two additional deletions were also generated (Figures 28 A and B). However, due to low concentrations of purified proteins, these deletion mutants could not be used in *in vitro* binding analysis.

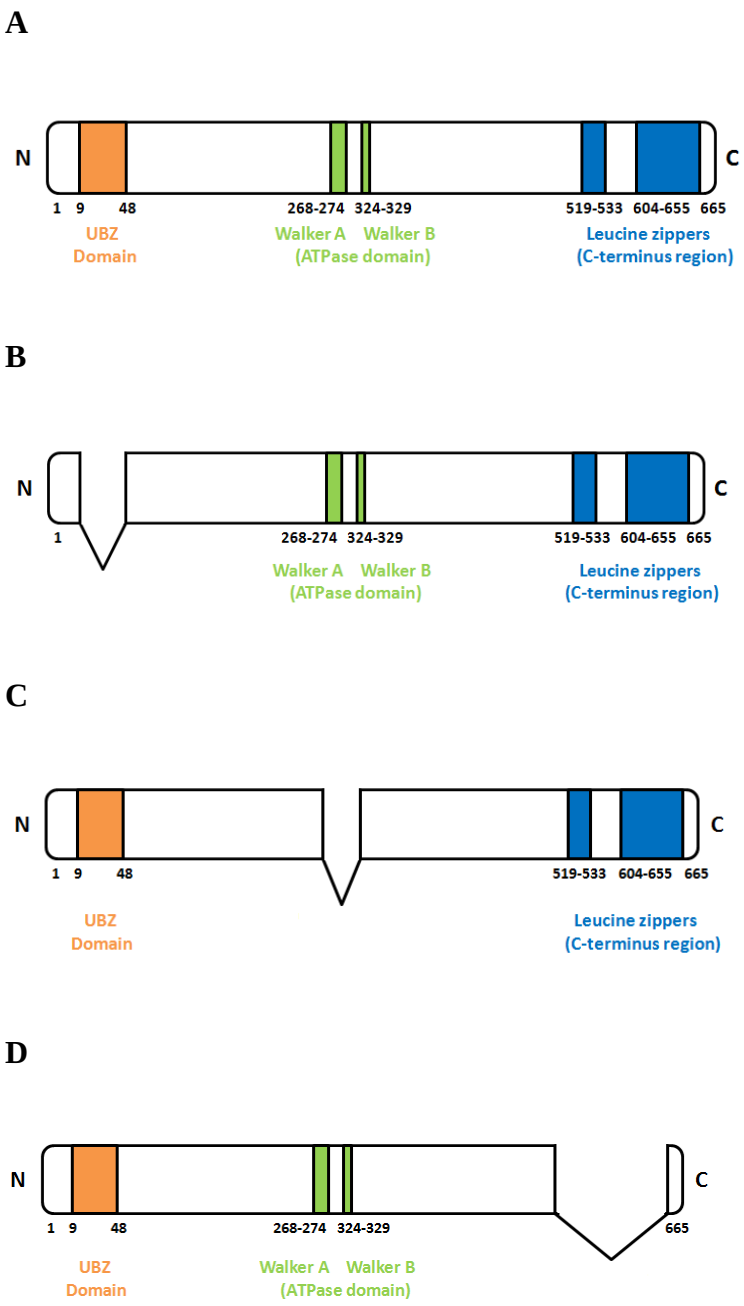
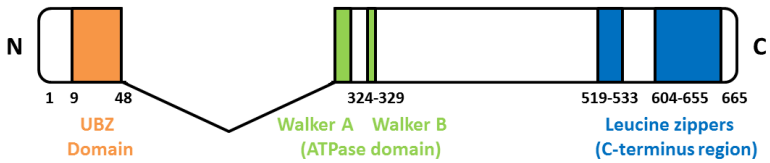
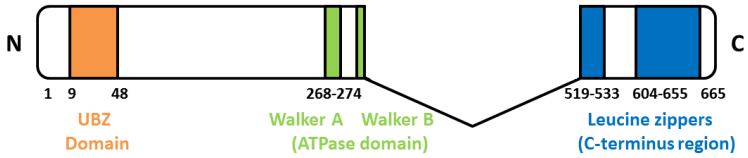



**Figure 27. Diagrammatic representation of WRNIP1 and three WRNIP1 deletion mutants** (A) Diagrammatic representation of WRNIP1's structure. UBZ domain is indicated in orange, ATPase domain, consisting of Walker A and Walker B motifs is indicated in green and two leucine zippers which make C-terminus region are indicated in blue. (B) Diagrammatic representation of UBZ deletion mutant of WRNIP. (C) Diagrammatic representation of ATPase domain deletion mutant of WRNIP1. (D) Diagrammatic representation of C-terminus deletion mutant of WRNIP1. These diagrammatic representations are not to scale.

**A**




**B**




**C**

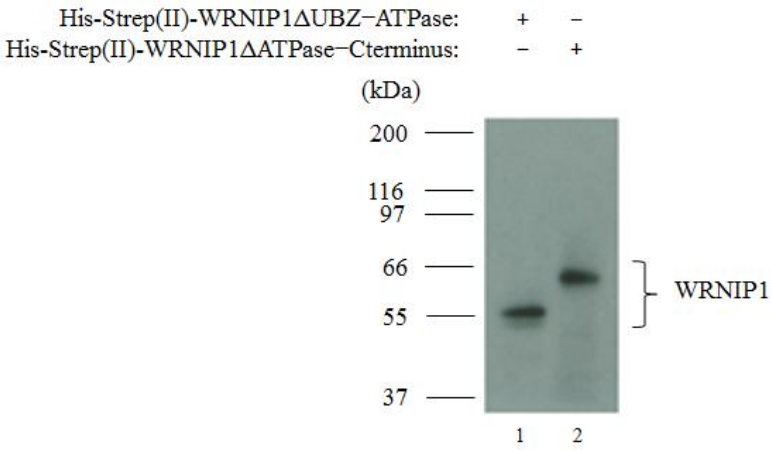
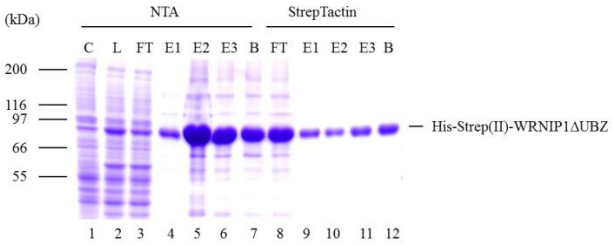


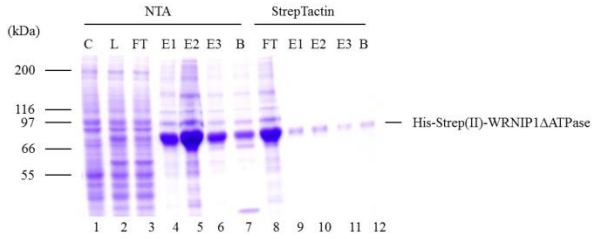

**Figure 28. Diagrammatic representation and Western blot analysis of two Sf9-purified WRNIP1 deletion mutants** (A) Diagrammatic representation of deletion mutant with deletion between UBZ and ATPase domains (His-Strep(II)-WRNIP1ΔUBZ−ATPase). This diagrammatic representation is not to scale. (B) Diagrammatic representation of deletion mutant with deletion between ATPase domain and C-terminus region (His-Strep(II)-WRNIP1ΔATPase−Cterminus). This diagrammatic representation is not to scale. (C) Western blot of purified His-Strep(II)-WRNIP1ΔUBZ−ATPase and His-Strep(II)-WRNIP1ΔATPase−Cterminus deletion mutants.

The deletions were introduced by PCR into the His- and Strep(II)-tagged WRNIP1-bearing vector pFastBac1-SHT with the use of previously designed primers (Materials and Methods). Subsequently, the deletion mutants were expressed in Sf9 insect cells and were purified after 72 hours of incubation in a standard lysis buffer (Figures 29 A, B and C). The resultant proteins (Figure 29 D) were applied in the *in vitro* binding, where Flag- and HA-tagged FANCD2 was subjected to binding with WRNIP1 and its deletion mutants. All the mutants were His- and Strep(II)-tagged and were expressed and purified from Sf9 insect cells (Figure 29 D). The results of this study indicated that none of the selected amino acid sequences of WRNIP1 was responsible for FANCD2 and WRNIP1 interaction (Figure 30).

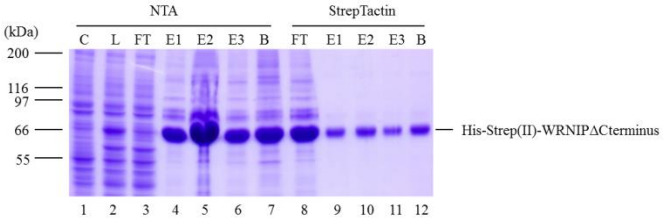
**A**




**B**




**C**




**D**

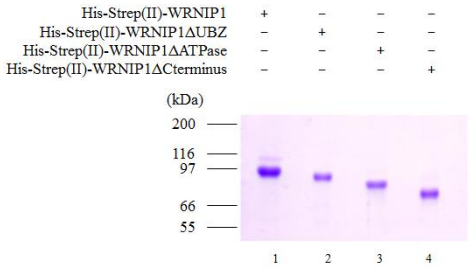



**Figure 29. Purification of WRNIP1 deletion mutants** (A) Coomassie blue stain of Sf9-purified WRNIP1 UBZ deletion mutant (His-Strep(II)-WRNIP1ΔUBZ). The order on a gel was as follows: 1) C – control Sf9 cells, 2) L – UBZ mutant lysate, 3) FT – flow-through, 4) NTA E1 – eluate 1, 5) NTA E2 – eluate 2, 6) NTA E3 – eluate 3, 7) NTA B – beads, 8) StrepTactin FT – flow-through, 9) StrepTactin E1 – eluate 1, 10) StrepTactin E2 – eluate 2, 11) StrepTactin E3 – eluate 3, 12) StrepTactin B – beads. (B) Coomassie blue stain of Sf9-purified WRNIP1 ATPase deletion mutant (His-Strep(II)-WRNIP1ΔATPase). The order on a gel was the same as for (A). (C) Coomassie blue stain of Sf9-purified WRNIP1 C-terminus deletion mutant (His-Strep(II)-WRNIP1ΔCterminus). The order on a gel was the same as in (A). (D) Coomassie blue stain of WRNIP1 and three WRNIP1 deletion mutants purified from Sf9 cells.

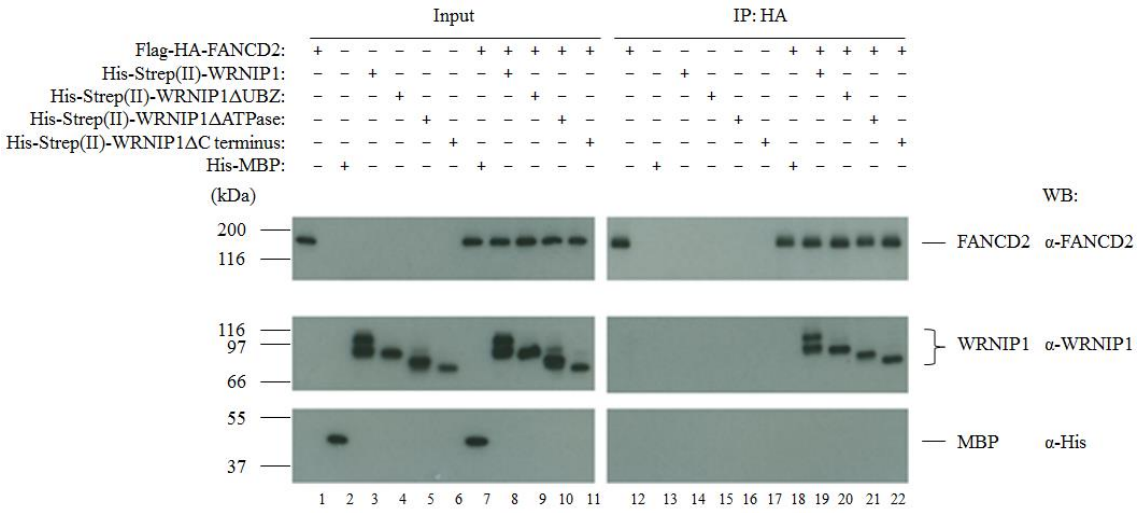



**Figure 30. FANCD2 interacts with WRNIP1 and WRNIP1 deletion mutants *in vitro*** Western blot of *in vitro* binding between Flag-HA-FANCD2, His-Strep(II)-WRNIP1 and His-Strep(II)-WRNIP1 deletion mutants. *In vitro* binding analysis shows that His-Strep(II)-WRNIP1 binds to Flag-HA-FANCD2 (lane 19). Flag-HA-FANCD2 interacts with three WRNIP1 deletion mutants: WRNIP1 UBZ deletion mutant (His-Strep(II)-WRNIP1ΔUBZ, lane 20), WRNIP1 ATPase deletion mutant (His-Strep(II)-WRNIP1ΔATPase, lane 21), WRNIP1 C-terminus deletion mutant (His-Strep(II)-WRNIP1ΔCterminus, lane 22). Flag-HA-FANCD2 does not interact with negative control (His-MBP, lane 18). WB indicates Western blot. Antibodies used in this experiment were α-FANCD2 (1:100 dilution), α-WRNIP1 (1:2000 dilution) and α-His (1:1000 dilution). His-MBP was obtained from Prof. Mark Howarth's laboratory.

### 5.5 *In vitro* binding between WRNIP1 and FANCI

After investigating the interaction between FANCD2 and WRNIP1, an interaction between WRNIP1 and the second component of the Fanconi anemia pathway, i.e. FANCI was examined. Flag- and HA-tagged FANCI (a baculovirus containing Flag- and HA-tagged FANCI was obtained from Chih-Chao Liang, Dr Martin Cohn's laboratory) and His- and Strep(II)-tagged WRNIP1 were purified from the Sf9 insect cells and subjected to *in vitro* binding, where the interaction between both proteins was examined and visualized by Western blotting. As in the case of WRNIP1-FANCD2 *in vitro* binding experiment, His-Strep(II)-WRNIP1 and Flag-HA-FANCI were mixed

together with BSA and binding buffer in the final volume of 10 µl. His-tagged MBP was used as a negative control. As expected, the Flag-HA-FANCI bound to α-HA beads, whereas WRNIP1 on its own did not bind to α-HA beads (Figure 31). MBP did not bind to α-HA beads and did not interact with FANCI. On the other hand, WRNIP1 was demonstrated to bind FANCI. During subsequent experiment, the increasing amounts of WRNIP1 (0.1, 0.2, 0.4 and 0.8 µg) were added to this *in vitro* binding mixture (Figure 32 A). The proteins were incubated together at 4°C for 1 h. After recovery of the incubation mixture, 10 µl of α-HA bead slurry was added to the proteins and was incubated together at 4°C for 30 minutes on the rotor (Figure 32 B). Subsequently, the α-HA beads were recovered from the Eppendorf tubes and were loaded on a column. Each column was washed with 3 ml of binding buffer containing 0.1% (v/v) Tween-20. 1X LDS/loading dye was used to elute proteins from the beads. The His-MPB served as a negative control. This study revealed that WRNIP1 was binding to FANCI in all the investigated amounts (Figure 32 A). Also, this study showed that MBP did not attach to the beads as it was anticipated. 0.2 µg WRNIP1 was at 1:1 molar ratio to FANCI. Thus, 0.4 µg of WRNIP1 and 0.8 µg of WRNIP1 was equivalent to 2:1 and 4:1 molar ratio of WRNIP1 to FANCI. Therefore, this would imply that more than one molecule of WRNIP1 could bind to FANCI.

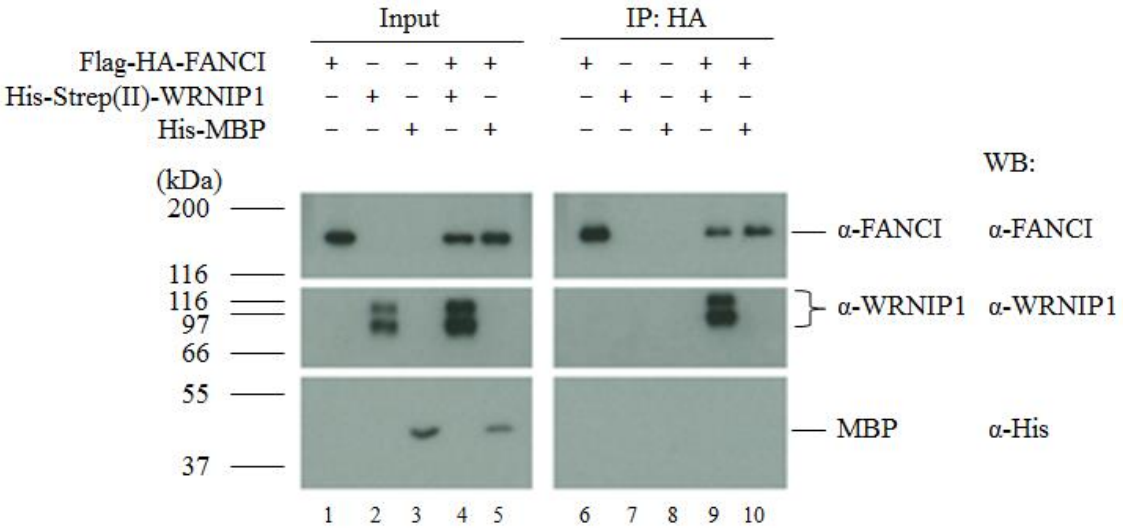
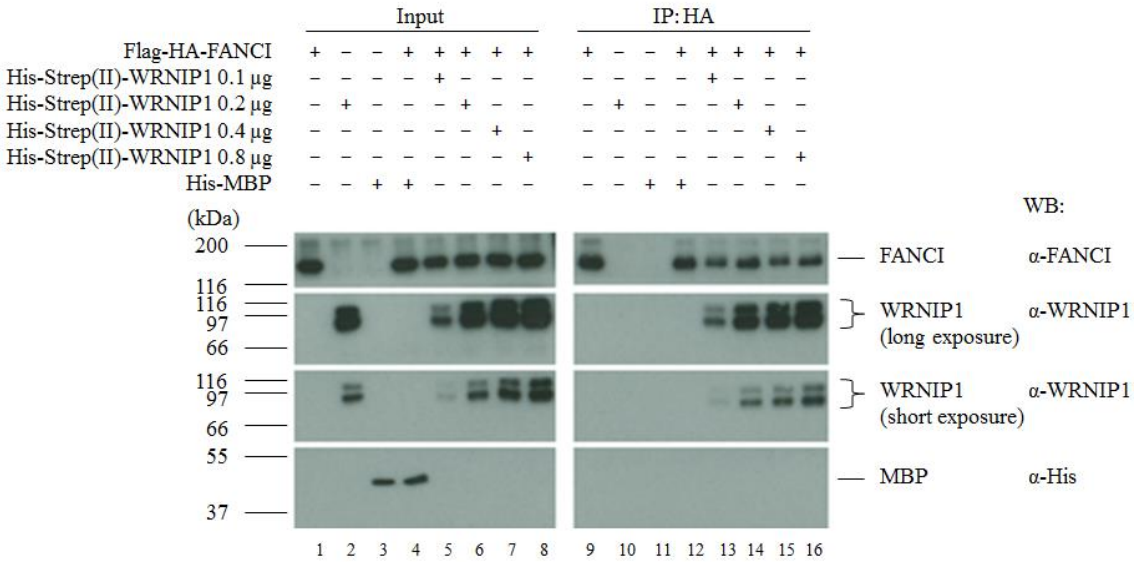



**Figure 31. WRNIP1 interacts with FANCI *in vitro*.** Western blot analysis showing *in vitro* binding between Flag-HA-FANCI and His-Strep(II)-WRNIP1. His-Strep(II)-WRNIP1 binds to Flag-HA-FANCI (lane 9). Flag-HA-FANCI does not interact with negative control (His-MBP, lane 10). WB indicates Western blot. Antibodies used in this experiment were α-FANCI (1:1000 dilution), α-WRNIP1 (1:2000 dilution) and α-His (1:1000 dilution). His-MBP was obtained from Prof. Mark Howarth's laboratory.

**A**




**B**

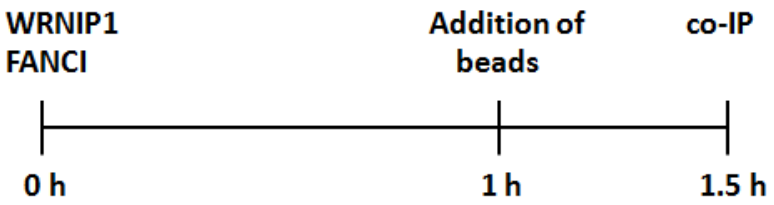


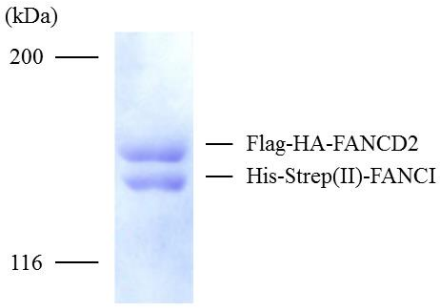

**Figure 32. WRNIP1 interacts with FANCI at various concentrations *in vitro*.** (A) Western blot analysis showing *in vitro* binding of Flag-HA-FANCI and His-Strep(II)-tagged WRNIP1. 0.1, 0.2, 0.4 and 0.8 µg of His-Strep(II)-WRNIP1 binds to Flag-HA-FANCI *in vitro*. His-MBP was used as a negative control and did not interact with Flag-HA-FANCI. His-MBP was obtained from Prof. Mark Howarth's laboratory. Antibodies used in this experiment were α-FANCI (1:1000 dilution), α-WRNIP1 (1:2000 dilution) and α-His (1:1000 dilution). (B) Diagrammatic representation of a timeline of *in vitro* binding between Flag-HA-FANCI and His-Strep(II)-WRNIP1.

## 5.6 *In vitro* binding between FANCD2/FANCI heterodimeric complex and WRNIP1

After establishing that WRNIP1 interacted with monomeric FANCD2 and monomeric FANCI *in vitro*, it was investigated whether WRNIP1 could interact with pre-formed heterodimeric FANCD2/FANCI complex. In order to achieve this, the baculoviruses containing Flag-HA-FANCD2 as well as His-Strep(II)-FANCI protein sequences were used (both baculoviruses were generated by Chih-Chao Liang, Dr Martin Cohn's laboratory). Subsequently, Sf9 insect cells were infected with both baculoviruses simultaneously and after 72-hour incubation, FANCD2/FANCI heterodimeric complex was purified with the use of α-Flag M2 agarose beads. The success of the purification was visualised by the Coomassie blue stain of FANC2/FANCI complex (Figure 33 A).

The purified constructs were used for *in vitro* binding experiment between pre-formed Flag-HA-FANCD2/His-FANCI complex and His-Strep(II)-WRNIP1. The Western blot analysis of *in vitro* showed that more WRNIP1 bound to heterodimeric FANCD2/FANCI complex (Figure 33 B, lane 17) than WRNIP1 which interacted with monomeric FANCD2 (Figure 33 B, lane 15). However, this was attributed to more WRNIP1 being loaded to that reaction mixture where FANCD2/FANCI complex was present (Figure 33 B, lanes 6 and 8). Therefore, WRNIP1 interacted with FANCD2/FANCI complex to a similar extent that WRNIP1 interacted with FANCD2. Furthermore, WRNIP1 did not obstruct the efficiency of binding of FANCD2/FANCI complex to the α-HA beads in the *in vitro* binding experiment. It was preliminarily suggested that the presence of WRNIP1 during the *in vitro* binding with FANCD2/FANCI did not influence the interaction between FANCD2 and FANCI.

**A**




**B**

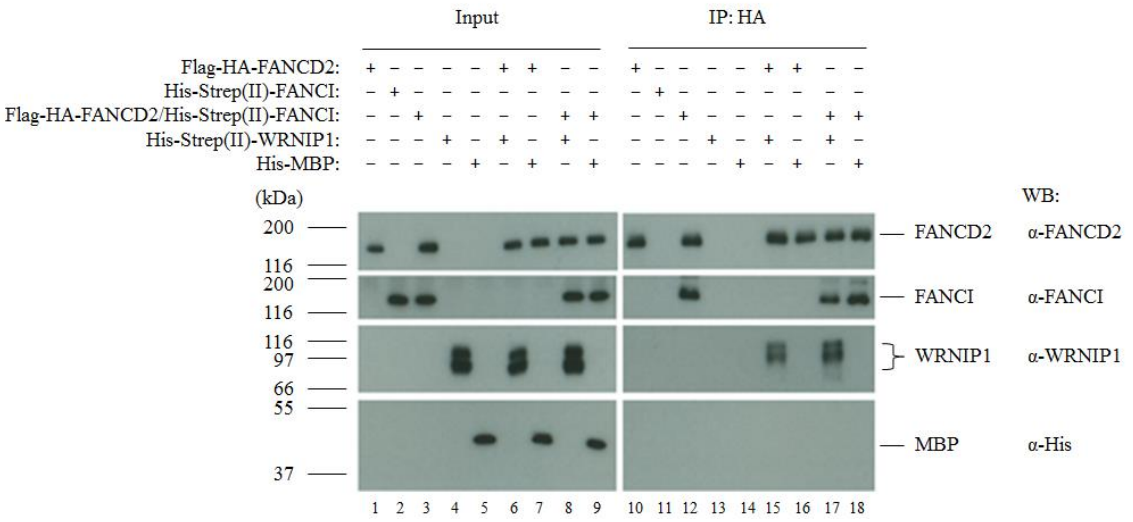



**Figure 33. WRNIP1 interacts with FANCD2/FANCI complex *in vitro*.** (A) Coomassie blue stain of Flag-HA-FANCD2/His-Strep(II)-FANCI (FANCD2/FANCI) heterodimeric complex purified from the Sf9 insect cells. (B) Western blot analysis showing *in vitro* binding between His-Strep(II)-WRNIP1 and FANCD2/FANCI complex (lane 17) as well as binding between His-Strep(II)-WRNIP1 and Flag-HA-FANCD2 (lane 15). His-MBP was used as a negative control and did not bind to either Flag-HA-FANCD2/His-Strep(II)-FANCI complex (lane 18) nor Flag-HA-FANCD2 (lane 16). Antibodies used in this experiment were α-FANCD2 (1:100 dilution), α-FANCI (1:1000 dilution), α-WRNIP1 (1:2000 dilution) and α-His (1:1000 dilution). His-MBP was obtained from Prof. Mark Howarth's laboratory.

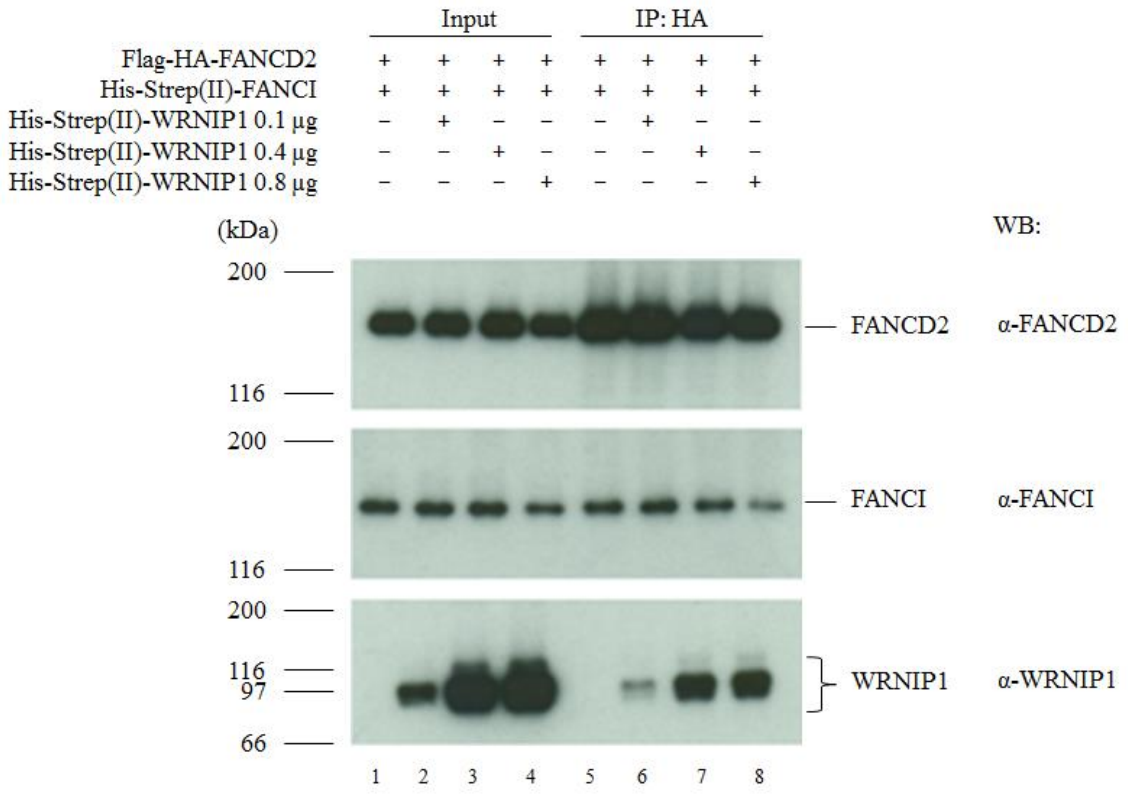
### 5.7 *In vitro* interaction between FANCD2, WRNIP1 and FANCI

It was established that WRNIP1 interacted with FANCD2 (see Section 5.3), FANCI (see Section 5.5) and FANCD2/FANCI complex (see Section 5.6). Therefore, it was suggested that WRNIP1 might compete with FANCI for a binding site on FANCD2. In an effort to establish whether the presence of WRNIP1 reduced the interaction between FANCD2 and FANCI, the three proteins were incubated together at 30°C for one hour in a binding buffer and were subjected to *in vitro* binding experiment. Afterwards, the 10 µl α-HA beads slurry was added to the proteins and the mixture was incubated at 4°C for 30 minutes on the rotor (Figure 34 B). The slurry containing proteins was loaded on the column. The column was washed with 3 ml of binding buffer containing 0.1% (v/v) Tween-20, which helped to remove unspecifically binding proteins. 50 µl of 1X LDS sample buffer/reducing agent was used to elute the proteins from the beads. All the proteins included in this experiment were added as monomers, i.e. there was no pre-formed complex used in this study. The increasing amounts of WRNIP1 were added to the *in vitro* binding mixture (Figure 34 A). The results of that experiment indicated that despite increasing amounts of WRNIP1 (from 0 to 0.4 µg), the binding between FANCD2 and FANCI remained uninterrupted. However, when WRNIP1 was increased to 0.8 µg, the amount of observed FANCI seemed to decrease. Moreover, the amount of WRNIP1 which was pulled down with FANCD2 and FANCI remained the same when 0.4 and 0.8 µg were added.

Second, in an effort to further establish whether WRNIP1 competed with FANCI for a binding site on FANCD2, the subsequent *in vitro* binding experiment was conducted. During that study, FANCD2 and increasing amounts of WRNIP1 (from 0 to 0.8 µg) were incubated together first for one hour at 30°C. Afterwards, FANCI was added to the

both proteins and was incubated with them for one hour at 30°C. Subsequently, 10 µl of α-HA beads slurry was added to the proteins and the Eppendorf tube was incubated at 4°C for 30 minutes on a rotor (Figure 35 B). The results of this *in vitro* binding study indicated that when WRNIP1 was added in increasing amounts to FANCD2, the amount of WRNIP1 which bound to FANCD2 was rising. The addition of FANCI did not disrupt this pattern (Figure 35 A).

**A**




**B**

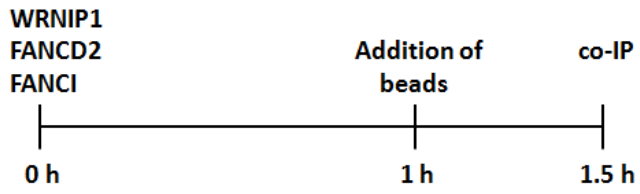
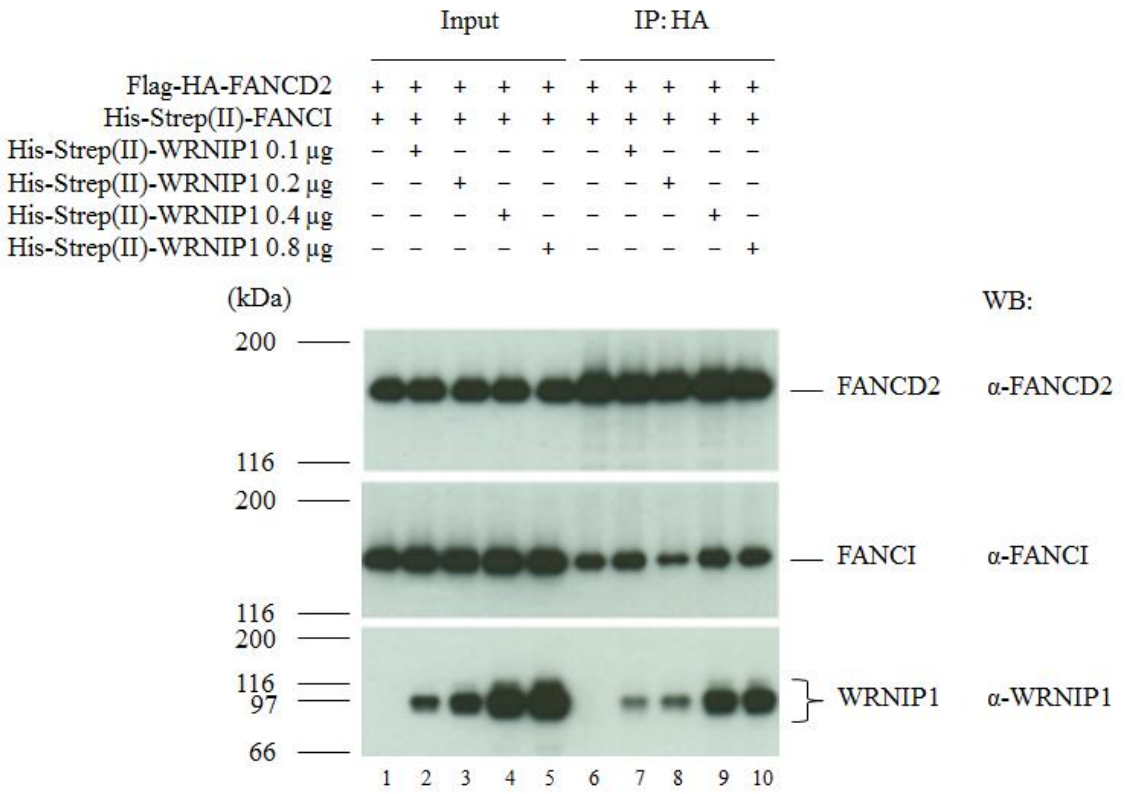



**Figure 34. WRNIP1 interacts with monomeric FANCD2 and monomeric FANCI *in vitro***

(A) Western blot showing the *in vitro* binding between monomeric FANCD2 (Flag-HA-FANCD2), monomeric WRNIP1 (His-Strep(II)-WRNIP1) and monomeric FANCI (His-Strep(II)-FANCI) where the three proteins were incubated together at 30°C for 1 h in a binding buffer. The amount of FANCD2 was 0.2 µg, the amount of FANCI was 0.2 µg and amount of WRNIP1 was increased from 0.1 to 0.8 µg. Antibodies used in this experiment were α-FANCD2 (1:100 dilution), α-FANCI (1:1000 dilution) and α-WRNIP1 (1:2000 dilution). (B) Diagrammatic representation of a timeline of *in vitro* binding between WRNIP1, FANCD2 and FANCI.

**A**




**B**

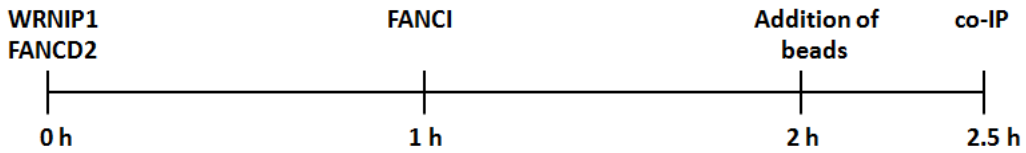



**Figure 35. WRNIP1 does not compete with FANCI for binding with FANCD2** (A) Western blot analysis showing *in vitro* binding where FANCD2 (Flag-HA-FANCD2) and WRNIP1 (His-Strep(II)-WRNIP1) were first incubated at 30°C for 1 h and then FANCI (His-Strep(II)-FANCI) was added to the binding mixture and the three proteins were incubated at 30°C for 1 h. The amount of FANCD2 was 0.2 µg, the amount of WRNIP1 was increased from 0.1 to 0.8 µg and the amount of FANCI was 0.2 µg. Antibodies used in this experiment were α-FANCD2 (1:100 dilution), α-FANCI (1:1000 dilution) and α-WRNIP1 (1:2000 dilution). (B) Diagrammatic representation of *in vitro* binding between WRNIP1, FANCD2 and FANCI.

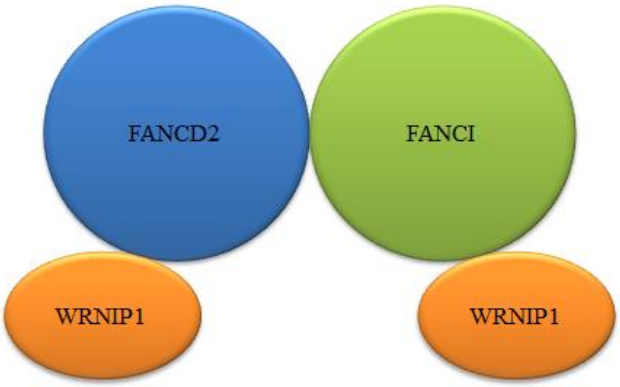
## 5.8 Discussion

This study revealed that WRNIP1 was able to interact with FANCD2 *in vitro*. The *in vitro* binding study conducted in the presence of the negative control (MBP) showed that WRNIP1 was binding to FANCD2 through a range of temperatures. This result indicated that WRNIP1 might play a role in the Fanconi anemia pathway as it was able to interact with FANCD2 which is a well-established Fanconi anemia component. This claim was corroborated by establishing WRNIP1's *in vitro* interaction with another major component of the Fanconi anemia pathway, i.e. FANCI. After demonstrating that WRNIP1 could interact with monomeric FANCD2 and monomeric FANCI, it was also shown that WRNIP1 could bind to heterodimeric FANCD2/FANCI complex. It should be noted, however, that the negative control used in this study (MBP) was His-tagged only. The lack of Strep(II) tag in MBP control could indicate that there is a possibility of His-Strep(II)-WRNIP1 interacting with Flag-HA-FANCD2 and/or Flag-HA-FANCI through its Strep(II) tag, thus resulting in inaccurate data. Therefore, both His- and Strep(II)-tagged negative control should be used in the future studies involving WRNIP1.

WRNIP1's *in vitro* interaction with two components of the Fanconi anemia pathway as well as heterodimeric FANCD2/FANCI complex posed a question whether WRNIP1 competed with FANCI for a binding site on FANCD2. The *in vitro* binding study involving all three proteins (FANCD2, FANCI and WRNIP1) showed that WRNIP1 was not competing with FANCI for a binding site on FANCD2. When all components were bound together or sequentially added, WRNIP1 still did not replace FANCI. This result suggested that WRNIP1 might have an alternative binding site to the one used by

FANCI when interacting with FANCD2. Also, this outcome indicated the possibility of WRNIP1's binding to the established Fanconi anemia proteins. First, one molecule of WRNIP1 could interact with both FANCD2 and FANCI simultaneously through two different domains (Figure 36 B). Second, two or more WRNIP1 molecules could bind to FANCD2 and FANCI (Figure 36 A). However, the exact mechanism of this interaction would need to be addressed by the future research.

**A**




**B**

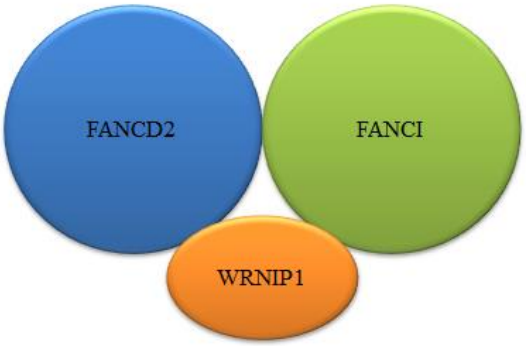



**Figure 36. FANCD2, FANCI and WRNIP1 interaction models** (A) Model of WRNIP1's interaction with FANCD2 and FANCI, where one molecule of WRNIP1 binds separately to FANCD2 and another monomeric WRNIP1 binds to FANCI (B) Model of WRNIP1's interaction with FANCD2 and FANCI, where one monomeric WRNIP1 binds to both FANCD2 and FANCI simultaneously.

WRNIP1 was suggested to form oligomers in several studies (Kawabe *et al.,* 2006; Tsurimoto *et al.,* 2005). As purified WRNIP1 was run on denaturing SDS-PAGE gels under reducing conditions, the possible oligomeric interactions could have been dissociated. Therefore, WRNIP1 must be run on native SDS-PAGE gels or on gel filtration column in order to establish whether it could form oligomers.

Figure 35 A showed that WRNIP1 was added in increasing concentrations to FANCD2. When 0.2 µg of WRNIP1 was added, the molar ratio of WRNIP1 to FANCD2 and FANCI was 1:1:1. Therefore, 0.4 µg of WRNIP1 resulted in molar ratio of 2:1:1 (molar ratio of WRNIP1:FANCD2:FANCI) and 0.8 µg WRNIP1 resulted in molar ratio of 4:1:1 (molar ratio of WRNIP1:FANCD2:FANCI). Figures 34 and 35 showed that there was no difference in band intensity when 0.4 µg and 0.8 µg WRNIP1 was added. This could indicate that 0.4 µg of WRNIP1 was the maximum amount of the protein, which could bind to FANCD2 and/or FANCI. Therefore, the molar ratio of WRNIP1:FANCD2:FANCI was 2:1:1. This corresponds to two molecules of WRNIP1 binding to one molecule of FANCD2 and one molecule of FANCI. This result would indicate that there is a possibility of WRNIP1's dimerization or one molecule of WRNIP binding to FANCD2 and another molecule of WRNIP1 binding to FANCI. It was also shown in this study that WRNIP1 could bind at 1:1, 2:1 and 4:1 molar ratio to FANCI. It could imply that four molecules of WRNIP1 could bind to FANCI at one time. However, when WRNIP1 interacted with both FANCD2 and FANCI, the molar ratio was 2:1:1, thus showing that presence of FANCD2 might somehow restrict the number of WRNIP1 molecules (dimers) which could interact with FANCI. It is speculated that this might be due to interaction between FANCD2 and FANCI which results in conformational rearrangement. Hence, based on these *in vitro* binding

experiments, the following models of WRNIP1 binding are suggested (Figure 37 A, B and C).

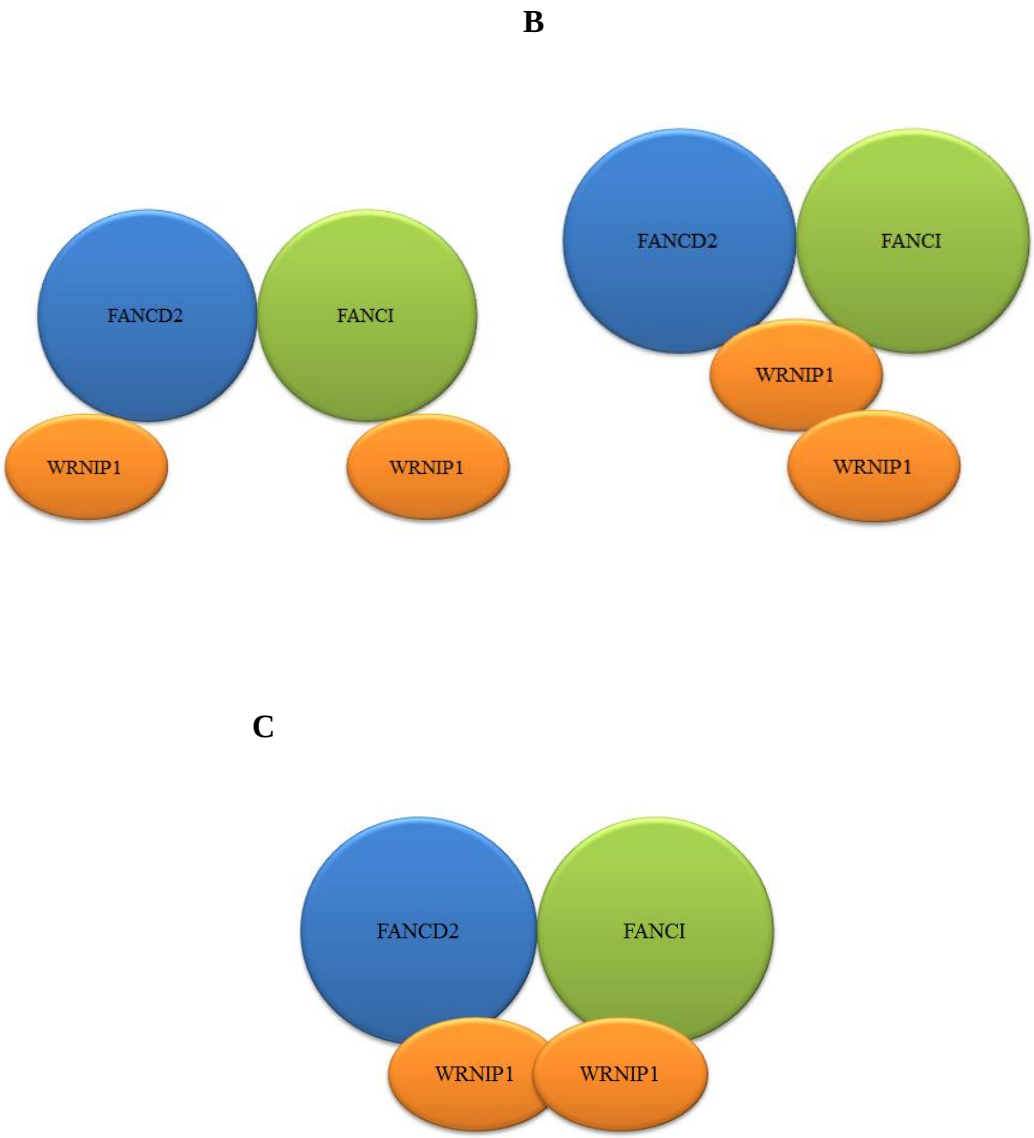



**Figure 37. Models of WRNIP1 interaction with FANCD2/FANCI complex** (A) A model of interaction between WRNIP1, FANCD2 and FANCI in which one molecule of WRNIP1 interacts with one molecule of FANCD2 and the second molecule of WRNIP1 interacts with FANCI. (B) A model of interaction between WRNIP1, FANCD2 and FANCI where WRNIP1 dimer interacts with FANCD2 and FANCI through one WRNIP1 molecule. (C) A model of interaction between WRNIP1, FANCD2 and FANCI in which WRNIP1 dimer interacts with FANCD2 and FANCI through two WRNIP1 molecules.

It was attempted to map a fragment of WRNIP1 which interacted with FANCD2. WRNIP1 was known to have two domains, namely UBZ and ATPase. Moreover, it had a predicted two leucine zippers at its C-terminus. Therefore, in order to establish a FANCD2 binding region on WRNIP1, the three WRNIP1 deletion mutants were expressed from Sf9 cells, i.e. UBZ, ATPase and C-terminus deletion mutants. These mutants were subjected to *in vitro* binding analysis with FANCD2. As a consequence, it was shown that all three purified WRNIP1 deletion mutants could bind to FANCD2 *in vitro*. This showed that the WRNIP1's fragment which was necessary for an interaction with FANCD2 was not identified yet. In order to establish which WRNIP1's fragment interacts with FANCD2, it will be necessary to make two more WRNIP1 deletion mutants, i.e. the first with a deletion spanning from UBZ to ATPase domain and the second with a deletion from ATPase to C-terminus region. It might be also a possibility that all mutants would bind to FANCD2. If this is the case, it might be necessary to assume that WRNIP1 binds to FANCD2 via multiple domains. Therefore, more than one deletion must be introduced into WRNIP1 in order to establish which WRNIP1 fragment binds FANCD2.

# 6 A study of ubiquitination of WRNIP1

## 6.1 Introduction

WRNIP1 was shown previously to be a heavily-modified protein by various post-translational modifications, i.e. ubiquitination, phosphorylation, sumoylation or acetylation (Bish *et al*. 2008). It was demonstrated that WRNIP1 migrated as a doublet on SDS-PAGE electrophoresis gels followed by Western blotting (Bish and Myers, 2007). It was suggested that WRNIP1 in its unmodified form migrated at 75 kDa. Although, several ubiquitination and sumoylation sites of WRNIP1 have been identified by the mass spectrometry (Bish and Myers, 2007), the role of these modifications was not established yet.

It was also demonstrated in the literature that the UBZ4 domain of WRNIP1 plays a role in its ubiquitination. Bish *et al.* (2008) indicated that a D37A mutation, which is located in the UBZ domain, completely abolishes WRNIP1's ubiquitination. Moreover, it was determined that lack of the UBZ domain inhibits the localization of WRNIP1 to the DNA damage sites, thus suggesting that either WRNIP1's ubiquitination or a structure of UBZ domain itself might influence its DNA repair capacity. Bish and Myers (2007) traced the abrogation of WRNIP1 ubiquitination by introduction of a single mutation into UBZ domain, i.e. D37A. This mutation inhibits both WRNIP1's ubiquitination as well as its localization to the DNA damage sites (Crosetto *et al*., 2008; Nomura *et al.*, 2012).

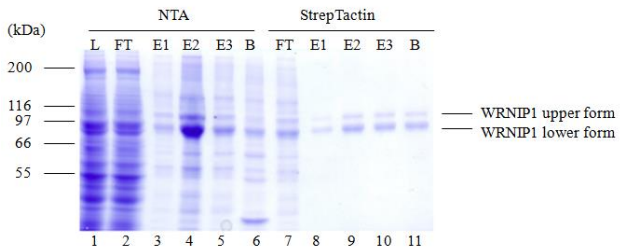
The initial aim of this study was to purify WRNIP1 from the Sf9 insect cells and apply it in *in vitro* binding study. However, unexpectedly, WRNIP1 was purified as a doublet and it was decided to investigate whether either upper or lower running form was

ubiquitinated by Western blotting. Furthermore, following the establishment that upper form was indeed ubiquitinated, the previously purified WRNIP1 deletion mutants were used to assess any alterations in ubiquitination. Finally, as ubiquitin forms various chains which serve various purposes in the cell (Ulrich and Walden, 2010), it was decided to determine what type of modification might be present in WRNIP1.

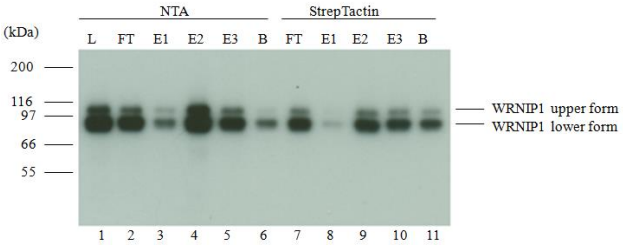
### 6.2 WRNIP1 has an ubiquitinated upper form

In order to use WRNIP1 in *in vitro* interaction studies, WRNIP1 was purified from the Sf9 insect cells and run on SDS-PAGE gel, followed by the Coomassie staining (Figure 38 A) and Western blotting (Figure 38 B) with α-WRNIP1 antibody. This analysis revealed that WRNIP1 was migrating in two forms, labelled as upper and lower form. The faster migrating lower form was not modified and the slower migrating upper form was suggested to be modified by post-translational modification. In order to establish whether both forms were exogenous proteins, i.e. introduced by the externally introduced DNA, the α-His Western blot was performed (Figure 38 C). That experiment showed that both forms of WRNIP1 were His-tagged and therefore were introduced to Sf9 insect cells via infection with baculovirus. In order to uncover the type of modification, the purified WRNIP1 was subjected to Western blot analysis, in which α-ubiquitin antibody was used (Figure 38 D). This analysis showed that upper form of WRNIP1 was ubiquitinated. However, the type of ubiquitination was not identified.

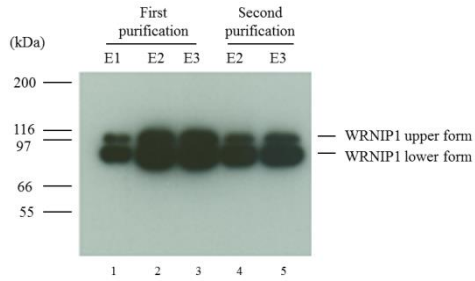
**A**




**B**




**C**




**D**

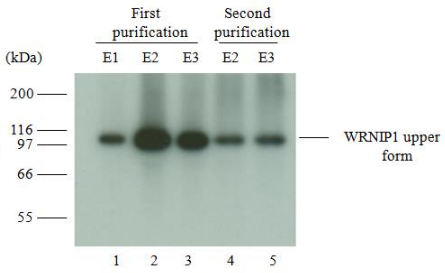



**Figure 38. Recombinant WRNIP1 purified from Sf9 cells has two forms** (A) Coomassie blue stain of recombinant WRNIP1 (His-Strep(II)-WRNIP1) purified from Sf9 insect cells. Order on a Coomassie: 1) NTA L – lysate, 2) NTA FT – flow-through, 3) NTA E1 – eluate 1, 4) NTA E2 – eluate 2, 5) NTA E3 – eluate 3, 6) NTA B – beads, 7) StrepTactin FT – flow-through, 8) StrepTactin E1 – eluate 1, 9) StrepTactin E2 – eluate 2, 9) StrepTactin E3 – eluate 3, 10) StrepTactin B – beads. (B) Western blot analysis of Sf9 purified WRNIP1, α-WRNIP1 antibody was used (1:2000 dilution). The order on the SDS-PAGE was the same as in (A). (C) Western blot analysis of Sf9 purified WRNIP1 eluates. The eluates were obtained from two $Ni^{2+}$-NTA and StrepTactin purifications. α-His antibody was used (1:1000 dilution). (D) Western blot analysis of Sf9 purified WRNIP1 eluates with α-ubiquitin antibody (FK2, 1:1000 dilution). Figures 38 A, B and C are the same as Figures 25 A, B and C.

In an effort to establish the type of WRNIP1's ubiquitination, the Western blot analysis was conducted where two antibodies detecting ubiquitinated proteins were used. FK1 antibody detected polyubiquitinated proteins only, whereas FK2 antibody detected both mono- and polyubiquitinated proteins. His- and Strep(II)-tagged WRNIP1 eluates were used in this experiment (Figure 39 A). This study revealed that both FK2 (Figure 39 B) and FK1 (Figure 39 C) antibodies bound to WRNIP1's upper form.

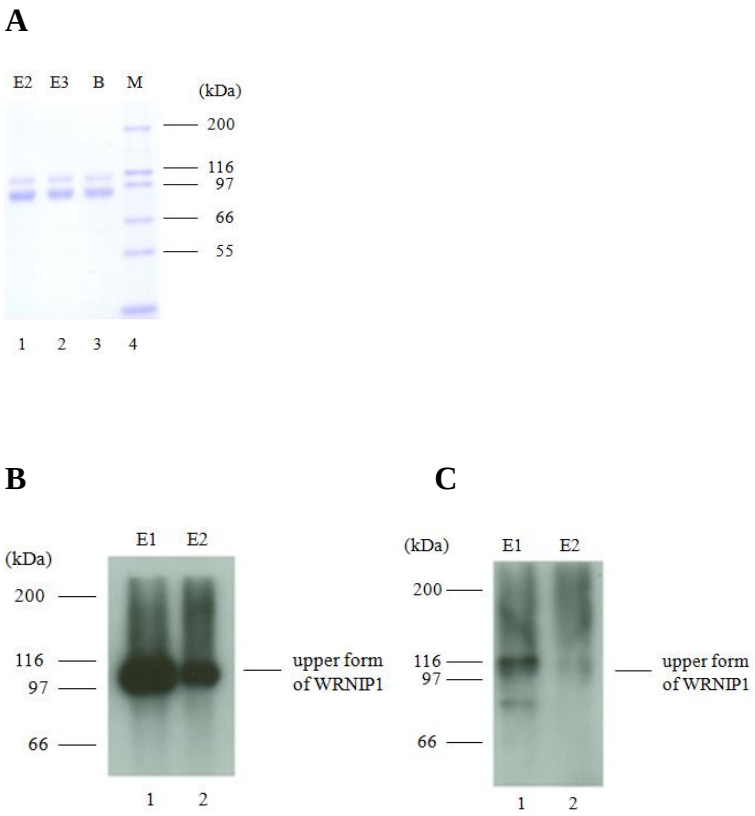


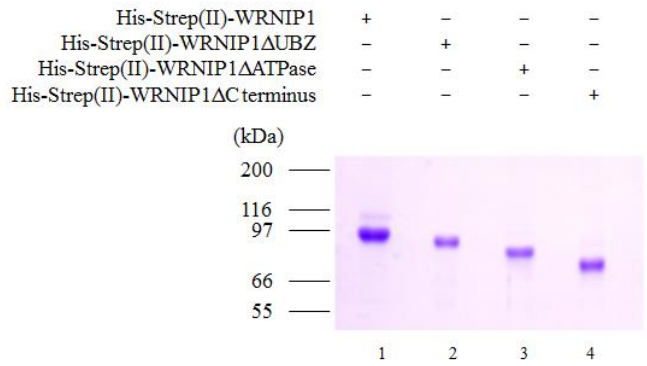

**Figure 39. Analysis of ubiquitination of WRNIP1's upper form** (A) Coomassie blue stain of $Ni^{2+}$-NTA and StrepTactin-purified WRNIP1 eluates (E2 and E3) and StrepTactin beads – B. Mark12 is indicated as M. (B) Western blot analysis showing StrepTactin eluates (E1 and E2) of WRNIP1 (His-Strep(II)-WRNIP1) and blotted with α-ubiquitin antibody (FK2, 1:1000 dilution). The Western blot shows the ubiquitinated upper form of WRNIP1. (C) Western blot analysis of $Ni^{2+}$-NTA and StrepTactin purified His-Strep(II)-WRNIP1 eluates (E1 and E2) which were blotted with α-ubiquitin FK1 antibody (1:1000 dilution).

### 6.3 UBZ domain directs WRNIP1's ubiquitination

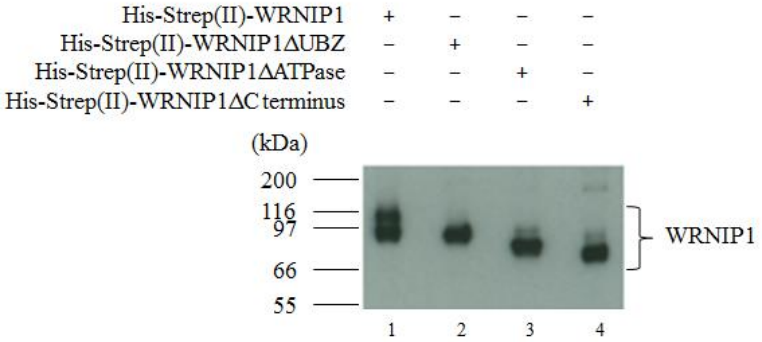
Following the establishment that WRNIP1 had ubiquitinated upper form which could be purified from the Sf9 insect cells, it was attempted to determine whether any of the previously generated WRNIP1 deletion mutants displayed alterations in ubiquitination levels.

Three WRNIP1 deletion mutants were generated by introducing the desired deletion into pFastBac1 vector already containing His- and Strep(II)-tagged WRNIP1 by the PCR with deletion-introducing primers (see Materials and Methods). The purified WRNIP1, WRNIP1 UBZ deletion mutant, WRNIP1 ATPase deletion mutant and WRNIP1 C-terminus deletion mutant were run on the SDS-PAGE gel and were stained with Coomassie (Figure 40 A). Moreover, Western blot analysis of the purified WRNIP1 and three deletion mutants was performed, where α-WRNIP1 antibody was used. This experiment revealed that WRNIP1 UBZ deletion mutant did not have upper ubiquitinated form (Figure 40 B). Finally, the Western blot analysis of purified WRNIP1 and three deletion mutants was conducted where α-ubiquitin antibody (FK2) was used. This investigation showed that UBZ deletion mutant could not interact with ubiquitin (Figure 40 C).

**A**




**B**




**C**

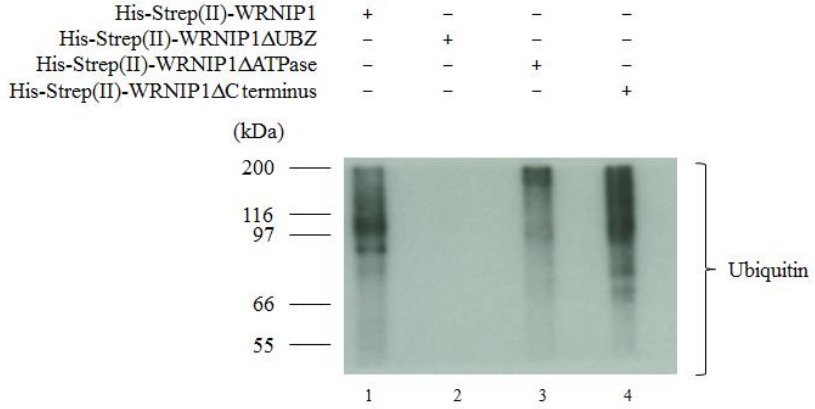



**Figure 40. Western blot analysis of the ubiquitination of WRNIP1 deletion mutants** (A) Coomassie blue stain of WRNIP1 (His-Strep(II)-WRNIP1) and UBZ (His-Strep(II)-WRNIP1ΔUBZ), ATPase (His-Strep(II)-WRNIP1ΔATPase) and C-terminus (His-Strep(II)-WRNIP1ΔCterminus) deletion mutants. (B) Western blotting of WRNIP1 and three WRNIP1 deletion mutants. α-WRNIP1 antibody was used (1:2000 dilution). (C) Western blot analysis of WRNIP1 and WRNIP1 deletion mutants' ubiquitination. α-Ubiquitin antibody was used (FK2, 1:1000 dilution). Figure 40 A is the same as Figure 29 D.

After establishing that UBZ domain deletion mutant of WRNIP1 was not able to be ubiquitinated, it was investigated with the use of PyMOL whether there were polar contacts (other than D37 of WRNIP1-R42 of ubiquitin) between UBZ domain of WRNIP1 and ubiquitin. It was suggested that mutation of residues responsible for the formation of such contacts, could abolish ubiquitination of WRNIP1. The PyMOL analysis revealed that two more polar contacts between UBZ of WRNIP1 and ubiquitin existed, i.e. N33 of UBZ and R42 of ubiquitin as well as A45 of UBZ and K48 of ubiquitin (Figure 41). It was demonstrated by our group that mutation of N33 also inhibits ubiquitination of WRNIP1 (data not shown).

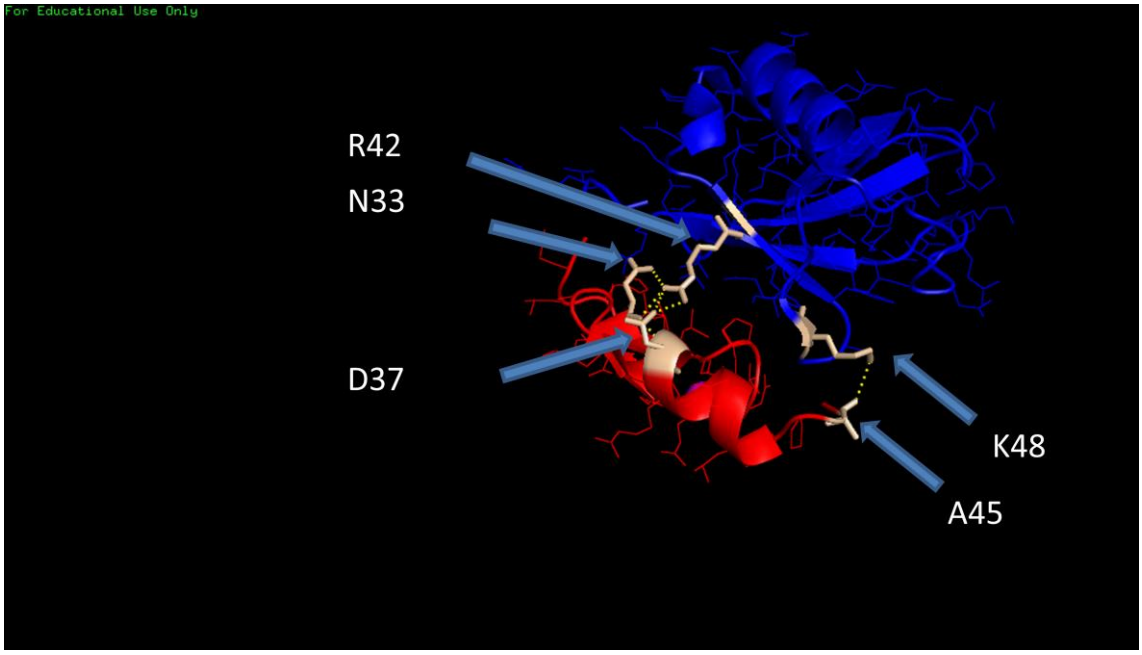
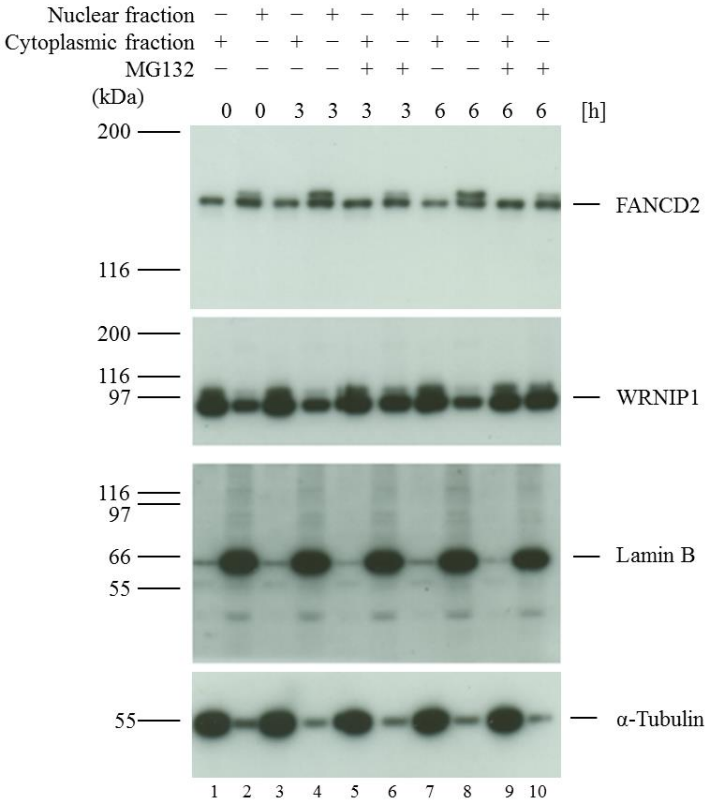



**Figure 41 Interactions between UBZ domain of WRNIP1 and ubiquitin.** UBZ domain of WRNIP1 is indicated in red and ubiquitin is indicated in blue. D37, N33 and A45 are amino acids of UBZ domain, whereas R42 and K48 indicate amino acids on ubiquitin.

## 6.4 WRNIP1's ubiquitinated upper form is not directed for proteasome degradation

After establishing that WRNIP1 had an abundant ubiquitinated upper form, it was analysed whether WRNIP1 upper form was localised to chromatin or cytoplasmic fraction. The HeLa cells were treated with 160 ng/ml MMC for 0, 3 or 6 h and fractionated into nuclear and cytoplasmic fractions. This experiment revealed that WRNIP1 upper form was more abundant in cytoplasmic fraction. Moreover, the upper form of WRNIP1 in both fractions did not change with the increasing time of incubation with MMC. When proteasome inhibitor (MG132) was used, the upper form of WRNIP1 was not much more visible in the nuclear fraction as compared to nuclear fraction which was not treated with MG132 (Figures 42 A and B).

**A**




**B**

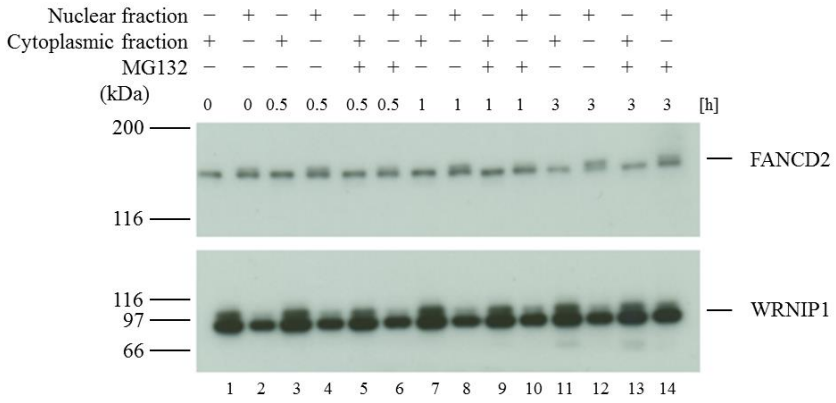



**Figure 42. WRNIP1's ubiquitination is not affected by proteasome inhibition** (A) The HeLa (HeLa.pSuper) cells were treated with MMC for 0, 3 and 6 h. Proteasome inhibitor (MG132) was used for each time point and cells were fractionated into nuclear and cytoplasmic fractions. Antibodies used in this experiment were α-FANCD2 (1:100 dilution), α-WRNIP1 (1:2000 dilution), α-Lamin B (1:200 dilution) and α-α-Tubulin (1:2000 dilution). (B) The HeLa (HeLa.pSuper) cells were treated with MMC for 0, 0.5, 1 and 3 h. Proteasome inhibitor (MG1322) was applied for each time point and cells were fractionated into nuclear and cytoplasmic fractions. Antibodies used in this experiment were α-FANCD2 (1:100 dilution) and α-WRNIP1 (1:2000 dilution).

## 6.5 Discussion

This study corroborated the previous result presented by Bish *et al.* (2008) that WRNIP1 had an ubiquitinated upper form which usually migrated at 105 kDa during SDS-PAGE gel analysis. This migration would suggest that WRNIP1 was polyubiquitinated or subjected to multiubiquitination. However, the form of ubiquitination could not be confirmed by this analysis. Both antibodies which were used in this study (i.e. FK1 and FK2) could identify the polyubiquitinated proteins and in this project they both revealed the presence of upper form of WRNIP1. It was shown however, that the WRNIP1's upper form was detected very weakly with FK1 antibody. On the other hand, the FK2 antibody resulted in a clearly visible upper form. Therefore, it is possible that WRNIP1 is multiubiquitinated. As it is known that unmodified WRNIP1 runs at 75 kDa on the SDS-PAGE gels, and the upper band is visible at around 105 kDa, it would suggest that WRNIP1 is multiubiquitinated at two or three different locations. It was also demonstrated that the upper form disappeared when UBZ domain of WRNIP1 was removed. Therefore, this domain of WRNIP1 played a role in its ubiquitination.

The fractionation study revealed that WRNIP1's ubiquitinated upper form was mostly localised to the cytoplasmic fraction. Moreover, no enrichment of WRNIP1's ubiquitinated upper form was observed after addition of a crosslinking agent MMC. This suggested that ubiquitination of WRNIP1 was not linked to the interstrand crosslink repair as the upper form was not increasing with longer MMC treatment. Moreover, after addition of proteasome inhibitor MG132 to the cells, the upper form of WRNIP1 was not enriched in the nuclear fraction. This outcome would suggest that

WRNIP1's ubiquitination does not play a role in proteasome targeting and degradation of WRNIP1.

# 7 Discussion and Conclusions

Werner helicase interacting protein 1 (WRNIP1) was discovered by the yeast two-hybrid assay performed by Kawabe *et al*. 2001 and established WRNIP1 as a binding partner of Werner helicase. Although, the two proteins interact physically, the functionality of that interaction is not known (Kawabe *et al.* 2006). WRNIP1 is also known to form molecular foci which formation is independent of cell cycle phase. The number of the foci was shown to increase after treatment of cells with replication fork stalling agents, i.e. hydroxyurea, UVC or topotecan (Crosetto *et al.,* 2008), thus indicating that WRNIP1 might play a role in a DNA repair. The notion that WRNIP1 is a DNA repair protein might be corroborated by the evidence of its interaction with various translesion repair proteins, such as Rad18 (Yoshimura *et al.,* 2009) or polymerase η (Yoshimura *et al.,* 2014). It was also shown that WRNIP1 binds to DNA and has a highest affinity to template-primer DNA (Kanamori *et al.,* 2011). This data suggested that WRNIP1 might function in translesion synthesis repair and it might play a role in exchange of polymerases and restart of a replication fork.

This project investigated a possible role of WRNIP1 in the Fanconi anemia pathway. The first part of this project addressed the question of whether WRNIP1 behaves like a typical Fanconi anemia pathway protein by testing its sensitivity to the ICL-inducing DNA damage. The response of WRNIP1 to various ICL-inducing agents, i.e. MMC, TMP-UVA and cisplatin was analysed through cell survival assays. Initially, the WRNIP1 knockdown cell line was compared to normal HeLa cells and the results revealed that WRNIP1 deficiency in cells exposed to MMC, but not cisplatin, resulted in lower survival of WRNIP1-depleted cells. Moreover, when WRNIP1 was knocked

out from the cells with the use of CRISPR/Cas9 technology, the sensitivity of this cell line to cisplatin increased, thus indicating that the residual levels of WRNIP1 in the HeLa WRNIP1 knockdown cells were sufficient to participate in resolution of cisplatin-induced DNA lesions. These results suggested that WRNIP1 might have participated in the repair of DNA damage. Furthermore, the outcomes of this study were corroborated by the subsequent clonogenic survival assay experiments involving WRNIP1 knockout cell line. The survival curves where a WRNIP1 knockout cell line was compared to normal cells revealed that upon treatment with MMC, TMP-UVA and cisplatin, all WRNIP1-depleted cell lines displayed sensitivity compared to normal cells. When WRNIP1-deficient HeLa Flp-in cells were complemented with EGFP-tagged WRNIP1, their sensitivity to MMC and TMP-UVA treatments partially decreased. Therefore, WRNIP1 might play some role in supporting a resolution of various ICLs. Overall, the first part of the study indicated that WRNIP1 similarly to the Fanconi anemia proteins fulfilled the criterion of the sensitivity to the ICL-inducing agents.

The second part of the study attempted to answer the question of whether WRNIP1 was a member of the Fanconi anemia pathway through establishing a functional link between WRNIP1 and FANCD2 through a series of *in vivo* experiments. First, it was examined if WRNIP1 was responding to the induction of ICLs in the nuclei of HeLa cells. As the Fanconi anemia proteins were involved in the resolution of ICLs, thus enrichment of WRNIP1 in the nuclear fraction or an alteration in its ubiquitination level might have indicated its participation in resolution of ICLs. However, after treatment with MMC and subsequent fractionation of cells with cytoskeletal buffer which resulted in cytoplasmic and nuclear fractions, there was only very gentle enrichment of WRNIP1 over the course of 24 h treatment, thus this outcome was concluded to be insignificant

(also no alteration in WRNIP1 levels was observed in UVC-treated cells). This result may have indicated that WRNIP1 did not react to induction of ICL. On the other hand, the lack of the alteration in WRNIP1 ubiquitination levels and its amount in the nuclear fraction could have suggested that the amount of WRNIP1 sufficient to resolve the DNA damage was already present in the chromatin. Therefore, no change was expected.

The fractionation experiments revealed that after WRNIP1 was knocked down from HeLa cells, which were subsequently treated with either MMC or TMP-UVA and fractionated into nuclear and cytoplasmic fractions, no changes in nuclear FANCD2 ubiquitination levels were observed. There was also no alteration in nuclear WRNIP1 ubiquitination levels when FANCD2 knockdown cell line was used. Moreover, it was suspected that the use of cytoskeletal buffer might have resulted in leakage of non-chromatin bound nuclear proteins into cytoplasmic fraction, thus rendering the identification of change of WRNIP1 levels more indiscernible. Hence, the alternative fractionation method was used where the cell nuclei were preserved in order to keep all the nuclear proteins inside the nucleus, and therefore identify any changes in WRNIP1 levels. However, similarly to the previous analysis, the Western blot analysis of nuclear proteins after induction of ICL, showed no alternation in FANCD2 ubiquitination levels in WRNIP1-depleted cell line as compared to control cells. Therefore, this study showed that fractionation experiments were not capable of providing any conclusive data on the involvement of WRNIP1 in the Fanconi anemia pathway.

Second, the cells were treated with genotoxic agent MMC and were subjected to immunofluorescence microscopy analysis where the formation of FANCD2 DNA repair foci was observed. The resultant number of FANCD2 foci was compared with number of foci in cells where WRNIP1 depletion was 95-99%. The outcome of that analysis

indicated that WRNIP1 deficiency did not significantly influenced the formation of the FANCD2 foci. Based on the fractionation and immunofluorescence results, no functional link between FANCD2 and WRNIP1 was found. There was still a possibility that WRNIP1 functions in the Fanconi anemia pathway but it does not influence FANCD2 foci formation nor it changes FANCD2 ubiquitination levels after being subjected to ICL-inducing treatments. WRNIP1 could still act downstream of FANCD2 in the Fanconi anemia pathway. However, this analysis was not sufficient to corroborate this conclusion.

As WRNIP1 was first identified to interact with FANCD2 either directly or indirectly by co-immunoprecipitation, we investigated whether WRNIP1 could interact with non-ubiquitinated FANCD2 or FANCI in *in vitro* binding experiments. It was shown that WRNIP1 was able to interact with both monomeric FANCD2 and monomeric FANCI. Moreover, WRNIP1 was demonstrated to bind to FANCD2 and FANCI, when the three monomeric components were mixed together. WRNIP1 could also bind to FANCD2/FANCI pre-formed heterodimeric complex. The binding between FANCD2 and FANCI was not interrupted by WRNIP1, thus leading to development of several hypothetical interaction models. In one model, one molecule of WRNIP1 would bind to FANCD2 and FANCI via two alternative domains. Alternatively, two WRNIP1 molecules might bind to both FANCD2 or FANCI at the same time or WRNIP1 would dimerize and bind to the FANCD2/FANCI complex.

After establishing the existence of interaction between WRNIP1 and FANCD2 *in vitro*, it was attempted to map a WRNIP1's domain which would interact with FANCD2. Three WRNIP1 deletion mutants were generated and purified from Sf9 cells, i.e. UBZ domain deletion mutant, ATPase domain deletion mutant, C-terminus deletion mutant.

Each of these mutants was shown to bind FANCD2 *in vitro*, thus indicating that the interaction region of WRNIP1 must be located to a sequence located between UBZ domain and ATPase domain. However, this hypothesis would need to be scientifically proven.

The last part of this project focused on characterization of WRNIP1 and its ubiquitination. It was found in this study that WRNIP1 is ubiquitinated both in HeLa and Sf9 cells. This result corroborated the finding from Bish and Myers (2007) who first showed that WRNIP1 was migrating as doublet on the SDS-PAGE gel. This project showed that the ubiquitinated form of WRNIP1 could be observed after purification from Sf9 insect cells and in the fractionation studies. The cell fractionation experiments revealed that WRNIP1's ubiquitinated form was present in both cytoplasmic and nuclear fractions of HeLa cells. Both fractionation methods revealed that WRNIP1's nuclear ubiquitinated form did not increase after treatment with ICL-inducing genotoxic agents. This result might provide some indication that WRNIP1 ubiquitinated form was not necessary for DNA repair. On the other hand, WRNIP1 which would have been necessary for DNA repair might have been already present in the nucleus. Thus, no increase in WRNIP1's ubiquitinated form nuclear fraction was necessary.

The type of ubiquitination was attempted to be established with the use of FK1 and FK2 α-ubiquitin antibodies, where FK1 was targeting polyubiquitin only, whereas FK2 targeted both monoubiquitinated and polyubiquitinated proteins. FK2 antibody was capable of robust detection of the upper form of WRNIP, whereas FK1 antibody resulted in a very weak band. Moreover, it was known that unmodified WRNIP1 run at 75 kDa on SDS-PAGE gels and upper band of WRNIP1 run at 105 kDa. Therefore, the

shift was equivalent to three ubiquitin molecules. Taken together these data may indicate that WRNIP1 was multiubiquitinated by three ubiquitin molecules.

This project provided preliminary evidence that WRNIP1 may be a possible candidate for acting in the Fanconi anemia pathway. The cell lines from which WRNIP1 was depleted showed higher sensitivity towards ICL-inducing agents (especially MMC) and the cell lines complemented with WRNIP1 showed partially reduced sensitivity towards MMC and TMP-UVA. Moreover, WRNIP1 was showed to interact *in vitro* with two members of the FA pathway, i.e. FANCD2 and FANCI and was has been suggested to form a complex with both of these proteins. However, the direct functional link between WRNIP1 and FANCD2 could not be established as WRNIP1 did not influence the formation of FANCD2 foci and it did not change the FANCD2 ubiquitination levels. This result might indicate, however, that WRNIP1 acts downstream of FANCD2 in the Fanconi anemia pathway. Therefore, WRNIP1 is recommended for further analysis and a model of WRNIP1 interaction within the FA pathway has been suggested (Figure 43). The proposed model demonstrates that WRNIP1 might interact with both FANCD2 and FANCI. Moreover, based on the *in vivo* results, WRNIP1 depletion did not affect the ubiquitination level of FANCD2, hence WRNIP1 is suggested to act downstream of FANCD2 ubiquitination, along with other Fanconi anemia downstream effector proteins.

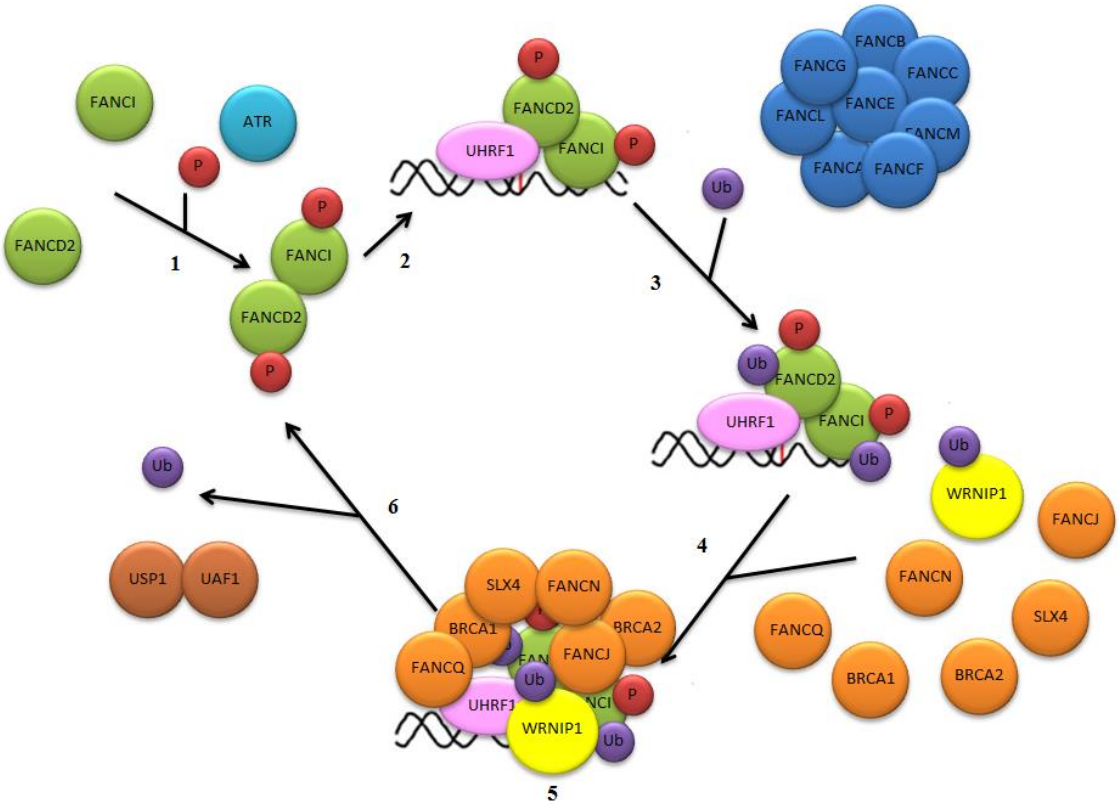



**Figure 43. Simplified diagrammatic representation of the Fanconi anemia ICL-repair pathway including WRNIP1** 1) Phosphorylation of FANCD2 and FANCI by ATR. 2) Sensing of ICL by UHRF1 and localisation of FANCD2/FANCI complex to ICL; recruitment of WRNIP1to ICL by FANCD2/FANCI complex 3) Monoubiquitination of FANCD2 and FANCI at lysine 561 and lysine 523, respectively, by E3 ligase activity of FANCL. 4) Recruitment of WRNIP1 and downstream effector proteins to ICL. 5) Assembly of DNA repair proteins at the ICL. 6) Deubiquitination of FANCD2 and FANCI by USP1/UAF1 complex and disassembly of DNA repair machinery. Not all known components of the Fanconi anemia pathway are included in this model.

# 8 Future Directions

The *in vitro* binding assays revealed that WRNIP1 bound to both established components of the Fanconi anemia pathway, i.e. FANCD2 and FANCI. The *in vitro* binding experiment was conducted, so that Flag- and HA-tagged FANCD2 bound to the α-HA sepharose beads and pulled down WRNIP1 with it. Similarly, both Flag- and HA-tagged FANCI interacted with WRNIP1. In order to corroborate the evidence that WRNIP1 binds *in vitro* to both FANCD2 and FANCI, it can be useful to investigate whether WRNIP1 is able to pull down FANCD2 as well as FANCI *in vitro*. This could be achieved by using StrepTactin beads for binding His- and Strep(II)-tagged WRNIP1 and observing whether FANCD2 and FANCI would be pulled down with it.

Three WRNIP1 deletion mutants were generated in an effort to map a binding site between FANCD2 and WRNIP1. However, the results of that study revealed that neither UBZ domain, ATPase domain nor C-terminus deletion mutants of WRNIP1 were responsible for the interaction with FANCD2. Therefore, it was suggested that two fragments of WRNIP1, i.e. one spanning between UBZ domain and ATPase domain (UBZ-ATPase) as well as the second fragment containing amino acid sequence between ATPase domain and C-terminus region (ATPase-Cterminus), might be responsible for ensuring interaction with FANCD2. Although, both of these deletion mutants were successfully cloned into pFastBac1 vector, their expression levels were very low in Sf9 insect cells. The Western blotting analysis demonstrated that both of these deletion mutants were generated but could not be used as the expression level were not sufficient for *in vitro* binding. Therefore, it is crucial to increase the expression levels of both WRNIP1 deletion mutants, purify them and use them in *in vitro* binding in order to determine the WRNIP1-FANCD2 interaction amino acid sequence. If both remaining

deletion mutants are expressed to the adequate level and show binding to FANCD2, it might indicate that the interaction between FANCD2 and WRNIP1 required a few domains. Hence, it may be necessary to generate WRNIP1 containing more than one domain deletion.

After mapping the domain responsible for WRNIP1-FANCD2 interaction, it would be necessary to investigate which fragment of WRNIP1 interacts with FANCI. In an effort to achieve this, all the previously generated WRNIP1 deletion mutants might be applied in that study.

The possibility of WRNIP1 dimerization has been discussed in this project. However, the sample preparation method as well as use of non-native SDS-PAGE gels ensured that any possible WRNIP1 complexes were disrupted. Therefore, it is recommended to purify WRNIP1 from Sf9 cells and define whether it exists as an oligomer through the use of native SDS-PAGE gels or gel filtration.

As WRNIP1 has been suggested to act downstream of FANCD2 in this project, thus it is hypothesised that depletion of WRNIP1 could result in a delay of DNA lesion repair (ICL repair) and longer time of FANCD2 retention at the damage site. In order to corroborate the hypothesis that WRNIP1 acts downstream of FANCD2, it is recommended to conduct an experiment which could examine the kinetics of DNA repair under the conditions of WRNIP1 deficiency. This could be achieved by live-cell imaging experiment in which FANCD2 with a fluorescent tag (e.g. EGFP) will be introduced to normal cells and WRNIP1-depleted cells. Subsequently, both types of cells will be treated with TMP and microirradiated at the specific sites with a laser beam. The fluorophore-tagged FANCD2 could be subsequently observed in real time to

accumulate at laser irradiation sites in both normal and WRNIP1-depleted cells and dissociate from the damage site after the DNA damage is repaired. The time from laser irradiation to dissociation from the damage site in normal and WRNIP1-depleted cells could be compared.

The WRNIP1 ubiquitination study has confirmed so far that WRNIP1 is highly ubiquitinated protein and that it can be purified from Sf9 insect cells as a doublet. The doublet was revealed to consist of non-ubiquitinated fast migrating form and ubiquitinated slower migrating form. It was attempted to identify the type of ubiquitination of the upper form via blotting with FK2 and FK1 α-ubiquitin antibodies. That analysis and calculation of molecular weight of the WRNIP1's upper form indicated that WRNIP1 might be polyubiquitinated or multiubiquitinated rather than monoubiquitinated. Further research would be necessary to determine the type of ubiquitination that WRNIP1 undergoes. This might be achieved by purification of His- and Strep(II)-tagged WRNIP1 from Sf9 insect cells and performing SDS-PAGE gel electrophoresis followed by the Coomassie staining. Afterwards, the upper form of WRNIP1, now visible on the SDS-PAGE gel, could be cut out of the gels and subjected to trypsin digestion and mass spectrometry. The outcomes of that study should reveal the type of ubiquitination of the upper form of WRNIP1. Simultaneously, an alternative approach might be applied in order to determine the type of WRNIP1's ubiquitination. So far, two antibodies able to target ubiquitinated proteins have been used in this research project, i.e. FK1 and FK2. However, there are various other commercially available antibodies which detect specific ubiquitin chains. These antibodies could be applied in this project by purifying WRNIP1 from Sf9 insect cells and subsequently performing gel electrophoresis and Western blotting analysis on the purified protein.

Western blotting with the antibodies able to detect specific ubiquitin chains could provide an answer whether upper form of WRNIP1 is mono- or polyubiquitinated. Moreover, such study might reveal the exact type of WRNIP1 polyubiquitination, if this post-translational modification is, indeed, occurring on WRNIP1's surface.

It was shown previously that WRNIP1 is a heavily-modified protein (Bish and Myers, 2007). This doctoral study confirmed that WRNIP1 is ubiquitinated. Moreover, it was shown for the first time that WRNIP1 could be purified as doublet from the Sf9 insect cells. It was also demonstrated that ubiquitination of WRNIP1 was very widespread by the Western blot study, where WRNIP1's ubiquitination was detected with α-ubiquitin (FK1 and FK2) antibodies and revealed a smear reaching far beyond the WRNIP1 upper form. If WRNIP1's ubiquitination is such an abundant post-translational modification and WRNIP1's upper form is conserved to such extent that it could be purified from the Sf9 insect cells, the question arises about a possible functionality of WRNIP1's ubiquitination. As protein ubiquitination may serve as a signal for localisation onto the DNA damage sites, it would be important to establish which ubiquitin modification of WRNIP1 may play this role. In order to achieve this, it would be necessary to mutate all known ubiquitins from Bish and Myers (2007) mass spectrometry study and subject mutated WRNIP1 to experiment which would explore its localisation to DNA damage site in the absence of given ubiquitin. In order to achieve this, the cells transfected with mutated WRNIP1 mutant may be treated first with ICL-inducing agent and afterwards subjected to UVA laser irradiation. This type of irradiation in combination with DNA damaging agent is able to introduce interstrand crosslinks into the chromatin. The accumulation, or lack thereof, of WRNIP1 mutant might be visualised with observation of fluorescent tag which should be introduced into WRNIP1.

# 9 Bibliography


Abdulovic, A. L. and Jinks-Robertson, S. (2005). The *in vivo* characterization of translesion synthesis across UV-induced lesions in *Saccharomyces cerevisiae*: insights into polζ- and polη-dependent frameshift mutations. *Genetics*. **172**, 1487-1498.

Acharya, N., Brahma, A., Haracska, L., Prakash, L. and Prakash, S. (2007). Mutations in ubiquitin binding UBZ motif of DNA polymerase η no not impair its function in translesion synthesis during replication. *Molecular and Cellular Biology*. **27**, 7266-7272.

Aggarwal, M., Banerjee, T., Sommers, J. A., Iannascoli, Ch., Pichierri, P., Shoemaker, R. H. and Brosh, Jr. R. M. (2013). Werner syndrome helicase has a critical role in DNA damage responses in the absence of a functional Fanconi anemia pathway. *American Association for Cancer Research*. **73**, 5497-5507.

Ahn, J. Y., Li, X., Davis, H. L. and Canman, C. E. (2002). Phosphorylation of threonine 68 promotes oligomerization and autophosphorylation of the Chk2 protein kinase via the forkhead-associated domain. *Journal of Biological Chemistry*. **277**, 19389-19395.

Alpi, A. F., Pace, P. E., Babu, M. M. and Patel, K. J. (2008). Mechanistic insight into site-restricted monoubiquitination of FANCD2 by UBET2, FANCL, and FANCI. *Molecular Cell*. **32**, 767-777.

Anand, R., Ranjha, L., Cannavo, E. and Cejka, P. (2016). Phosphorylated CtIP functions as a co-factor of the MRE11-RAD50-NBS1 endonuclease in DNA end resection. *Molecular Cell*. **64**, 940-950.

Aparicio, T., Baer, R. and Gautier, J. (2014). DNA double-strand break pathway choice and cancer. *DNA Repair (Amst)*. **19**, 169-175.

Bakker, S. T., de Winter, J. P. and te Riele, H. (2013). Learning from a paradox: recent insights into Fanconi anaemia through studying mouse models. *Disease Models and Mechanisms*. **6**, 40-47.

Bannister, A. J. and Kouzarides, T. (2011). Regulation of chromatin by histone modifications. *Cell Research*. **21**, 381-395.

Bergoglio, V., Boyer, A.-S., Walsh, E., Naim, V., Legube, G., Lee, M. Y. W. T., Rey, L., Rosselli, F., Cazaux, Ch., Eckert, K. A. and Hoffmann, J.-S. (2013). DNA synthesis by Pol η promotes fragile site stability by preventing under-replicated DNA in mitosis. *Journal of Cell Biology*. **201**, 395-408.

Bish, R. A. and Myers, M. P. (2007). Werner helicase-interacting protein 1 binds polyubiquitin via its zinc finger domain. *Journal of Biological Chemistry*. **282**, 23184-23193.

Bish, R. A., Fregoso, O. I., Piccini, A. and Myers, M. P. (2008). Conjugation of complex polyubiquitin chains to WRNIP1. *Journal of Proteome Research*. **7**, 3481-3489.

Bluteau, D., Masliah-Planchon, J., Clairmont, C., Rousseau, A., Ceccaldi, R., Dubois d'Enghien, C., Bluteau, O., Cuccuini, W., Gachet, S., Peffault de Latour, R., Leblanc, T., Socié, G., Baruchel, A., Stoppa-Lyonnet, D., D'Andream A. D. and Soulier, J. (2016). Biallelic inactivation of REV7 is associated with Fanconi anemia. *The Journal of Clinical Investigation.* **126**, 3580-3584.

Bogliolo, M., Schuster, B., Stoepker, Ch., Derkunt, B., Su, Y., Raams, A., Trujillo, J. P., Minguillón, J., Ramírez, M. J., Pujol, R., Casado, J. A., Baños, R., Rio, P., Knies, K., Zúñiga, Sh., Benítez, J., Bueren, J. A., Jaspers, N. G. J., Schärer, O. D., de Winter, J. P., Schindler, D. and Surrallés, J. (2013). Mutations in *ERCC4*, encoding the DNA-repair endonuclease XPF, cause Fanconi anemia. *The American Journal of Human Genetics*. **92**, 800-806.

Boisvert, R. A. and Howlett, N. G. (2014). The Fanconi anemia ID2 complex: dueling saxes at the crossroads. *Cell Cycle*. **13**, 2999-3015.

Bomar, M. G., Pai, M.-T., Tzeng, Sh.-R., Li, Sh. Sh.-Ch. and Zhou, P. (2006). Structure of the ubiquitin-binding zinc finger domain of human DNA Y-polymerase η. *EMBO reports.* **8**, 247-251.

Branzei, D. and Foiani, M. (2008). Regulation of DNA throughout the cell cycle. *Nature Reviews Molecular Cell Biology*. **9**, 297-308.

Branzei, D. and Foiani, M. (2010). Maintaining genome stability at the replication fork. *Nature Reviews Molecular Cell Biology*. **11**, 208-219.

Broderick, R., Nieminuszczy, J., Baddock, H. T., Deshpande, R. A., Gileadi, O., Paull, T. T., McHugh, P. J. and Niedzwiedz, W. (2016). EXD2 promotes homologous recombination by facilitating DNA end resection. *Nature Cell Biology*. **18**, 271-280.

Brosh, R. M. Jr. and Cantor, Sh. B. (2014). Molecular and cellular functions of the FANCJ DNA helicase defective in cancer and in Fanconi anemia. *Frontiers in Genetics*. **5**, 1-14.

Brosh, R. M. Jr. and Waheed, J. (2002). Biochemical characterization of the DNA substrate specificity of Werner syndrome helicase. *The Journal of Biological Chemistry*. **277**, 23236-23245.

Budzowska, M., Graham, T. G., Sobeck, A., Waga, S. and Walter, J. C. (2015). Regulation of the Rev1-pol zeta complex during bypass of a DNA interstrand cross-link. *EMBO Journal*. **34**, 1971-1985.

Buisson, R., Niraj, J., Pauty, J., Maity, R., Zhao, W., Coulombe, Y., Sung, P. and Masson, J.-Y. (2014). Breast cancer proteins PALB2 and BRCA2 stimulate polymerase η in recombination-associated DNA synthesis at blocked replication forks. *Cell Reports*. **6**, 553-564.

Cai, Z., Chehab, N. H. and Pavletich, N. P. (2009). Structure and activation mechanism of the CHK2 DNA damage checkpoint kinase. *Molecular Cell*. **35**, 818-829.

Cannavo, E. and Cejka, P. (2014). Sae2 promotes dsDNA endonuclease activity within Mre11-Rad50-Xrs2 to resect DNA breaks. *Nature*. **514**, 122-125.

Ceccaldi, R., Sarangi, P and D'Andrea, A. D. (2016). The Fanconi anaemia pathway: new players and new functions. *Nature Reviews: Molecular Cell Biology*. **17**, 337-349.

Chang, D. J. and Cimprich, K. A. (2009). DNA damage tolerance: When it's OK to make mistakes. *Nature Chemical Biology*. **5**, 82-90.

Chapman, J. R., Taylor, M. R. and Boulton, S. J. (2012). Playing the end game: DNA double-strand break repair pathway choice. *Molecular Cell*. **47**, 497-510.

Chaudhury, I., Stroik, D. R. and Sobeck, A. (2014). FANCD2-controlled chromatin access of the Fanconi-associated nuclease FAN1 is crucial for the recovery of stalled replication forks. *Molecular and Cellular Biology*. **34**, 3939-3954.

Chen, X., Wilson, J. B., McChesney, P., Williams, S. A., Kwon, Y., Longerich, S., Marriott, A. S., Sung, P., Jones, N. J. and Kupfer, G. M. (2014). The Fanconi anemia proteins FANCD2 and FANCJ interact and regulate each other's chromatin localization. *The Journal of Biological Chemistry*. **289**, 25774-25782.

Cho-Park, P. F. and Steller, H. (2013). Proteasome regulation by ADP-ribosylation. *Cell*. 614-627.

Ciccia, A., Constantinou, A. and West, S. C. (2003). Identification and characterization of the human mus81-eme1 endonuclease. *Journal of Biological Chemistry*. **278**, 25172-25178.

Ciccia, A. and Elledge, S. J. (2010). The DNA damage response: making it safe to play with knives. *Molecular Cell*. **40**, 179-204.

Ciccia, A., McDonald, N. and West, S. C. (2008). Structural and functional relationships of the XPF/MUS81 family of proteins. *Annual Review of Biochemistry*. **77**, 259-287.

Cimprich, K. A. and Cortez, D. (2008). ATR: and essential regulator of genome integrity. *Nature Reviews Molecular Cell Biology*. **9**, 616-627.

Cohn, M. A. and D'Andrea, A. D. (2008). Chromatin recruitment of DNA repair proteins: lessons from the Fanconi anemia and double-strand break repair pathways. *Molecular Cell Review*. **32**, 306-312.

Cohn, M. A., Kee, Y. Haas, W., Gygi, S. P. and D'Andrea, A. D. (2008). UAF1 is a subunit of multiple deubiquitinating enzyme complexes. *The Journal of Biological Chemistry*. **284**, 5343-5351.

Collis, S. J., Ciccia, A., Deans, A. J., Horejsi, Z., Martin, J. S., Maslen, S. L., Skehel, J. M., Elledge, S. J., West, S. C. and Boulton, S. J. (2008). FANCM and FAAP24 function in ATR-mediated checkpoint signaling independently of the Fanconi anemia core complex. *Molecular Cell*. **32**, 313-324.

Cox, L. S. and Mason, P. A. (2013). The role of WRN helicase/exonuclease in DNA replication. *InTech*. 219-254.

Crosetto, N., Bienko, M., Hibbert, R. G., Perica, T., Ambrogio, C., Kensche, T., Hofmann, K., Sixma, T. K. and Dikic, I. (2008). Human Wrnip1 is localized in replication factories in a ubiquitin-binding zinc finger-dependent manner. *The Journal of Biological Chemistry*. **283**, 35173-35185.

Crossan, G. P., van der Weyden, L., Rosado, I. V., Langevin, F., Gaillard, P.-H. L., McIntyre, R. E., Gallagher, F., Kettunen, M. I., Lewis, D. Y., Brindle, K., Arends, M. J., Adams, D. J. and Patel, K. J. (2011). Disruption of mouse Slx4, a regulator of structure-specific nucleases, phenocopies Fanconi anemia. *Nature Genetics*. **43**, 147-152.

Cruz-Garcia, A., López-Saavedra, A. and Huertas, P. (2014). BRCA1 accelerates CtIP-mediated DNA-end resection. *Cell Reports*. **9**, 451-459.

Cumming, G., Fidler, F. and Vaux, D. L. (2007). Error bars in experimental biology. *The Journal of Cell Biology*. **177**, 7-11.

Daley, J. M., Niu, H., Miller, A. S. and Sung, P. (2015). Biochemical mechanism of DSB end resection and its recombination. *DNA Repair (Amst).* **32,** 66-74.

D'Andrea, A. D. (2013). BRCA1: a missing link in the Fanconi anemia/BRCA pathway. *Cancer Discovery*. **3**, 376-378.

Dao, K.-H. T., Rotelli, M. D., Brown, B. R., Yates, J. E., Rantala, J., Tognon, C., Tyner, J. W., Druker, B. J. and Bagby, G. C. (2013). The PI3K/Akt1 pathway enhances steady-state levels of FANCL. *Molecular Biology of the Cell.* **24**, 2582-2592.

Davis, A. J., Chen, B. P. and Chen, D. J. (2014). DNA-PK: a dynamic enzyme in a versatile DSB repair. *DNA Repair (Amst)*. **17**, 21-29.

De Ioannes, P., Malu, S., Cortes, P. and Aggarwal, A. K. (2012). Structural basis of DNA ligase IV-Artemis interaction in nonhomologous end-joining. *Cell Reports*. **2**, 1505-1512.

de Winter, J. P. and Joenje, H. (2009). The genetic and molecular basis of Fanconi anemia. *Mutation Research*. **668**, 11-19.

de Winter, J. P., Rooimans, M., van Der Weel, L., van Berkel, C., Alon, N., Bosnoyan-Collins, L., de Groot, J., Zhi, Y., Waisfisz, Q. and Pronk, J. (2000). The Fanconi anaemia gene FANCF encodes a novel protein with homology to ROM. *Nature Genetics*. **24**, 15-16.

de Winter, J. P., Waisfisz, Q., Rooimans, M., van Berkel, C., Bosnoyan-Collins, L., Alon, N., Carreau, M., Bender, O., Demuth, I. and Schindler, D. (1998). The Fanconi anaemia group G gene FANCG is identical with XRCC9. *Nature Genetics*. **20**, 281-283.

Deans, A. J. and West, S. C. (2011). DNA interstrand crosslink repair and cancer. *Nature Reviews Cancer*. **11**, 467-480.

Deans, A. J. (2012). Fanconi proteins get histones moving. *The EMBO Journal*. **31**, 3511-3512.

Dellaire, G. and Bazett-Jones, D. P. (2007). Beyond repair foci: subnuclear domains and the cellular response to DNA damage. *Cell Cycle*. **6**, 1864-1872.

Dikic, I., Wakatsuki, S. and Walters, K. J. (2009). Ubiquitin-binding domains – from structures to functions. *Nature Reviews Molecular Cell Biology*. **10**, 659-671.

Dong, Y. P., Seki, M., Yoshimura, A., Inoue, E., Furukawa, Sh., Tada, Sh. and Enomoto, T. (2007). WRN functions in a RAD18-dependent damage avoidance pathway. *Biological and Pharmaceutical Bulletin.* **30**, 1080-1083.

Dolan, D., Nelson, G., Zupanic, A., Smith, G. and Shanley, D. (2013). Systems modelling of NHEJ reveals the importance of redox regulation of Ku70/80 in the dynamics of DNA damage foci. *PLoS ONE*. **8**

Downs, J. A. and Jackson, S. P. (2004). A means to a DNA end: the many roles of Ku. *Nature Reviews Molecular Cell Biology*. **5**, 367-378.

Dronkert, M. L. G. and Kanaar, R. (2001). Repair of DNA interstrand cross-links. *Mutation Research*. **486**, 217-247.

Drugmand, J.-Ch., Schneider, Y.-J. and Agathos, S. N. (2012). Insect cells as factories for biomanufacturing. *Biotechnology Advances*. **30**, 1140-1157.

Duquette, M. L., Zhu, Q., Taylor, E. R., Tsay, A. J., Shi, L. Z., Berns, M. W. and McGowan, C. H. (2012). CtIP is required to initiate replication-dependent interstrand crosslink repair. *PLOS Genetics*. **8**, 1-14.

Dupré, A., Boyer-Chatenet, L., Sattler, R. M., Modi, A. P., Lee, J. H., Nicolette, M. L., Kopelovich, L., Jasin, M., Baer, R., Paull, T. T. and Gautier, J. (2008). A forward chemical genetic screen reveals an inhibitor of the Mre11-Rad50-Nbs1 complex. *Nature Chemical Biology*. **4**, 119-125.

Durando, M., Tateishi, S. and Vaziri, C. (2013). A non-catalytic role of DNA polymerase η in recruiting Rad18 and promoting PCNA monoubiquitination at stalled replication forks. *Nucleic Acids Research*. **41**, 3079-3093.

Escribano-Diaz, C., Orthwein, A., Fradet-Turcotte, A., Xing, M., Young, J. T. F., Tkáč, J., Cook, M. A., Rosebrock, A. P., Munro, M., Canny, M. D., Xu, D. and Durocher, D. (2013). A cell cycle-dependent regulatory circuit composed of 53BP1-RIF1 and BRCA1-CtIP controls DNA repair pathway choice. *Molecular Cell*. **49**, 872-883.

Falck, J., Coates, J. and Jackson, S. P. (2005). Conserved modes of recruitment of ATM, ATR and DNA-PKcs to sites of DNA damage. *Nature*. **434**, 605-611.

Farmer, H., McCabe, N., Lord, C. J., Tutt, A. N. J., Johnson, D. A., Richardson, T. B., Santarosa, M., Dillon, K. J., Hickson, I., Knights, C., Martin, N. M. B., Jackson, S. P., Smith, G. C. M. and Ashworth, A. (2005). Targeting the DNA repair defect in *BRCA* mutant cells as a therapeutic strategy. *Nature*. **434**, 917-921.

Fei, P., Yin, J. and Wang, W. (2005). New advances in the DNA damage response network of Fanconi anemia and BRCA proteins: FAAP95 replaces BRCA2 as the true FANCB protein. *Cell Cycle*. **4**, 80-86.

Fu, D., Dudimah, F. D., Zhang, J., Pickering, A., Paneerselvam, J., Palrasu, M., Wang, H. and Fei, P. (2013). Recruitment of DNA polymerase eta by FANCD2 in the early response to DNA damage. *Cell Cycle*. **12**, 803-809.

Fujimoto, M. and Yokosawa, H. (2005). Production of antipolyubiquitin monoclonal antibodies and their use for characterisation and isolation of polyubiquitinated proteins. *Methods in Enzymology*. **399**, 75-86.

Furuse, M., Nagase, Y., Tsubouchi, H., Murakami-Murofushi, K., Shibata, T. and Ohta, K. (1998). Distinct roles of two separable *in vitro* activities of yeast Mre11 in mitotic and meiotic recombination. *EMBO Journal*. **17**, 6412-6425.

Garcia-Higuera, I., Taniguchi, T., Ganesan, Sh., Meyn, M. S., Timmers, C., Hejna, J., Grompe, M. and D'Andrea, A. (2001). Interaction of the Fanconi anemia proteins and BRCA1 in a common pathway. *Molecular Cell*. **7**, 249-262.

Garner, E., Kim, Y., Lach, F. P., Kottemann, M. C. and Smogorzewska, A. (2013). Human GEN1 and SLX4-associated nucleases MUS81 and SLX1 are essential for the resolution of replication-induced Holliday junctions. *Cell Reports*. **5**, 207-215.

Garner, E. and Smogorzewska, A. (2011). Ubiquitylation and the Fanconi anemia pathway. *FEBS Letters*. **585**, 2853-2860.

Geng, L., Huntoon, C. J. and Karnitz, L. M. (2010). Rad18-mediated ubiquitination of PCNA activates the Fanconi anemia DNA repair network. *The Journal of Cell Biology*. **191**, 249-257.

Goodsell, D. S. (2001). The molecular perspective: ultraviolet light and pyrimidine dimmers. *The Oncologist*. **6**, 298-299.

Gravel, S., Chapman, J. R., Magill, C. and Jackson, S. P. (2008). DNA helicases Sgs1 and BLM promote DNA double-stand break resection. *Genes and Development.* **22**, 2767-2772.

Gravells, P., Hoh, L., Solovieva, S., Patil, A., Dudziec, E., Rennie, I. G., Sisley, K. and Bryant, H. E. (2013). Reduced FANCD2 influences spontaneous SCE and RAD51 foci formation in uveal melanoma and Fanconi anaemia. *Oncogene*. **32**, 1-9.

Gregory, R. C., Taniguchi, T. and D'Andrea, A. D. (2003). Regulation of the Fanconi anemia pathway by monoubiquitination. *Seminars in Cancer Biology*. **13**, 77-82.

Guervilly, J.-H., Takedachi, A., Naim, V., Scaglione, S., Chawhan, Ch., Lovera, Y., Despras, E., Kuraoka, I., Kannouche, P., Rosselli, F. and Gaillard, P.-H. L. (2015). The SLX4 complex is a SUMO E3 ligase that impacts on replication stress outcome and genome stability. *Molecular Cell*. **57**, 123-137.

Haglund, K. and Stenmark, H. (2006). Working out coupled monoubiquitination. *Nature Cell Biology*. **8**, 1218-1219.

Hanson, P. I. and Whiteheart, S. W. (2005). AAA+ proteins: have engine, will work. *Nature Reviews Molecular Cell Biology*. **6**, 519-529.

Hayashi, T., Seki, M., Inoue, E., Yoshimura, A., Kusa, Y., Tada, S. and Enomoto, T. (2008). Vertebrate WRNIP1 and BLM are required for efficient maintenance of genome stability. *Genes & Genetic Systems*. **83**, 95-100.

Haynes, B., Saadat, N., Myung, B. and Shekhar, M. P. V. (2015). Crosstalk between translesion synthesis, Fanconi anemia network, and homologous recombination repair pathways in interstrand DNA crosslink repair and development of chemoresistance. *Mutation Research*. **763**, 258-266.

Helchowski, C. M., Show, L. F., Roberts, K. H., Chute, C. L. and Canman, Ch. E. (2013). A small ubiquitin binding domain inhibits ubiquitin-dependent protein recruitment to DNA repair foci. *Cell Cycle*. **12**, 3749-3758.

Higgs, M. R., Reynolds, J. J., Winczura, A., Blackford, A. N., Borel, V., Miller, E. S., Zlatanou, A., Nieminuszczy, J., Ryan, E. L., Davies, N. J., Stankovic, T., Boulton, S. J., Niedzwiedz, W. and Stewart, G. S. (2015). BOD1L is required to suppress deleterious resection of stressed replication forks. *Molecular Cell.* **59**, 462-477.

Hishida, T., Iwasaki, H., Ohno, T., Morishita, T. and Shinagawa, H. (2001). A yeast gene, MGS1, encoding a DNA-dependent $AAA^+$ ATPase is required to maintain genome stability. *PNAS*. **98**, 8283-8289.

Hishida, T., Ohya, T., Kubota, Y., Kamada, Y. and Shinagawa, H. (2006). Functional and physical interaction of yeast Mgs1 with PCNA: impact on *RAD6*-dependent DNA damage tolerance. *Molecular and Cellular Biology*. **26**, 5509-5517.

Ho, T. V. and Schärer, O. D. (2010). Translesion DNA synthesis polymerases in DNA interstrand crosslink repair. *Environmental and Molecular Mutagenesis*. **51**, 552-566.

Hodson, Ch. and Walden, H. (2012). Towards a molecular understanding of the Fanconi anemia core complex. *Anemia*. 1-10.

Hofmann, K. (2009). Ubiquitin-binding domains and their role in the DNA damage response. *DNA Repair*. **8**, 544-556.

Hopfner, K. P., Karcher, A., Craig, L., Woo, T. T., Carney, J. P. and Tainer, J. A. (2001). Structural biochemistry and interaction architecture of the DNA double-stand break repair Mre11 nuclease and Rad50-ATPase. *Cell*. **105**, 473-485.

Howlett, N. G., Taniguchi, T., Olson, S., Cox, B., Waisfisz, Q., de Die-Smulders, Ch., Persky, N., Grompe, M., Joenje, H., Pals, G., Ikeda, H., Fox, E. A. and D'Andrea, A. D. (2002). Biallelic inactivation of *BRCA2* in Fanconi anemia. *Science*. **297**, 606-609.

Huang, T. T. and D'Andrea, A. D. (2006). Regulation of DNA repair by ubiquitylation. *Nature Reviews Molecular Cell Biology*. **7**, 323-334.

Huang, Y., Leung, J. W. C., Lowery, M., Matsushita, N., Wang, Y., Shen, X., Huong, D., Takata, M., Chen, J. and Li L. (2014). Modularized functions of the Fanconi anemia core complex. *Cell Reports*. **7**, 1849-1857.

Huen, M. S. Y. and Chen, J. (2008). The DNA damage response pathways: at the crossroad of protein modifications. *Cell Research*. **18**, 8-16.

Ishiai, M., Kitao, H., Smogorzewska, A., Tomida, J., Kinomura, A., Uchida, E., Saberi, A., Kinoshita, E., Kinoshita-Kikuta, E., Koike, T., Tashiro, S., Elledge, S. J. and Takata,

M. (2008). FANCI phosphorylation functions as a molecular switch to turn on the Fanconi anemia pathway. *Nature Structural & Molecular Biology*. **15**, 1138-1146.

Jackson, D. G. and Dent, Sh. Y. R. (2013). Chromatin: receiver and quarterback for cellular signals. *Cell*. **152**, 685-689.

Jackson, S. P. and Bartek, J. (2009). The DNA-damage response in human biology and disease. *Nature*. **461**, 1071-1078.

Jackson, S. P. and Durocher, D. (2013). Regulation of DNA damage responses by ubiquitin and SUMO. *Molecular Cell Review*. **49**, 795-807.

Jacquemont, C. and Taniguchi, T. (2007). Proteasome function is required for DNA damage response and Fanconi anemia pathway activation. *Cancer Research*. **67**, 7395-7405.

Jiang, W., Crowe, J. L., Liu, X., Nakajima, S., Wang, Y., Li, C., Lee, B. J., Dubois, R. L., Liu, C., Yu, X., Lan, L. and Zha, S. (2015). Differential phosphorylation of DNA-PKcs regulates the interplay between end-processing and end-ligation during nonhomologous end-joining. *Molecular Cell*. **58**, 172-186.

Jones, M. J. K. and Huang, T. T. (2012). The Fanconi anemia pathway in replication stress and DNA crosslink repair. *Cellular and Molecular Life Sciences.* **69**, 3963-3974.

Jones, P. A. (2012). Functions of DNA methylation: islands, start sites, gene bodies and beyond. *Nature Reviews Genetics*. **13**, 484-492.

Joo, W., Xu, G., Persky, N. S., Smogorzewska, A., Rudge, D. G., Buzovetsky, O., Elledge, S. J. and Pavletich, N. P. (2011). Structure of the FANCI-FANCD2 complex: insights into the Fanconi anemia DNA repair pathway. *Science.* **333**, 312-316.

Kaddar, T. and Carreau, M. (2012). Fanconi anemia proteins and their interacting partners: a molecular puzzle. *Anemia*. 1-11.

Kakarougkas, A. and Jeggo, P. A. (2014). DNA DSB repair pathway choice: an orchestrated handover mechanism. *The British Journal of Radiology*. **87**, 20130685.

Kanamori, M., Seki, M., Yoshimura, A., Tsurimoto, T., Tada, S. and Enomoto, T. (2011). Werner interacting protein 1 promotes binding of Werner protein to template-primer DNA. *Biological and Pharmaceutical Bulletin*. **34**, 1314-1318.

Kanu, N., Zhang, T., Burrell, R. A., Chakraborty, A., Cronshaw, J., Costa, C. D., Grönroos, E., Pemberton, H. N., Anderton, E., Gonzalez, L., Sabbioneda, S., Ulrich, H. D., Swanton, C. and Behrens, A. (2015). RAD18, WRNIP1 and ATMIN promote ATM signalling in response to replication stress. *Oncogene*. 1-11.

Kass, E. M. and Jasin, M. (2010). Collaboration and competition between DNA double-strand break repair pathways. *FEBS Letters*. **584**, 3703-3708.

Kaur, S., White, T. E., DiGuilio, A., L. and Glavy, J. S. (2010). The discovery of Werner helicase interacting protein (WHIP) association with the nuclear pore complex. *Cell Cycle*. **9**, 3106-3111.

Kawabe, Y-I., Branzei, D., Hayashi, T., Suzuki, H., Masuko, T., Onoda, F., Heo, S-J., Ikeda, H., Shimamoto, A., Furuichi, Y., Seki, M. and Enomoto, T. (2001). A novel protein interacts with the Werner's syndrome gene product physically and functionally. *The Journal of Biological Chemistry*. **276**, 20364-20369.

Kawabe, Y-I., Seki, M., Yoshimura, A., Nishino, K., Hayashi, T., Takeuchi, T., Iguchi, S., Kusa, Y., Ohtsuki, M., Tsuyama, T., Imamura, O., Matsumoto, T., Furuichi, Y., Tada, S. and Enomoto, T. (2006). Analyses of the interaction of WRNIP1 with Werner syndrome protein (WRN) *in vitro* and in the cell. *DNA Repair*. **5**, 816-828.

Kee, Y. and D'Andrea, A. D. (2010). Expanded roles of the Fanconi anemia pathway in preserving genomic stability. *Genes & Development*. **24**, 1680-1694.

Kim, H. and D'Andrea, A. D. (2012). Regulation of DNA cross-link repair by the Fanconi anemia/BRCA pathway. *Genes & Development*. **26**, 1393-1408.

Kim, H., Dejsuphong, D., Adelmant, G., Ceccaldi, R., Yang, K., Marto, J. A. and D'Andrea, A. D. (2014). Transcriptional repressor ZBTB1 promotes chromatin remodeling and translesion DNA synthesis. *Molecular Cell*. **54**, 107-118.

Kim, J. M., Kee, Y., Gurtan, A. and D'Andrea, A. (2008). Cell cycle-dependent chromatin loading of the Fanconi anemia core complex by FANCM/FAAP24. *Blood*. **111**, 5215-5222.

Kim, Y., Spitz, G. S., Veturi, U., Lach, F. P., Auerbach, A. D. and Smogorzewska, A. (2012). Regulation of multiple DNA repair pathways by the Fanconi anemia protein SLX4. *Blood*, **121**, 54-63.

Klein Douwel, D., Boonen, R. A. C. M., Long, D. T., Szypowska, A. A., Räschle, M., Walter, J. C. and Knipscheer, P. (2014). XPF-ERCC1 acts in unhooking DNA interstrand crosslinks in cooperation with FANCD2 and FANCP/SLX4. *Molecular Cell*. **54**, 460-471.

Knipscheer, P., Räschle, M., Smogorzewska, A., Enoiu, M., Ho, T. V., Schärer, O. D., Elledge, S. J. and Walter, J. C. (2009). The Fanconi anemia pathway promotes replication-dependent DNA interstrand cross-link repair. *Science*. **326**, 1698-1701.

Kottemann, M. C. and Smogorzewska, A. (2013). Fanconi anaemia and the repair of Watson and Crick DNA crosslinks. *Nature*. **493**, 356-363.

Kowalczykowski, S. C. (2015). An overview of the molecular mechanisms of recombinational DNA repair. *Cold Spring Harbor Perspectives in Biology.* **7**, 7.

Kratz, K., Schöpf, B., Kaden, S., Sendoel, A., Eberhard, R., Lademann, C., Cannavó, E., Sartori, A. A., Hengartner, M. O. and Jiricny, J. (2010). Seficiency of FANCD2-associated nuclease KIAA1018/FAN1 sensitizes cells to interstand crosslinking agents. **142**, 77-88.

Kupfer, G. M, Naf, D., Garcia-Higuera, I., Wasik, J., Cheng, A., Yamashita, T., Tipping, A., Morgan, N., Mathew, C. G. and D'Andrea, A. D. (1999). A patient-derived mutant from the Fanconi anemia protein, FANCA, is defective in nuclear accumulation. *Experimental Hematology*. **27**, 587-593.

Kupfer, G. M., Naf, D., Suliman, A., Pulsipher, M. and D'Andrea, A. D. (1997). The Fanconi anemia proteins, FAA and FAC interact to form a nuclear complex. *Nature Genetics*. **17**, 487-490.

Kusumoto-Matsuo, R., Ghosh, D., Karmakar, P., May, A., Ramsden, D. and Bohr, V. A. (2014). Serines 440 and 467 in the Werner syndrome protein are phosphorylated by DNA-PK and affect its dynamics in response to DNA double strand breaks. *Aging (Albany, NY)*. **6**, 70-81.

Lachaud, Ch., Castor, D., Hain, K., Muñoz, I., Wilson, J., MacArtney, T. J., Schindler, D. and Rouse, J. (2014). Distinct functional roles for the two SLX4 ubiquitin-binding UBZ domains mutated in Fanconi anemia. *Journal of Cell Science*. **127**, 2811-2817.

Le Breton, C., Hennion, M., Arimondo, P. B. and Hyrien, O. (2011). Replication-fork stalling and processing at a single psolaren interstrand crosslink in Xenopus egg extracts. *PLoS ONE*. **6**, 1-10.

Lee, J.-H. and Paull, T. T. (2005). ATM activation by DNA double-strand breaks through the Mre11-Rad50-Nbs1 complex. *Science*. **308**, 551-554.

Lehmann, A. R. (2003). DNA repair-deficient diseases, xeroderma pigmentosum, Cockayne syndrome and trichothiodystrophy. *Biochimie*. **85**, 1101-1111.

Leung, J. W. C., Wang, Y., Fong, K. W., Huen, M. S. Y., Li, L. and Chen, J. (2012) Fanconi anemia (FA) binding protein FAAP20 stabilizes FA complementation group A (FANCA) and participates in interstrand crosslink repair. *Proceedings of the National Academy of Sciences*. **109**, 4491-4496.

Liang, C.-C., Li, Z., Lopez-Martinez, D., Nicholson, W. V., Vénien-Bryan, C. and Cohn, M. A. (2016). The FANCD2-FANCI complex is recruited to DNA interstrand crosslinks before monoubiquitination of FANCD2. *Nature Communications.* **7**, 1-10.

Liang, C.-C., Zhan, B., Gygi, S. P. and Cohn, M. A. (2015). UHRF1 is a sensor for DNA interstrand crosslinks and recruits FANCD2 to initiate the Fanconi anemia pathway. *Cell Reports*. **10**, 1-10.

Lieber, M. R., Ma, Y., Pannicke, U. and Schwarz, K. (2003). Mechanism and regulation of human non-homologous DNA end-joining. *Nature Reviews Molecular Cell Biology*. **4**, 712-720.

Ling, C., Ishiai, M., Ali, A. M., Medhurst, A. L., Neveling, K., Kalb, R., Yan, Z., Xue, Y., Oostra, A. B., Auerbach, A. D., Hoatlin, M. E., Schindler, D., Joenje, H., de Winter, J. P., Takata, M., Ruhikanta, A. and Wang, W. (2007). FAAP100 is essential for activation of the Fanconi anemia-associated DNA damage response pathway. *EMBO J*. **26**, 2104-2114.

Liu, T., Ghosal, G., Yuan, J., Chen, J. and Huang, J. (2010). FAN1 acts with FANCI-FANCD2 to promote DNA interstrand cross-link repair. *Science*. **329**, 693-696.

Liu, T. and Huang, J. (2016). DNA end resection: facts and mechanisms. *Genomics Proteomics Bioinformatics*. **14**, 126-130.

Long, D. T., Joukov, V., Budzowska, M. Walter, J. C. (2014). BRCA1 promotes unloading of the CMG helicase from a stalled DNA replication fork. *Molecular Cell*. **56**, 174-185.

Longerich, S., Filippo, J. S., Liu, D. and Sung, P. (2009). FANCI binds branched DNA and is monoubiquitinated by UBE2T-FANCL. *Journal of Biological Chemistry*. **284**, 23182-23186.

Longerich, S., Kwon, Y., Tsai, M.-Sh., Hlaing, A. S., Kupfer, G. M. and Sung, P. (2014). *Nucleic Acids Research*. 1-14.

Lopez-Martinez, D., Liang, C.-C. and Cohn, M. A. (2016). Cellular response to DNA interstrand crosslinks: the Fanconi anemia pathway. *Cellular and Molecular Life Sciences*. **73**, 3097-3114.

Low, T. Y., Magliozzi, R., Guardavaccaro, D. and Heck, A. J. R. (2013). Unraveling the ubiquitin-regulated signaling networks by mass spectrometry-based proteomics. *Proteomics*. **13**, 526-537.

Lukas, C., Falck, J., Bartkova, J., Bartek, J. and Lukas, J. (2003). Distinct spatiotemporal dynamics of mammalian checkpoint regulators induced by DNA damage. *Nature Cell Biology*. **5**, 255-260.

Lukas, J., Lukas, C. and Bartek, J. (2011). More than just a focus: the chromatin response to DNA damage and its role in genome integrity maintenance. *Nature Cell Biology*. **13**, 1161-1169.

Ma, Y., Pannicke, U., Schwarz, K. and Lieber, M. R. (2002). Hairpin opening and overhang processing by an Artemis/DNA-dependent protein kinase complex in nonhomologous end joining and V(D)J recombination. *Cell*. **108**, 781-794.

Ma, Y., Schwarz, K. and Lieber, M. R. (2005). The Artemis:DNA-PKcs endonuclease cleaves DNA loops, flaps and gaps. *DNA Repair (Amst)*. **4**, 845-851.

MacKay, C., Déclais, A.-C., Lundin, C., Agostinho, A., Deans, A. J., MacArtney, T. J., Hofmann, K., Gartner, A., West, S. C., Helleday, T., Lilley, D. M. J. and Rousem J. (2010). Identification of KIAA1018/FAN1, a DNA repair nuclease recruited to DNA damage by monoubiquitinated FANCD2. *Cell*. **142**, 65-76.

Mah, L.-J., El-Osta, A. and Karagiannis, T. C. (2010). γH2AX: a sensitive molecular marker of DNA damage and repair. *Leukemia*. **24**, 679-686.

Mailand, N., Gibbs-Seymour, I. and Bekker-Jensen, S. (2013). Regulation of PCNA-protein interactions for genome stability. *Nature Reviews Molecular Cell Biology*. **14**, 269-282.

Malkova, A. and Haber, J. E. (2012). Mutations arising during repair of chromosome breaks. *Annual Review of Genetics*. **46**, 455-473.

Malumbres, M. and Barbacid, M. (2009). Cell cycle, CDKs and cancer: a changing paradigm. *Nature Reviews*. **9**, 153-167.

Mamrak, N. E., Shimamura, A. and Howlett, N. G. (2016). Recent discoveries in the molecular pathogenesis of the inherited bone marrow failure syndrome Fanconi anemia. *Blood Reviews.*

Marteijn, J. A., Lans, H., Vermeulen, W. and Hoeijmakers, J. H. J. (2014). Understanding nucleotide excision repair and its roles in cancer and ageing. *Nature Reviews Molecular Cell Biology*. **15**, 465-481.

Matsuoka, S., Ballif, B. A., Smogorzewska, A., McDonald, E. R. 3rd, Hurov, K. E., *et al.* (2007). ATM and ATR substrate analysis reveals extensive protein networks responsive to DNA damage. *Science.* **316**, 1160-1166.

Meetei, A. R., Medhurst, A. L., Ling, C., Xue, Y., Singh, T. R., Bier, P., Steltenpool, J., stone, S., Dokal, I., Mathew, C. G., Hoatlin, M., Joenje, H., de Winter, J. P. and Wang, W. (2005). A human ortholog of archaeal DNA repair protein Hef is defective in Fanconi anemia complementation group M. *Nature Genetics*. **37**, 958-963.

Meetei, A. R., Yan, Z. and Wang, W. (2004). FANCL replaces BRCA1 as the likely ubiquitin ligase responsible for FANCD2 monoubiquitination. *Cell Cycle*. **3**, 174-176.

Mimori, T. and Hardin, J. A. (1986). Mechanism of interaction between Ku protein and DNA. *Journal of Biological Chemistry.* **261**, 10375-10379.

Mimitou, E. P. and Symington, L. S. (2008). Sae2, Exo1 and Sgs1 collaborate in DNA double-strand break processing. *Nature.* **455**, 770-774.

Mimitou, E. P. and Symington, L. S. (2010). Ku prevents Exo1 and Sgs1-dependent resection of DNA ends in the absence of a functional MRX complex or Sae2. *EMBO Journal*. **29**, 3358-3369.

Mirchandani, K. D. and D'Andrea, A. D. (2006). The Fanconi anemia/BRCA pathway: a coordinator of cross-link repair. *Experimental Cell Research*. **312**, 2647-2653.

Modesti, M., Hesse, J. E. and Gellert, M. (1999). DNA binding to Xrcc4 protein is associated with V(D)J recombination but not with stimulation of DNA ligase IV activity. *EMBO Journal*. **18**, 2008-2018.

Moldovan, G.-L. and D'Andrea, A. D. (2009). How the Fanconi anemia pathway guards the genome. *Annual Review of Genetics*. **43**, 223-249.

Moldovan, G.-L. and D'Andrea, A. D. (2012). To the rescue: the Fanconi anemia genome stability pathway salvages replication forks. *Cancer Cell*. **22**, 5-6.

Moldovan, G.-L., Pfander, B. and Jentsch, S. (2007). PCNA, the maestro of the replication fork. *Cell*. **129**, 665-679.

Moser, J., Kool, H., Giakzidis, I., Caldecott, K., Mullenders, L. H. F. and Fousteri, M. I. (2007). Sealing of chromosomal DNA nicks during nucleotide excision repair requires XRCC1 and DNA Ligase III in a cell-cycle-specific manner. *Molecular Cell*. **27**, 311-323.

Mouw, K. W. and D'Andrea, A. D. (2014). Crosstalk between the nucleotide excision repair and Fanconi anemia/BRCA pathways. *DNA Repair*. **19**, 130-134.

Murina, O., von Aesch, Ch., Karakus, U., Ferretti, L. P., Bolck, H. A., Hänggi, K. and Sartori, A. A. (2014). FANCD2 and CtIP cooperate to repair DNA interstrand crosslinks. *Cell Reports*. **7**, 1030-1038.

Nakanishi, K., Taniguchi, T., Ranganathan, V., New, H. V., Moreau, L. A., Stotsky, M., Mathew, C. G., Kastan, M. B., Weaver, D. T. and D'Andrea, A. D. (2002). Interaction of FANCD2 and NBS1 in the DNA damage response. *Nature Cell Biology*. **4**, 913-920.

Niimi, A., Brown, S., Sabbioneda, S., Kannouche, P. L., Scott, A., Yasui, A., Green, C. M. and Lehmann, A. R. (2008). Regulation of proliferating cell nuclear antigen ubiquitination in mammalian cells. *PNAS*. **105**, 16125-16130.

Nijman, S. M. B., Huang, T. T., Dirac, A. M. G., Brummelkamp, T. R., Kerkhoven, R. M., D'Andrea, A. D. and Bernards, R. (2005). The deubiquitinating enzyme USP1 regulates the Fanconi anemia pathway. *Molecular Cell*. **17**, 331-339.

Nimonkar, A. V., Genschel, J., Kinoshita, E., Polaczek, P., Campbell, J. L., Wyman, C., Modrich, P. and Kowalczykowski, S. C. (2011). BLM-DNA2-RPA-MRN and EXO1-BLM-RPA-MRN constitute two DNA end resection machineries for human DNA break repair. *Genes and Development*. **25**, 350-362.

Niu, H., Chung, W. H., Zhu, Z., Kwon, Y., Zhao, W., Chi, P., Prakash, R., Seong, C., Liu, D., Lu, L., Ira, G. and Sung, P. (2010). Mechanism of the ATP-dependent DNA end-resection machinery from *Saccharomyces cerevisiae*. **467**, 108-111.

Nomura, H., Yoshimura, A., Edo, T., Kanno, S-I., Tada, S., Seki, M., Yasui, A. and Enomoto, T. (2012). WRNIP1 accumulates at laser light irradiated sites rapidly via its ubiquitin-binding zinc finger domain and independently from its ATPase domain. *Biochemical and Biophysical Research Communications*. **417**, 1145-1150.

Nussenzweig, A. and Nussenzweig, M. C. (2007). A backup DNA repair pathway moves to the forefront. *Cell*. **131**, 223-225.

Ochi, T., Blackford, A. N., Coates, J., Jhujh, S., Mehmood, S., Tamura, N., Travers, J., Wu, Q., Draviam, V. M., Robinson, C. V., Blundell, T. L. and Jackson, S. P. (2015). DNA repair. PAXX, a paralog of XRCC4 and XLF, interacts with Ku to promote DNA double-strand break repair. *Science*. **347**, 185-188.

O'Donovan, P. J. and Livingston, D. M. (2010). BRCA1 and BRCA2: breast/ovarian cancer susceptibility gene products and participants in DNA double-strand break repair. *Carcinogenesis*. **31**, 961-967.

Ohmori, H., Friedberg, E. C., Fuchs, R. P., Goodman, M. F., Hanaoka, F., Hinkle, D., Kunkel, T. A., Lawrence, C. W., Livneh, Z., Nohmi, T., Prakash, L., Prakash, S., Todo, T., Walker, G. C., Wang, Z. and Woodgate, R. (2001). The Y-family of DNA polymerases. *Molecular Cell*. **8**, 7-8.

Oliver, A. W., Paul, A., Boxall, K. J., Barrie, S. E., Aherne, G. W., Gerrett, M. D., Mittnacht, S. and Pearl, L. H. (2006). Trans-activation of the DNA-damage signalling protein kinase Chk2 by T-loop exchange. *EMBO Journal*. **25**, 3179-3190.

Osorio, A., Bogliolo, M., Fernández, V., Barroso, A., de la Hoya, M., Caldés, T., Lasa, A., Ramón y Cajal, T., Santamariña, M., Vega, A., Quiles, F., Lázaro, C., Díez, O., Fernández, D., González-Sarmiento, R., Durán, M., Fernández Piqueras, J., Marín, M., Pujol, R., Surrallés, J. and Benítez, J. (2013). Evaluation of rare variants in the new Fanconi anemia gene *ERCC4* (*FANCQ*) as familial breast/ovarian cancer susceptibility alleles. *Human Mutation*. **34**, 1615-1618.

Ouyang, J., Garner, E., Hallet, A., Nguyen, H. D., Rickman, K. A., Gill, G., Smogorzewska, A. and Zou, L. (2015). Noncovalent interactions with SUMO and ubiquitin orchestrate distinct functions of the SLX4 complex in genome maintenance. *Molecular Cell*. **57**, 108-122.

Pace, P., Johnson, M., Tan, W. M., Mosedale, G., Sng, C., Hoatlin, M., de Winter, J., Joenje, H., Gergely, F. and Patel, K. J. (2002). FANCE: the link between Fanconi anaemia complex assembly and activity. *EMBO*. **21**, 3414-3423.

Panier, S. and Boulton, S. J. (2014). Double-strand break repair: 53BP1 comes into focus. *Nature Reviews Molecular Cell Biology*. **15**, 7-18.

Park, H. K., Wang, H., Zhang, J., Datta, S. and Fei, P. (2010). Convergence of Rad6/Rad18 and Fanconi anemia tumor suppressor pathways upon DNA damage. *PLoS ONE*. **5**, 1-7.

Park, J., Long, D. T., Lee, K. Y., Abbas, T., Shibata, E., Negishi, M., Luo, Y., Schimenti, J. C., Gambus, A., Walter, J. C. and Dutta, A. (2013). The MCM8-MCM9 complex promotes RAD51 recruitment to DNA damage sites to facilitate homologous recombination. *Molecular and Cellular Biology*. **33**, 1632-1644.

Park, J. Y., Virts, E. L., Jankowska, A., Wiek, C., Othman, M., Chakraborty, S. C., Vance, G. H., Alkuraya, F. S., Hanenberg, H. and Andreassen, P. R. (2016). Complementation of hypersensitivity to DNA interstrand crosslinking agents demonstrates that XRCC2 is a Fanconi anaemia gene. *Journal of Medical Genetics*. **53**, 672-680.

Parrilla-Castellar, E. R., Arlander, S. J. H. and Karnitz, L. (2004). Dial 9-1-1 for DANN damage: the Rad9-Hus1-Rad1 (9-1-1) clamp complex. *DNA Repair*. **3**, 1009-1014.

Parsons, J. L. and Dianov, G. L. (2013). Co-ordination of base excision repair and genome stability. *DNA Repair*. **12**, 326-333.

Paull, T. T. and Gellert, M. (1999). Nbs1 potentiates ATP-driven DNA unwinding and endonuclease cleavage by the Mre11/Rad50 complex. *Genes and Development*. **13**, 1276-1288.

Paull, T. T., Rogakou, E. P., Yamazaki, V., Kirchgessner, C. U., Gellert, M. and Bonner, W. M. (2000). A critical role for histone H2AX in recruitment of repair factors to nuclear foci after DNA damage. *Current Biology*. **10**, 886-895.

Pauty, J., Rodrigue, A., Couturier, A., Buisson, R. and Masson, J.-Y. (2014). Exploring the roles of PALB2 at the crossroads of DNA repair and cancer. *Biochemical Journal*. **460**, 331-342.

Petermann, E. and Helleday, T. (2010). Pathways of mammalian replication fork restart. *Nature Reviews Molecular Cell Biology*. **11**, 683-687.

Petermann, E., Keil, C. and Oei, S. L. (2006). Roles of DNA ligase III and XRCC1 in regulating the switch between short patch and long patch BER. *DNA Repair*. **5**, 544-555.

Peters, J. E. and Craig, N. L. (2001). Tn7: smarter than we thought. *Nature Reviews Molecular Cell Biology*. **2**, 806-814.

Pinder, J. B., Attwood, K. M. and Dallaire, G. (2013). Reading, writing, and repair: the role of ubiquitin and the ubiquitin-like proteins in DNA damage signaling and repair. *Frontiers in Genetics*. **4**, 1-14.

Pinto, C., Kasaciunaite, K., Seidel, R. and Cejka, P. (2016). Human DNA2 possesses a cryptic DNA unwinding activity that functionally integrates with BLM or WRN helicases. *eLife*. **5**, 1-24.

Polito, D., Cukras, S., Wang, X., Spence, P., Moreau, L., D'Andrea, A. D. and Kee, Y. (2014). The carboxy terminus of FANCE recruits FANCD2 to the FA E3 ligase complex to promote the Fanconi anemia DNA repair pathway. *The Journal of Biological Chemistry*. **289**, 7003-7010.

Raghunandan, M., Chaudhury, I., Kelich, S. L., Hanenberg, H. and Sobeck, A. (2015). FANCD2, FANCJ and BRCA2 cooperate to promote replication fork recovery independently of the Fanconi Anemia core complex. *Cell Cycle*. **14**, 342-353.

Rajendra, E., Garaycoechea, J. I., Patel, K. J. and Passmore, L. A. (2014). Abundance of the Fanconi anaemia core complex is regulated by the RuvBL1 and RuvBL2 AAA+ ATPases. *Nucleic Acids Research*. **42**, 13736-13748.

Rajendra, E., Oestergaard, V. H., Langevin, F., Wang, M., Doman, G. L. and Patel, K. J. (2014). The genetic and biochemical basis of FANCD2 monoubiquitination. *Molecular Cell*. **54**, 858-869.

Rego, M. A., Kolling, F. W. IV, Vuono, E. A., Mauro, M. and Howlett, N. G. (2012). Regulation of the Fanconi anemia pathway by a CUE ubiquitin-binding domain in the FANCD2 protein. *Blood*. **120**, 2109-2117.

Reid, S., Schindler, D., Hanenberg, H., Barker, K., Hanks, S., Kalb, R., Neveling, K., Kelly, P., Seal, S., Freund, M., Wurm, M., Batish, S. D., Lach, F. P., Yetgin, S., Neitzel, H., Ariffin, H., Tischkowitz, M., Mathew, C. G., Auerbach, A. D. and Rahman, N. (2007). Biallelic mutations in PALB2 cause Fanconi anemia subtype FA-N and predispose to childhood cancer. *Nature Genetics*. **39**, 162-164.

Reinhardt, H. Ch. and Yaffe, M. B. (2009). Kinases that control the cell cycle in response to DNA damage: Chk1, Chk2, and MK2. *Current Opinion in Cell Biology*. **21**, 245-255.

Renaud, E. and Rosselli, F. (2013). FANC pathway promotes UV-induced stalled replication forks recovery by acting both upstream and downstream Polη and Rev1. *PLoS ONE*. **8**, 1-13.

Rickman, K. A., Lach, F. P., Abhyankar, A., Donovan, F. X., Sanborn, E. M., Kennedy, J. A., Sougnez, C., Gabriel, S. B., Elemento, O., Chandrasekharappa, S. C., Schindler, D., Auerbach, A. D. and Smogorzewska, A. (2015). *Cell Reports*. **12**, 35-41.

Roy, R., Chun, J. and Powell, S. N. (2012). BRCA1 and BRCA2: different roles in a common pathway of genome protection. *Nature Reviews Cancer*. **12**, 68-78.

Sale, J. E., Lehmann, A. R. and Woodgate, R. (2012). Y-family DNA polymerases and their role in tolerance of cellular damage. *Nature Reviews Molecular Cell Biology*. **13**, 141-152.

Salewsky, B., Schmiester, M., Schindler, D., Digweed, M. and Demuth, I. (2012). The nuclease hSNM1B/Apollo is linked to the Fanconi anemia pathway via its interaction with FANCP/SLX4. *Human Molecular Genetics*. **21**, 4948-4956.

Sarbajana, Sh., Davies, D. and West, S. C. (2014). Roles of SLX1-SLX4, MUS81-EME1, and GEN1 in avoiding genome instability and mitotic catastrophe. *Genes & Development.* **28**, 1124-1136.

Sareen, A., Chaudhury, I., Adams, N. and Sobeck, A. (2012). Fanconi anemia proetins FANCD2 and FANCI exhibit different DNA damage responses during S-phase. *Nucleic Acids Research*. **40**, 8425-8439.

Sato, K., Ishiai, M., Toda, K., Furukoshi, S., Osakabe, A., Tachiwana, H., Takizawa, Y., Kagawa, W., Kitao, H., Dohmae, N., Obuse, Ch., Kimura, H., Takata, M. and Kurumizaka, H. (2012). Histone chaperone activity of Fanconi anemia proteins, FANCD2 and FANCI, is required for DNA crosslink repair. *The EMBO Journal*. **31**, 3524-3536.

Satyanarayana, A. and Kaldis, P. (2009). Mammalian cell-cycle regulation: several Cdks, numerous cyclins and diverse compensatory mechanisms. *Oncogene*. **28**, 2925-2939.

Saugar, I., Parker, J. L., Zhao, S. and Ulrich, H. D. (2012). The genome maintenance factor Mgs1 is targeted to sites of replication stress by ubiquitinated PCNA. *Nucleic Acids Research*. **40**, 245-257.

Sawyer, S. L., Tian, L., Kähkönen, M., Schwartzentruber, J., Kircher, M., Majewski, J., Dyment, D. A., Innes, A. M., Boycott, K. M., Moreau, L. A., Moilanen, J. S. and Greenberg, R. A. (2014). Biallelic mutations in *BRCA1* cause a new Fanconi anemia subtype. *Cancer Discovery*. **5**, 135-142.

Schärer, O. D. (2005). DNA interstrand crosslinks: natural and drug-induced DNA adducts that induce unique cellular responses. *ChemBioChem*. **6**, 27-32.

Schlacher, K., Wu, H. and Jasin, M. (2012). A distinct replication fork protection pathway connects Fanconi anemia tumor suppressors to RAD51-BRCA1/2. *Cancer Cell*. **22**, 106-116.

Sertic, S., Evolvi, C., Tumini, E., Plevani, P., Muzi-Falconi, M. and Rotondo, G. (2013). Non-canonical CRL4A/4B$^{CDT2}$ interacts with RAD18 to modulate post replication repair and cell survival. *PLoS ONE*. **8**, 1-15.

Sherratt, D. J., Søballe, B., Barre, F.-X., Filipe, S., Lau, I., Massey, T. and Yates, J. (2004). Recombination and chromosome segregation. *Philosophical Transactions B.* **359**, 61-69.

Shibata, A., Moiani, D., Arvai, A. S., Perry, J., Harding, S. M., Genois, M. M., Maity, R., van Rossum-Fikkert, S., Kertokalio, A., Romoli, F., Ismail, A., Ismalaj, E., Petricci, E., Neale, M. J., Bristow, R. G., Masson, J. Y., Wyman, C., Jeggo, P. A. and Tainer, J. A. (2014). DNA double-stand break repair pathway choice is directed by distinct MRE11 nuclease activities. *Molecular Cell.* **53**, 7-18.

Shiloh, Y. and Lehmann, A. R. (2004). Maintaining integrity. *Nature Cell Biology.* **6**, 923-928.

Shuck, S. C., Short, E. A. and Turchi, J. J. (2008). Eukaryotic nucleotide excision repair: from understanding mechanisms to influencing biology. *Cell Research*. **18**, 64-72.

Shukla, P., Solanki, A., Ghosh, K. and Vundinti, B. R. (2013). DNA interstrand cross-link repair: understanding role of Fanconi anemia pathway and therapeutic implications. *European Journal of Haematology*. **91**, 381-393.

Shibata, T., Hishida, T., Kubota, Y., Han, Y.-W., Iwasaki, H. and Shinagawa, H. (2005). Functional overlap between RecA and MgsA (RarA) in the rescue of stalled replication forks in *Escherichia coli*. **10**, 181-191.

Siebler, H. M., Lada, A. G., Baranovskiy, A. G., Tahirov, T. H. and Pavlov, Y. I. (2014).

Singh, T. R., Saro, D., Ali, A. M., Zheng, X. F., Du, C. H., Killen, M. W., Sachpatzidis, A., Wahengbam, K., Pierce, A. J., Xiong, Y., Sung, P. and Meetei, R. (2010). MHF1-

MHF2, a histone-fold-containing protein complex, participates in the Fanconi anemia pathway via FANCM. *Molecular Cell*. **37**, 879-886.

Smogorzewska, A., Matsuoka, S., Vinciguerra, P., McDonald, E. R. III, Hurov, K. E., Luo, J., Ballif, B. A., Gygi, S. P., Hofmann, K., D'Andrea, A. D. and Elledge, S. J. (2007). Identification of the FANCI protein, a monoubiquitinated FANCD2 paralog required for DNA repair. *Cell*. **129**, 289-301.

Sommers, J. A., Banerjee, T., Hinds, T., Wold, M. S., Lei, M. and Brosh, Jr. M. (2014). Novel function of Fanconi anemia group J or RECQ1 helicase to disrupt protein-DNA complexes in a replication protein A-stimulated manner. *The Journal of Biological Chemistry*. **289**, 19928-19941.

Soria, G., Polo, S. E. and Almouzni, G. (2012). Prime, repair, restore: the active role of chromatin in the DNA damage response. *Molecular Cell*. **46**, 722-734.

Sørensen, C. S., Hansen, L. T., Dziegielewski, J., Syljuåsen, R. G., Lundin, C., Bartek, J. and Helleday, T. (2005). The cell-cycle checkpoint kinase Chk1 is required for mammalian homologous recombination repair. *Nature Cell Biology*. **7**, 195-201.

Stecklein, Sh. R. and Jensen, R. A. (2012). Identifying and exploiting defects in the Fanconi anemia/BRCA pathway in oncology. *Translational Research*. **160**, 178-197.

Stoepker, Ch., Hain, K., Schuster, B., Hilhorst-Hofstee, Y., Rooimans, M. A., Steltenpool, J., Oostra, A. B., Eirich, K., Korthof, E. T., Nieuwint, A. W. M., Jaspers, N. G. J., Bettecken, T., Joenje, H., Schindler, D., Rouse, J. and de Winter, J. P. (2011). SLX4, a coordinator of structure-specific endonucleases, is mutated in a new Fanconi anemia subtype. *Nature Genetics*. **43**, 138-141.

Strande, N. T., Waters, C. A. and Ramsden, D. A. (2012). Resolution of complex ends by nonhomologous end joining – better to be lucky than good? *Genome Integrity*. **3**, 10.

Sturzenegger, A., Burdova, K., Kanagaraj, R., Levikova, M., Pinto, C., Cejka, P. and Janscak, P. (2014). DNA2 cooperates with the WRN and BLM RecQ helicases to mediate long-range DNA end resection in human cells. *The Journal of Biological Chemistry*. **289**, 27314-27326.

Sung, P. and Klein, H. (2006). Mechanism of homologous recombination: mediators and helicases take on regulatory functions. *Nature Reviews Molecular Cell Biology*. **7**, 739-750.

Svendsen, J. M., Smogorzewska, A., Sowa, M. E., O'Connell, B. C., Gygi, S. P., et al. (2009). Mammalian BTBD12/SLX4 assembles a Holliday junction resolvase and is required for DNA repair. *Cell*. **138**, 63-77.

Taniguchi, T. and D'Andrea, A. D. (2006). Molecular pathogenesis of Fanconi anemia: recent progress. *Blood*. **107**, 4223-4233.

Terai, K., Abbas, T., Jazaeri, A. A. and Dutta, A. (2010). $CRL4^{Cdt2}$ E3 ubiquitin ligase monoubiquitinates PCNA to promote translesion DNA synthesis. *Molecular Cell*. **37**, 143-149.

Thompson, L. H. and Hinz, J. M. (2009). Cellular and molecular consequences of defective Fanconi anemia proteins in replication-coupled DNA repair: mechanistic insights. *Mutation Research*. **668**, 54-72.

Timmers, C., Taniguchi, T., Hejna, J., Reifsteck, C., Lucas, L., Bruun, D., Thayer, M., Cox, B., Olson, S., D'Andrea, A. D., Moses, R. and Grompe, M. (2001). Positional cloning of a novel Fanconi anemia gene, FANCD2. *Molecular Cell*. **7**, 241-248.

Tsubouchi, H. and Ogawa, H. (1998). A novel *mre11* mutation impairs processing of double-stand breaks of DNA during both mitosis and meiosis. *Molecular and Cellular Biology*. **18**, 260-268.

Trujillo, J. P., Mina, L. B., Pujol, R., Bogliolo, M., Andrieux, J., Holder, M., Schuster, B., Schindler, D. and Surrallés, J. (2012). On the role of FAN1 in Fnconi anemia. *Blood*. **120**, 86-89.

Trujillo, K. M. and Sung, P. (2001). DNA structure-specific nuclease activities in the *Saccharomyces cerevisiae* Rad50*Mre11 complex. *Journal of Biological Chemistry*. **276**, 35458-35464.

Trujillo, K. M., Yuan, S. S., Lee, E. Y. and Sung, P. (1998). Nuclease activities in a complex of human recombination and DNA repair factors Rad50, Mre11, and p95. *Journal of Biological Chemistry*. **273**, 21447-21450.

Tsurimoto, T., Shinozaki, A., Yano, M., Seki, M. and Enomoto, T. (2005). Human Werner helicase interacting protein 1 (WRNIP1) functions as a novel modulator for DNA polymerase δ. *Genes to Cells.* **10**, 13-22.

Ulrich, H. D. (2009). Regulating post-translational modifications of the eukaryotic replication clamp PCNA. *DNA Repair*. **8**, 461-469.

Ulrich, H. D. and Takahashi, T. (2013). Readers of PCNA modifications. *Chromosoma*. **122**, 259-274.

Ulrich, H. D. and Walden, H. (2010). Ubiquitin signalling in DNA replication and repair. *Nature Reviews Molecular Cell Biology*. **11**, 479-489.

Unno, J., Itaya, A., Taoka, M., Sato, K., Tomida, J., Sakai, W., Sugasawa, K., Ishiai, M., Ikura, T., Isobe, T., Kurumizaka, H. and Takata, M. (2014). FANCD2 binds CtIP

and regulates DNA-end resection during DNA interstrand crosslink repair. *Cell Reports*. **7**, 1039-1047.

van Attikum, H. and Gasser, S. M. (2009). Crosstalk between histone modifications during the DNA damage response. *Trends in Cell Biology*. **19**, 207-217.

van Gent, D. C., Hoeijmakers, J. H. J. and Kanaar, R. (2001). Chromosomal stability and the DNA double-standed break connection. *Nature Reviews Genetics.* **2**, 196-206.

van Oers, M. M. (2011). Opportunities and challenges for the baculovirus expression system. *Journal of Invertebrate Pathology*. **107**, S3-S15.

Vaux, D. L. (2012). Research methods: know when your numbers are significant. *Nature*. **492**, 180-181.

Vaz, F., Hanenberg, H., Schuster, B., Barker, K., Wiek, C., Erven, V., Neveling, K., Endt, D., Kesterton, I., Autore, F., Fraternali, F., Freund, M., Hartmann, L., Grimwade, D., Roberts, R. G., Schaal, H., Mohammed, S., Rahman, N., Schindler, D. and Mathew, C. G. (2010). Mutation of the RAD51C gene in a Fanconi anemia-like disorder. *Nature Genetics*. **42**, 406-409.

Voets, T., Janssens, A., Droogmans, G. and Nilius, B. (2004). Outer pore architecture of a Ca2+-selective TRP channel. *Journal of Biological Chemistry*. **279**, 15223-15230.

Walden, H. and Deans, A. J. (2014). The Fanconi anemia DNA repair pathway: structural and functional insights into a complex disorder. *Annual Review of Biophysics.* **43**, 257-278.

Walker, J. R., Corpina, R. A. and Goldberg, J. (2001). Structure of the Ku heterodimer bound to DNA and its implications for double-stand break repair. *Nature.* **412**, 607-614.

Wang, A. T., Kim, T., Wagner, J. E., Conti, B. A., Lach, F. P., Huang, A. L., Molina, H., Sanborn, E. M., Zierhut, H., Cornes, B. K., Abhyankar, A., Sougnez, C., Gabriel, S. B., Auerbach, A. D., Kowalczykowski, S. C. and Smogorzewska, A. (2015). A dominant mutation in human RAD51 reveals is function in DNA interstrand crosslink repair independent of homologous recombination. *Molecular Cell*. **59**, 478-490.

Wang, A. T., Sengerova, B., Cattell, E., Inagawa, T., Hartley, J. M., Kiakos, K., Burgess-Brown, N. A., Swift, L. P., Enzlin, J. H., Schofield, C. J., Gileadi, O., Hartley, J. A. and McHugh, P. J. (2011). Human SNM1A and XPF-ERCC1 collaborate to initiate DNA interstrand cross-link repair. *Genes and Development.* **25**, 1859-1870.

Wang, A. T. and Smogorzewska, A. (2015). SnapShot: Fanconi anemia and associated proteins. *Cell*. **160**, 354-354.

Wang, R., Persky, N. S., Yoo, B., Ouerfelli, O., Smogorzewska, A., Elledge, S. J. and Pavletich, N. P. (2014). Mechanism of DNA interstrand cross-link processing by repair nuclease FAN1. *Science*. **346**, 1127-1130.

Wang, W. (2007) Emergence of a DNA-damage response network consisting of Fanconi anaemia and BRCA proteins. *Nature Reviews Genetics*. **8**, 735-748.

Wang, X., Andreassen, P. R. and D'Andrea, A. D. (2004). Functional interaction of monoubiquitinated FANCD2 and BRCA2/FANCD1 in chromatin. *Molecular and Cellular Biology*. **24**, 5850-5862.

Wang, Y., Leung, J. W., Jiang, Y., Lowery, M. G., Do, H., Vasquez, K. M., Chen, J., Wang, W. and Li, L. (2013). FANCM and FAAP24 maintain genome stability via cooperative as well as unique functions. *Molecular Cell*. **49**, 1-13.

Warmerdam, D. O. and Kanaar, R. (2010). Dealing with DNA damage: relationships between checkpoint and repair pathways. *Mutation Research/Reviews in Mutation Research*. **704**, 2-11.

Welchman, R. L., Gordon, C. and Mayer, R. J. (2005). Ubiquitin and ubiquitin-like proteins as multifunctional signals. *Nature Reviews Molecular Cell Biology*. **6**, 599-609.

Wiese, C., Hinz, J. M., Tebbs, R. S., Nham, P. B., Urbin, S. S., Collins, D. W., Thompson, L. H. and Schild, D. (2006). Disparate requirements for the Walker A and B ATPase motifs of human RAD51Din homologous recombination. *Nucleic Acids Research*. **34**, 2833-2843.

Williams, R. S., Dodson, G. E., Limbo, O., Yamada, Y., Williams, J. S., Guenther, G., Classen, S., Glover, J. N., Iwasaki, H., Russell, P. and Tainer, J. A. (2009). Nbs1 flexibly tethers Ctp1 and Mre11-Rad50 to coordinate DNA double-stand break processing and repair. *Cell*. **139**, 87-99.

Williams, S. A., Longerich, S., Sung, P., Vaziri, C. and Kupfer, G. M. (2011). The E3 ubiquitin ligase Rad18 regulates ubiquitilation and chromatin loading of FANCD2 and FANCI. *Blood*. **117**, 5078-5087.

Williams, H. L., Gottesman, M. E. and Gautier, J. (2012). Replication-independent repair of DNA interstrand crosslinks. *Molecular Cell*. **47**, 140-147.

Wood, R. D. (2010). Mammalian nucleotide excision repair proteins and interstrand crosslink repair. *Environmental and Molecular Mutagenesis*. **51**, 520-526.

Wojtaszek, J. L., Wang, S., Kim, H., Wu, Q., D'Andrea, A. D. and Zhou, P. (2014). Ubiquitin recognition by FAAP20 expands the complex interface beyond the canonical UBZ domain. *Nucleic Acids Research*. 1-9.

Xing, M., Yang, M., Huo, W., Feng, F., Wei, L., Jiang, W., Ning, S., Yan, Z., Li, W., Wang, Q., Hou, M., Dong, C., Guo, R., Gao, G., Zha, S., Lan, L., Liang, H. and Xu, D. (2015). Interactome analysis identifies a new paralogue of XRCC4 in non-homologous end joining DNA repair pathway. *Nature Communications.* **6**, 6233.

Yamamoto, K. N., Kobayashi, S., Tsuda, M., Kurumizaka, H., Takata, M., Kono, K., Jiricny, J., Takeda, S. and Hirota, K. (2011). Involvement of SLX4 in interstrand cross-link repair is regulated by the Fanconi anemia pathway. *PNAS*. **108**, 6492-6496.

Yan, Z., Delannoy, M., Ling, C., Daee, D., Osman, F., Muniandy, P. A., Shen, X., Oostra, A. B., Du, H., Steltenpool, J., Lin, T., Schuster, B., Decaillet, C., Stasiak, A., Stasiak, A., Stone, S., Hoatlin, M, E., Schindler, D., Woodcock, C. L., Joenje, H., Sen, R., de Winter, J. P., Li, L., Seidman, M. M., Whitby, M. C., Myung, K. and Constantinou, A. (2010). A histone-fold complex and FANCM form a conserved DNA remodeling complex to maintain genome stability. *Molecular Cell.* **37**, 865-878.

Yang, K., Guo, R. and Xu, D. (2016). Non-homologous end joining: advances and frontiers. *Acta Biochimica et Biophysica Sinica.* **48**, 632-640.

Yang, K., Moldovan, G.-L. and D'Andrea, A. D. (2010). RAD18-dependent recruitment of SNM1A to DNA repair complexes by a ubiquitin-binding zinc finger. *The Journal of Biological Chemistry*. **285**, 19085-19091.

Yang, K., Weinacht, Ch. P. and Zhuang, Z. (2013). Regulatory role of ubiquitin in eukaryotic DNA translesion synthesis. *Biochemistry*. **52**, 3217-3228.

Yeo, J. E., Lee, E. H., Hendrickson, E. and Sobeck, A. (2014). CtIP mediates replication fork recovery in a FANCD2-regulated manner. *Human Molecular Genetics*. 1-28.

Yoshimura, A., Seki, M., Kanamori, M., Tateishi, S., Tsurimoto, T., Tada, S. and Enomoto, T. (2009). Physical and functional interaction between WRNIP1 and RAD18. *Genes and Genetic Systems*. **84**, 171-178.

Yoshimura, A., Kobayashi, Y., Tada, Sh., Seki, M. and Enomoto, T. (2014). WRNIP1 functions upstream of DNA polymerase η in the UV-induced DNA damage response. *Biochemical and Biophysical Research Communications.* **452**, 48-52.

Yuasa, M. S., Masutani, Ch., Hirano, A., Cohn, M. A., Yamaizumi, M., Nakatani, Y. and Hanaoka, F. (2006). A human DNA polymerase η complex containing Rad18, Rad6 and Rev1; proteomic analysis and targeting of the complex to the chromatin-bound fraction of cells undergoing fork arrest. *Genes to Cells*. **11**, 731-744.

Zeman, M. K. and Cimprich, K. A. (2014). Causes and consequences of replication stress. *Nature Cell Biology*. **16**, 2-9.

Zhang, J., Dewar, J. M., Budzowska, M., Motnenko, A., Cohn, M. A. and Walter, J. C. (2015). DNA interstrand cross-link repair requires replication fork convergence. *Nature Structural & Molecular Biology*. **22**, 242-247.

Zhang, J. and Walter, J. C. (2014). Mechanism and regulation of incisions during DNA interstrand cross-link repair. *DNA Repair*. **19**, 135-142.

Zhu, B., Yan, K., Li, L., Lin, M., Zhang, S., He, Q., Zheng, D., Yang, H. and Shao, G. (2014). K63-linked ubiquitination of FANCG is required for its association with the Rap80-BRCA1 complex to modulate homologous recombination repair of DNA interstrand crosslinks. *Oncogene*. 1-12.

Zhu, Z., Chung, W. H., Shim, E. Y., Lee, S. E. and Ira, G. (2008). Sgs1 helicase and two nucleases Dna2 and Exo1 resect DNA double-strand break ends. *Cell*. **134**, 981-994.